

TECHNISCHE UNIVERSITÄT MÜNCHEN

Lehrstuhl für Ernährungsphysiologie

**Plasma and tissue metabolite profiling
in mouse models of obesity and diabetes**

Pieter Johan Giesbertz

Vollständiger Abdruck der von der Fakultät Wissenschaftszentrum Weihenstephan für Ernährung, Landnutzung und Umwelt der Technischen Universität München zur Erlangung des akademischen Grades eines

Doktors der Naturwissenschaften

genehmigten Dissertation.

Vorsitzender: Univ.-Prof. Dr. H. Witt

Prüfer der Dissertation: 1. Univ.-Prof. Dr. H. Daniel
2. Univ.-Prof. Dr. M. Klingenspor

Die Dissertation wurde am 12.05.2016 bei der Technischen Universität München eingereicht und durch die Fakultät Wissenschaftszentrum Weihenstephan für Ernährung, Landnutzung und Umwelt am 09.09. 2016 angenommen.

CONTENT

INTRODUCTION	4
Rationale.....	4
A short résumé on obesity-induced type 2 diabetes	4
Insulin signaling, energy balance and glucose homeostasis	5
Obesity-induced insulin resistance.....	5
Increased insulin output from β -cells counterbalances insulin resistance	6
β -cell exhaustion results in type 2 diabetes.....	7
The course of diabetes development.....	8
Metabolite profiling in diabetes research.....	9
Metabolite profiling to discover markers of insulin resistance and diabetes.....	9
Acylcarnitines as markers of mitochondrial and peroxisomal pathways of fatty acid and amino acid oxidation and their alterations in diabetic states.....	11
Three animal models representing individual stages of diabetes progression.....	13
Leptin-signaling defective ob/ob and db/db mice as models for insulin resistance and type 2 diabetes	14
Streptozotocin-treated insulin-deficient mice as model for type 1 diabetes or end-stage type 2 diabetes	15
MATERIALS AND METHODS	17
Chemicals.....	17
Mouse models.....	17
Leptin-signaling deficient ob/ob and db/db mice	18
Streptozotocin-induced insulin-deficient diabetic mice	18
Plasma, urine, and tissue collection	18
Metabolite profiling	19
Untargeted broad-metabolite profiling with in-house GC-MS	19
Untargeted broad-metabolite profiling in cooperation with Metanomics health GmbH	20
Targeted amino acid profiling via LC-MS/MS and aTRAQ™ labeling	21
Targeted acylcarnitine profiling via LC-MS/MS and butylation: method development and application to mouse samples.....	21
Additional methods.....	23
Osmolarity measurements in urine.....	23
Plasma insulin measurements using ELISA.....	23
Gene expression analyses using quantitative real-time PCR	23
Statistical analysis and computational data integration	24

PUBLICATION 1	26
PUBLICATION 2	27
PUBLICATION 3	28
PUBLICATION 4 (in preparation).....	29
JOURNALS' PERMISSIONS TO INCLUDE ARTICLES.....	31
DISCUSSION	33
Mouse models display phenotypic changes characterizing individual stages of diabetes progression in humans	33
Plasma metabolite signatures in mice represent corresponding changes observed in human diabetes	34
Novel metabolite markers of obesity and diabetes in plasma.....	35
A branched-chain amino acid signature observed in all three models.....	36
White adipose tissue as important regulator of circulating BCAA levels in healthy states and insulin-resistant conditions.....	37
A novel LC-MS/MS method to quantify acylcarnitines from individual routes of amino acid and fatty acid breakdown.....	39
Signatures of acylcarnitine and acyl-CoA give insight into altered amino acid and fatty acid oxidation in tissues.....	40
Odd-numbered acylcarnitines as products of α -oxidation and elongation of amino acid-derived odd-numbered carbon primers.....	41
Impairment of the electron transport chain as a possible cause of alterations in the BCAA degradation pathways.....	43
CONCLUSION AND FUTURE PERSPECTIVES	48
SUMMARY	51
ZUSAMMENFASSUNG.....	51
SAMENVATTING.....	54
ABBREVIATIONS.....	56
BIBLIOGRAPHY	57
APPENDIX	64
ACKNOWLEDGEMENT/DANKSAGUNG/DANKWOORD	69
PUBLICATION LIST	70
CURRICULUM VITAE	71
ERKLÄRUNG	72

INTRODUCTION

Rationale

Understanding the diverse metabolic impairments in diseases like diabetes or the metabolic syndrome is a challenge. Both genetics and profiling approaches such as transcriptomics and proteomics have shown the complexity of these diseases and have demonstrated the difficulty in giving meaning to the observed changes. Metabolite profiling now adds a new layer of complexity to that via the identification of marker metabolites of insulin resistance and diabetes. Analysis of the metabolite changes is considered to improve diagnosis, allow disease prediction and add to the understanding of disease mechanisms. Over 50 metabolites have meanwhile been identified in human plasma that associate with insulin resistance and type 2 diabetes. However, in many cases it is not known why these metabolite changes in plasma occur and which metabolic processes in tissues contribute to the observed alterations in the plasma profiles.

Metabolites in blood are the result of uptake into and release from tissues. Within the experimental work underlying this thesis, metabolite profiles of plasma but and a number of tissues were analyzed in mice to better understand the contribution of individual organs to plasma metabolite concentration changes observed in insulin resistance and diabetes. The choice of three different mouse models representing different stages of diabetes development (obesity/insulin resistance, type 2 diabetes, type 1 diabetes/late type 2 diabetes) allowed the comparison of metabolite profiles in different stages of disease progression and across tissues based on a broad metabolite profiling approach combined with targeted analyses of pathway-specific metabolites. The following questions were addressed:

1. Do the mice display the same plasma metabolite changes as found in humans with insulin resistance and diabetes?
2. Can model-specific changes in metabolite concentrations be identified that mark specific developmental stages of diabetes and thus help to better understand the etiology and causality?
3. Which tissue-specific metabolite patterns relate to changes in plasma metabolite concentrations?
4. Can individual pathways be identified as origins of metabolite changes in plasma?

A short résumé on obesity-induced type 2 diabetes

Insulin signaling, energy balance and glucose homeostasis

Energy homeostasis is the result of a subtle regulation of anabolic and catabolic processes. Insulin is responsible for the major signal of anabolic adaptation and is involved in cell growth and differentiation. It promotes substrate storage in liver, muscle, and adipose tissue by affecting carbohydrate, lipid, and protein metabolism. Furthermore, insulin is responsible for a tight regulation of blood glucose levels via inhibition of hepatic gluconeogenesis and stimulation of hepatic glycolysis, via stimulation of glucose uptake into skeletal muscle and adipose tissue, and by activation of glycogen synthesis in liver and muscle. Maintenance of normal blood glucose levels relies on sufficient glucose-stimulated insulin secretion from β -cells and the proper metabolic responses of tissues to insulin. Organs directly responsive to insulin are liver, muscle, and adipose tissue, but other tissues are affected indirectly. Insulin signaling is thus central for control of energy balance and glucose homeostasis.

Obesity-induced insulin resistance

Obesity has been identified as a major cause of insulin resistance and type 2 diabetes. The pathogenesis of obesity-induced insulin resistance has not been completely clarified yet, but multiple mechanisms have been proposed and various aberrations in the insulin-signaling pathway have been identified. Accumulation of triglycerides in adipose tissue of obese individuals causes a large increase in adipose tissue mass accompanied by alterations in endocrine and metabolic functions of adipose tissue [1]. Secretion of adiponectin is reduced [2-4], while secretion of leptin is increased [5]. Adiponectin has been shown to improve insulin signaling and is known as an important stimulator of mitochondrial processes [6, 7]. Impaired adiponectin signaling is associated with a decreased mitochondrial capacity [8] and an increase in intermediates of mitochondrial oxidation which contribute to insulin resistance in peripheral tissues like adipose tissue and muscle [9]. The importance of adiponectin signaling is also demonstrated by a correction of disturbances of the muscle metabolome and whole body homeostasis in high-fat fed animals upon adiponectin administration [10]. Similarly, hepatic lipid accumulation is antagonized by adiponectin [11]. Leptin reduces food intake and body weight by hypothalamic [12] and peripheral processes [13]. However, in most obese individuals leptin sensitivity is reduced. Mechanisms for reduced leptin signaling are a defective leptin transport across the blood-brain barrier [14, 15] and an attenuation of leptin receptor signaling to which variations of leptin and leptin receptor genes contribute [16, 17].

Leptin resistance seems associated with endoplasmic reticulum stress which in turn inhibits leptin-induced STAT3 signaling [18]. A prolonged exposure of rat adipocytes to leptin has been shown to reduce adipocyte responsiveness to insulin [19] and chronic hyperleptinemia may therefore promote insulin resistance.

Besides alterations in hormone secretion, adipose tissue of obese individuals displays and increased secretion of proinflammatory cytokines such as TNF- α , IL-6, MCP-1 and RBP-4. TNF- α directly affects insulin signaling in skeletal muscle and adipose tissue [20, 21], as well as in liver [22]. RBP-4 induces insulin resistance via reduction of PI-3K signaling in muscle and increases gluconeogenesis in liver [23, 24]. The role of IL-6 in the induction of insulin resistance remains controversial. Strongest evidence for an induction of insulin resistance by IL-6 has been found in liver [25]. In contrast to its role in liver, IL-6 was demonstrated to increase glucose transport and glucose metabolism in human skeletal muscle [26]. Other cytokines like the monocyte chemoattractant protein 1 (MCP-1) recruit macrophages into the adipose tissue which produce additional cytokines, resulting in a state of chronic low-grade inflammation, directly affecting insulin sensitivity and metabolic processes [27-29].

A consequence of adipose tissue inflammation and adipocyte insulin resistance is an increased lipolysis rate followed by a release of non-esterified fatty acids (NEFA) and glycerol into the circulation [30]. The increased delivery of NEFA to skeletal muscle results in an increased accumulation of intramyocellular acyl-CoAs, di- and triacylglycerols and ceramides [31]. These intracellular lipids in turn inhibit glucose transport into skeletal muscle by affecting proteins in the insulin signaling cascade [32-34].

In summary, the progressive expansion of adipose tissue is accompanied by altered endocrine and metabolic function in combination with an enhanced inflammatory tone and an increased lipolysis rate which all contribute to reduced insulin responsiveness in peripheral and hepatic tissues in a prediabetic state known as insulin resistance.

Increased insulin output from β -cells counterbalances insulin resistance

Reduced tissue responsiveness to insulin is compensated by an increased pancreatic secretion of insulin [35]. At least in rats this is accompanied by an increased β -cell mass and size [36-38]. In addition, a reduced insulin clearance in states of decreased insulin sensitivity has been shown [39-41]. These factors lead to hyperinsulinemia [42]. As long as pancreatic β -cells are

able to compensate for the insulin resistance, euglycemia is maintained. Hyperinsulinemia per se causes metabolic alterations and contributes itself to insulin resistance [43]. Most prominent is the partial insulin resistance observed in the liver, in which suppression of FOXO-mediated gluconeogenic pathways by insulin is impaired but insulin-stimulated fatty acid *de novo* lipogenesis via SREBP-1c remains intact [44-46]. As a consequence, fatty acid *de novo* lipogenesis is overstimulated, contributing to the observed dyslipidemia and hepatosteatosis in obese and type 2 diabetic individuals [47]. Furthermore, the extent of insulin resistance, and thus the extent of insulin action, might vary between tissues. It has now become clear that the prediabetic states of impaired glucose tolerance (IGT) and impaired fasting glucose (IFG) exist in parallel rather than as sequential stages since they originate from insulin resistance in liver and muscle respectively [48]. Although type 2 diabetes is not yet diagnosed in these conditions due to a compensatory insulin output that prevents hyperglycemia, prediabetic individuals already hold metabolic alterations that distinguish them from healthy individuals.

β-cell exhaustion results in type 2 diabetes

Obesity is the major risk factor for type 2 diabetes, although most individuals who are obese do not develop diabetes. The progression from a prediabetic to a diabetic state develops in individuals that are unable to sustain the compensatory response by the β -cells. The prediction whether and when an individual will progress from a prediabetic insulin-resistant stage to a stage of pancreatic failure and type 2 diabetes is a major challenge and is essential for proper and timely intervention. Factors involved in the development of β -cell dysfunction can be of genetic origin but can also be acquired defects, including defective insulin biosynthesis and secretion [49] and mitochondrial dysfunction associated with increased oxidative stress [50]. The result is a lack to completely compensate for hepatic and/or peripheral insulin resistance in a state called relative insulin deficiency, in which individuals are hyperinsulinemic but where the insulin resistance outpaces insulin secretion [51]. An important implication of this is the failure to further inhibit hepatic glucose production, which is the primary determinant of the fasting plasma glucose concentration. Once hyperglycemia has established, other factors such as glucolipotoxicity [52], islet inflammation [53] and oxidative stress [54] enhance the progression of β -cell deterioration leading to β -cell failure associated with increased β -cell death by apoptosis.

The course of diabetes development

It becomes evident that the time course of diabetes initiation and progression features distinct metabolic and physiologic stages which depend on β -cell function and tissue responsiveness to insulin. A summary of the major events in the time course of diabetes development is given in Figure 1.

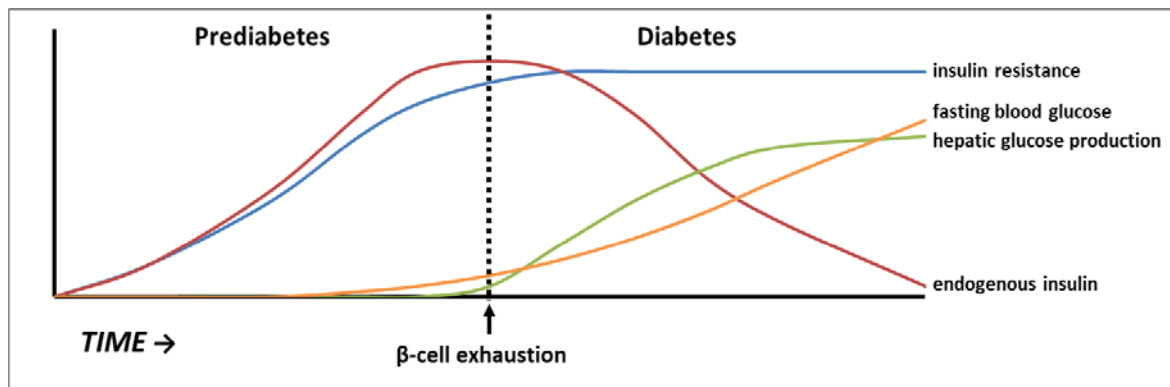


Figure 1. A simplified representation of the paradigm of diabetes development.

A rise in insulin resistance, for which the major causative factor is obesity, is accompanied by a compensatory increase in insulin output. This compensatory insulin response maintains normal blood glucose levels. At a certain time point, β -cells can no longer increase their insulin output to compensate for the progressive insulin resistance and fasting blood glucose levels can no longer be maintained at a normal level. At the time point of β -cell exhaustion, insulin output decreases and hepatic glucose production can no longer be effectively suppressed. As a result, blood glucose levels further rise. This state of hyperglycemia can still be accompanied by insulin levels which are elevated compared to a healthy state. This condition of relative insulin deficiency enhances β -cell deterioration and can lead to absolute insulin deficiency.

Metabolite profiling in diabetes research

In the last decade, metabolite profiling has become an element in diabetes research to identify metabolite changes marking insulin resistance and diabetes to improve diagnosis and allow early prediction of the disease. Furthermore, exploration of alterations in metabolite levels is thought to improve fundamental understanding of disease development and its associated metabolic perturbations. Of course, identification of novel disease-marking metabolites will aid the fundamental understanding of disease development, while improved understanding will support the discovery of disease-related metabolite markers. Here, the use of metabolomics to identify metabolite markers of insulin resistance and diabetes is described and the interpretation of acylcarnitine profiles to study changes in mitochondrial pathways of amino acid and fatty acid oxidation is described.

Metabolite profiling to discover markers of insulin resistance and diabetes

Diagnosis and monitoring of insulin resistance and glucose homeostasis are done by determining blood glucose and glycated hemoglobin A1c (HbA1c, as a measure for long-term hyperglycemia) and via a homeostasis model assessment as a measure of insulin resistance and β -cell function [55]. While these are good diagnostic procedures, the early identification of individuals at risk for diabetes remains challenging and requires markers with proper prediction quality for identification of subgroups at risk [56]. Metabolite profiling has become an explorative tool for metabolites with diagnostic and predictive quality for diabetes. Over 50 metabolites have meanwhile been reported as potential biomarkers. Despite large variation between studies, a number of metabolite changes have been replicated in multiple studies (see Table 1). Most prominent are elevations of branched-chain amino acids and their derivatives, including branched-chain keto acids, branched-chain fatty acids and acylcarnitines [57-63]. Increases of these metabolites have been reported for very early stages in diabetes development and remain high at all stages including diabetic ketoacidosis [61] and type 1 diabetes [64, 65]. Increased levels of aromatic amino acids (phenylalanine, tyrosine [59]) and reductions in glycine levels [66] as well as elevations of 2-hydroxybutyrate [67] and 2-aminoadipate [68] were reported in early stages of insulin resistance. In contrast, other metabolite changes relate specifically to severe states of hyperglycemia and increased catabolism in late glucose intolerant and diabetic states. These include increases of several

hexoses and amino-sugars like fructosamine [69, 70], as well as glyoxylate [69] related to protein glycation. Another prominent marker of hyperglycemia, 1,5-anhydroglucitol, is strongly reduced in plasma in hyperglycemic states and reflects a reduced renal reabsorption which is competitive with glucose [69, 70].

Table 1. Metabolite biomarkers most often reported as associated with obesity, prediabetic conditions, and diabetes.

Metabolite marker	Direction of change	Condition	Literature
Branched-chain amino acids (Val, Leu, Ile)	↑	Obesity, IFG, IGT, T2DM, T1DM	[57, 59-65, 71-75]
Aromatic amino acids (Tyr, Phe)	↑	Obesity, IR, T2DM	[57, 59, 62, 63, 71, 75, 76]
Glycine	↓	Obesity, T2DM	[60, 61, 66, 72, 76]
2-hydroxybutyrate	↑	IFG, IGT, T2DM	[58, 67, 69, 72]
3-hydroxybutyrate	↑	IGT, T2DM	[69, 77]
1,5-anhydroglucitol	↓	IFG, T2DM	[58, 69, 70, 77]
Lysophosphatidylcholine C18:2 / Linoleylglycerophosphocholine	↓	Obesity, IR, T2DM	[66, 67, 72, 78]
Lactate	↑	IFG, IGT, T2DM	[58, 69, 79]
Sugar amines (fructosamine)	↑	IFG, IGT, T2DM	[69, 70]

Furthermore, late stages of diabetes progression are characterized by increased levels of ketone bodies (3-hydroxybutyrate, acetone, acetoacetate, [69, 77, 80]) and lactate [58, 69, 79], in conditions of ketoacidosis and lactic acidosis. It is striking to realize that many of these metabolite concentration changes are known for many decades. As an example, the famous studies describing changes in circulating amino acid levels in obese and diabetic humans from Philip Felig date back to the early 1970s [60, 61]. Improved lipidomics technologies now identify an increasing number of lipid species from various classes that change in insulin resistant and diabetic conditions. One of the most promising biomarkers in this field is the decrease in linoleyl-glycerophosphocholine concentrations, which is already being used in the clinical setting for diabetes prediction [81, 82]. Similarly, various other lipids containing linoleic acid as well as free linoleic acid were reported to be decreased in plasma in obesity and T2DM [66, 83-85]. Furthermore, besides prominent increases in long-chain saturated and mono-unsaturated fatty acids, a general decrease of lysophosphatidylcholines and sphingomyelins has been observed in obesity and diabetes [71, 76, 78]. Arachidonic acid is discussed in the context of diabetes as well, but both increases [71] and decreases [77] have been reported in type 2 diabetes. Different directions of change have also been reported for odd-numbered and branched-chain fatty acids [58, 67, 77]. In contrast to the rather limited panel of amino

acids and organic solutes from well-described biochemical pathways which offer starting points for interpretation of molecular mechanisms and association with altered enzyme activities, the interpretation of lipidomics changes often remains at the biomarker level and the information necessary to understand molecular mechanisms of disease is currently limited.

In summary, whereas changes in plasma levels of various amino acids and other solutes have been described over 40 years ago and are now “rediscovered” in metabolomics studies to predict and diagnose insulin resistance and type 2 diabetes, the advance in lipidomics technologies offers a whole new panel of metabolites for which interpretation is currently very challenging as the biological information available on origin and fate of the molecules is very limited.

Acylcarnitines as markers of mitochondrial and peroxisomal pathways of fatty acid and amino acid oxidation and their alterations in diabetic states

Obesity and diabetes are characterized by changes in fatty acid and amino acid metabolism. Acylcarnitines are metabolic products derived from mitochondrial and peroxisomal oxidation of fatty acids and amino acids. These molecules are formed via the conversion of acyl-CoA intermediates of mitochondrial fatty acid and amino acid oxidation by the action of carnitine transferases [86]. Whereas conjugation to carnitine is essential for fatty acids to be imported into the mitochondria for oxidation, a release of acylcarnitines into the cytosol and from there into circulation becomes important in conditions of impaired mitochondrial utilization in which export of acylcarnitines may be considered as a spill-over to prevent unwanted effects of fatty acids in free form and/or in form of CoA-derivatives that can be toxic when accumulating [87, 88]. Four carnitine transferases have been identified that allow the conversion of the whole range of acyl-CoA species into acylcarnitines [89]. While most acylcarnitine species are derived from β -oxidation of fatty acids, branched-chain amino acid breakdown gives rise to specific branched-chain and odd-numbered acylcarnitine species [59, 90]. In addition, dicarboxylic acylcarnitines are formed in amino acid oxidation [91] and fatty acid ω -oxidation [92]. It has not been completely clarified how acylcarnitines reach the circulation (both OCTN2 and CPT2/CACT were reported to be involved [93, 94]), but the determination of acylcarnitine profiles in plasma and urine is widely used to identify inherited disorders of mitochondrial and peroxisomal oxidation processes [95]. More recently, changes

in acylcarnitine concentrations in plasma were found to associate with obesity and impaired insulin signaling (see Table 2).

Table 2. Acylcarnitine markers described in obesity, insulin resistance and T2DM.

Acylcarnitine markers in IR and T2DM	Direction of change	Condition	Literature
BCAA-derived acylcarnitines (C3, C5s, isoC4)	↑	Obesity, T2DM	[59, 62, 67, 83]
Succinylcarnitine (C4-DC)	↑	T2DM	[96]
Acetylcarnitine (C2)	↑	IGT, T2DM	[66, 71, 83]
Medium-chain acylcarnitines (C8, C10)	↑	IGT, IFG	[58, 67, 77, 97, 98]
Linoleoylcarnitine (C18:2)	↓	T2DM	[83]

The various oxidation pathways give rise to many isomeric acylcarnitine species. Since obesity and diabetes are characterized by changes in both fatty acid and amino acid metabolism, quantification of individual isomeric compounds is important to be able to identify changes of individual pathways of fatty acid and amino oxidation. The common measurement approach using direct infusion tandem mass spectrometry (MS/MS) does not allow this, due to the lack of chromatography [99]. Recent studies reported a successful chromatographic separation of isomeric acylcarnitine species [100-103], although the identification of the exact compound often remains elusive and the abundance of many species in biological samples is often too low for robust detection and quantification. As part of this thesis, an LC-MS/MS method was developed that includes the quantification of low-abundant forms with a special focus on amino acid derived and odd-numbered acylcarnitine species as putative diabetes markers. The method was applied to quantify acylcarnitine concentrations in plasma and tissues in the mouse models of obesity and diabetes to better understand mitochondrial and peroxisomal changes of fatty acid and amino acid oxidation and how these processes affect changes in plasma metabolite markers.

Three animal models representing individual stages of diabetes progression

For many metabolites reported as diabetes markers in human plasma, the metabolic origin is often not known. In contrast to humans in which tissues are hard to obtain for analysis, animals such as mice allow the collection of organs and tissues for fundamental studies of metabolic processes. Rodents with characteristics of insulin resistance and type 2 diabetes similar to humans include species with genetic (e.g. *ob/ob* mice, ZDF rats), nutritional (e.g. high-fat diet induced obesity), chemical (e.g. streptozotocin-induced diabetes), or experimental (e.g. surgery-induced diabetes) origin [104]. While all models have their advantages and disadvantages (see [104]), an important classification should be made based on the robustness of the pancreas to compensate for a decrease in insulin sensitivity. The choice of a model prone or resistant to β -cell failure depends on which aspect of the metabolic syndrome is aimed to study. Thus, models that are rather resistant to developing β -cell failure and diabetes (e.g. *ob/ob* mice, Zucker fatty rats) are suitable to study obesity-induced insulin resistance and hepatic steatosis, whereas models prone to β -cell failure (e.g. *db/db* mice, Zucker diabetic rats) can be used to study hyperglycemia-associated pathologies like diabetic nephropathy and neuropathy.

Box 1. Mouse models studied in this thesis.

C57BL/6J-*Lep*^{ob/ob} : „diabetes-resistant“

Defective leptin production

Hyperphagia > Obesity > Insulin-resistance > ***Pancreas hypertrophy*** > transitory hyperglycemia

C57BLKS/J-*Lepr*^{db/db} : „diabetes-prone“

Deficient leptin receptor B

Hyperphagia > Obesity > Insulin-resistance > ***Pancreas atrophy*** > marked hyperglycemia > ketotic > progressive weight loss

C57BL/6J: streptozotocin-induced type I diabetes

Intraperitoneal streptozotocin-injection (180 mg/kg BW) > pancreas destruction

Non-obese, insulin-deficiency, severe hyperglycemia, ketotic, weight loss

Another important criterion is the presence or absence of obesity. While obesity models allow the study of obesity-induced insulin resistance and diabetes, non-obesity models allow the

study of insulin-deficient conditions per se, dissociated from obesity. The latter group includes chemically-induced diabetes models by use of alloxan or streptozotocin which are toxic to pancreatic β -cells. It also includes genetic rodent models such as the AKITA mouse, lacking the *ins2* gene [105] and rodent models with spontaneous autoimmunity or a virally-induced immune response leading to β -cell destruction.

For the present thesis, mouse models representing disease conditions from early obesity-induced insulin resistance to late diabetic ketoacidosis were studied (see Box 1), with the *ob/ob* and *db/db* mice as models for obesity and diabetes-resistant or diabetes-prone conditions, respectively and streptozotocin-treated C57BL6/J mice for a non-obese insulin-deficient condition.

Leptin-signaling defective ob/ob and db/db mice as models for insulin resistance and type 2 diabetes

Described in 1950 [106] and 1966 [107] respectively as to result from naturally-occurring gene mutations, the C57BL6/J-*Lep*^{ob/-} mice and C57BLKS-*Lepr*^{db/-} mice, in the remaining text called *ob/ob* and *db/db* mice respectively, are now known to be defective in leptin signaling [108]. In *ob/ob* mice this is due to an autosomal recessive mutation in the leptin gene whereas in *db/db* mice an autosomal recessive mutation in the gene coding for the leptin receptor isoform B is the cause [109, 110]. Leptin, predominantly produced in adipose tissue, is a key satiety hormone, regulating energy intake and expenditure [12]. Hence, homozygous mutant mice from both strains are highly hyperphagic and develop massive obesity as well as a strong insulin resistance. Importantly, the *ob/ob* mice are on the diabetes-resistant C57BL6/J background whereas the *db/db* mice have a diabetes-prone C57BLKS/J background which is a mixture of C57BL6/J and DBA (dilute brown agouti) strains [111]. As a result, the C57BLKS/J strain has about one in every eight of its genes from the DBA strain, which has an unstable pancreas which is more prone to developing β -cell exhaustion. As a consequence, while both strains develop obesity and insulin resistance as a result of impaired leptin signaling, the *ob/ob* mice are able to compensate for the increasing insulin demand with a hypertrophy and hyperplasia of pancreatic β -cells [112]. The result is a hyperglycemia that is only transient until around 14 to 16 weeks of age, followed by a normalization of blood glucose levels. Body weight, however, continues to increase and mice may reach weights of up to 120 grams [107], which is more than four times the weight of a wild-type control animal. The mice furthermore

show a severe steatosis of the liver. In contrast, in *db/db* mice, β -cell expansion fails and islet atrophy occurs. Hyperinsulinemia develops within one month, followed by a steady decrease in insulin levels and a severe hyperglycemia. After four months of age, animals become ketotic and lose weight. These animals don't survive longer than 8 to 10 months. Important to note is the study by Hummel et al. in 1972 who transferred the *db* mutation into a C57BL6/J background. These C57BL6/J-*db/db* mice showed the same development as *ob/ob* mice, demonstrating that the genetic background is responsible for the different susceptibility to develop diabetes and that it is not the different defects of leptin hormone or leptin receptor [113]. Similarly, when introducing the *ob* gene into the C57BL6 background, mice develop severe diabetes [114]. Thus, *ob/ob* mice serve as a model of prediabetes with obesity-induced insulin resistance but without impairment of pancreatic β -cell function, while *db/db* mice serve as model for a more advanced stage of diabetes development with relative insulin deficiency and hyperglycemia.

Streptozotocin-treated insulin-deficient mice as model for type 1 diabetes or end-stage type 2 diabetes

A common method to induce insulin-deficiency in rodents, mostly in rats, is the use of the cytotoxic chemicals alloxan and streptozotocin. Both are selectively toxic to pancreatic β -cells due to their selective uptake via GLUT2 transporters, which are dominantly present in β -cells [115]. The mechanisms of cytotoxicity of the two compounds are different. Streptozotocin used here consists of a glucose and a methylnitrosurea moiety. The latter has alkylating properties, responsible for DNA damage and destruction of β -cells [115]. Rodents treated with a high dose of streptozotocin display a triphasic blood glucose response. A first hyperglycemic phase one hour after drug administration is the result from an inhibition of mitochondrial energy production and processing of insulin in secretory granules leading to a reduced insulin secretion. A second phase, typically four to eight hours after drug administration, is marked by a strong hypoglycemia. This is the result of the membrane rupture of β -cells and secretory granules leading to a release of the complete insulin store into the circulation. A final fourth phase is a permanent hyperglycemia resulting from a loss of β -cells. In the final phase, streptozotocin-treated mice display severe hyperglycemia and glucosuria accompanied by hyperglycemia-related pathologies such as neuropathy, cardiomyopathy and retinopathy [115]. Furthermore, a hyperlipidaemia and ketoacidosis is observed. Thus, high dose

streptozotocin-treated mice offer a model for non-obese absolute insulin-deficient hyperglycemia which occurs as a final stage in type 2 diabetes and in type 1 diabetes.

MATERIALS AND METHODS

An overview on the study workflow in this thesis is provided in Figure 2. Three different mouse models of obesity and diabetes were studied. Plasma, urine, and tissues were collected. Metabolite profiling was performed using targeted and untargeted GC-MS and LC-MS/MS approaches. Additional methods included osmolarity measurements of urine, determination of plasma insulin levels and selected gene expression analyses. Statistical analysis and computational data integration was done using the statistical software environment R [116]. All steps are discussed in detail in the subsequent paragraphs.

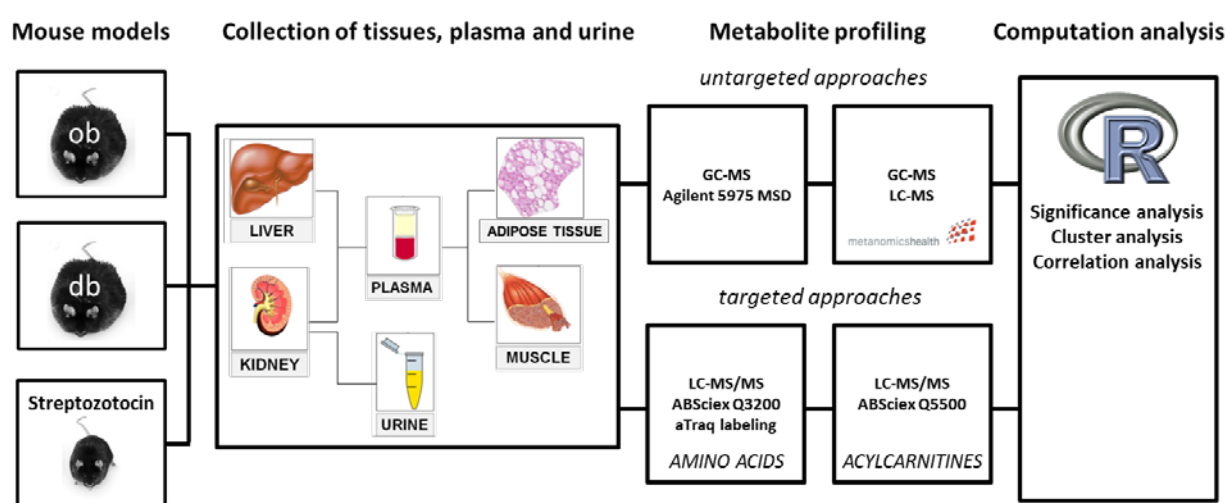


Figure 2. Overview of the workflow in this thesis.

Chemicals

Chemicals were obtained from Sigma-Aldrich, Roth, and Merck, unless stated differently in the corresponding sections.

Mouse models

Three mouse models with phenotypic characteristics resembling different stages of diabetes progression were studied. Leptin-resistant *ob/ob* and *db/db* mice are models of obesity-induced insulin resistance with or without hyperglycemia, respectively. High-dose streptozotocin-treated insulin-deficient mice resemble a condition of absolute insulin-deficient diabetes, as occurring in an end-point stage of type 2 diabetes and in type 1 diabetes.

A control group of wild-type mice was included for every model. For *ob/ob* and *db/db* mice, these were wild-type mice of the corresponding background strain. For streptozotocin-treated mice, these were wild-type mice treated with citrate buffer.

Leptin-signaling deficient ob/ob and db/db mice

Male *db/db* mice and C57BLKS/J wild-type littermates ($n=6-10$ per group) were purchased from Charles River Laboratories (Sulzfeld, Germany) at an age of 5 weeks. Male *ob/ob* mice and C57BL6/J wild-type littermates ($n=6-10$ per group), bred at the Research Center of Nutrition and Food Sciences (ZIEL), were obtained at the age of 5 weeks. Mice were kept on a standard-chow diet (ssniff V1534-0 R/M-H) for 3 weeks and were then placed on a chemically defined control diet (CCD; ssniff E15000-04 EF R/M Kontrolle) for 12 weeks. All mice had ad libitum access to food and water and were housed in the same open mouse facility. Body weight was determined weekly, and blood glucose was measured shortly before the end of the feeding trial. Animals were killed in a non-fasted state at an age of 20 weeks. Animal handling was conducted in accordance with the Principles of Laboratory Care and was approved by the Veterinary Inspection Services.

Streptozotocin-induced insulin-deficient diabetic mice

C57BL6/N mice ($n=10$) at an age of 12 weeks were injected intraperitoneally with a single high dose of streptozotocin (180 mg/kg body weight; streptozotocin was dissolved in 0.1 M citric acid buffer). C57BL6/N mice ($n=10$) injected intraperitoneally with citric acid buffer were used as controls. All mice were kept at a standard chow diet (ssniff V1534-0 R/M-H) during the whole study and were not fasted. Mice were killed five days post-injection. Body weight and blood glucose were measured daily. Blood glucose was measured using tail-vein puncture. All experiments were conducted according to the German guidelines for animal care and were approved by the state of Bavaria (Regierung von Oberbayern) ethics committee (Reference number: 55.2.1-54-2532-22-11).

Plasma, urine, and tissue collection

For all mice in the study, the procedure of sample collection was kept the same. For *ob/ob* and *db/db* mice, urine was collected shortly before killing and was snap-frozen in liquid nitrogen. For streptozotocin-treated mice, urine was collected daily and was snap-frozen in

liquid nitrogen. All mice were anaesthetized with isoflurane. Before killing, blood was collected via retro-orbital puncture into EDTA-coated tubes and was centrifuged for 10 minutes at 1200 g and 4°C. Plasma was separated and snap-frozen in liquid nitrogen. Animals were killed using cervical dislocation. Tissues were collected and immediately snap-frozen in liquid nitrogen. All samples were stored at -80°C until the day of measurement.

Metabolite profiling

Metabolite profiling was performed using four different platforms combining untargeted and targeted approaches. Broad metabolite profiles were established via in-house GC-MS measurements and via LC- and GC-MS measurements in cooperation with Metanomics Health GmbH (Berlin, Germany). A targeted LC-MS/MS analysis using aTraq labeling was used to measure amino acids. A second targeted LC-MS/MS method to measure acylcarnitine species was developed, validated, and applied to mouse samples.

Untargeted broad-metabolite profiling with in-house GC-MS

For broad metabolite profiling of plasma, urine, liver, kidney and muscle in-house GC-MS analyses were performed as a semi-quantitative approach. Tissues were ground in liquid nitrogen using pestle and mortar prior to extraction. Metabolites were extracted from 10 to 20 mg tissue (wet weight), 50 µl urine, and 100 µl plasma, using 1 ml of ice-cold methanol containing paracetamol (0.5 mg/ml) as internal standard. Samples were shaken for 10 minutes at 4°C and were then centrifuged for 5 minutes at 14.000 g. 900 µl of the supernatant was transferred to a new tube and vacuum-dried.

Derivatization of dried samples was performed in a two-step process. First, to stabilize carbonyl moieties in the metabolites, 30 µl methoxyaminehydrochloride (20 mg/ml in pyridine) was added to the dried sample and samples were shaken at 30°C for 90 minutes. Second, samples were silylated by addition of 30 µl of the trimethylsilyl (TMS) reagent N-Methyl-N-(trimethylsilyl) trifluoroacetamide (MSTFA) and 40 minutes shaking at 50°C. The solution was then centrifuged for 7 minutes at 14.000 g and 45µl of the pellet was transferred to a glass vial.

Gas chromatographic separation and mass spectrometric analysis was performed using an HP Agilent 7890 gas chromatograph coupled to an Agilent 5975 Quadrupole mass spectrometer

(Agilent technologies, Böblingen, Germany). A sample volume of 1 μ l was injected and separation was performed on a VF-5ms capillary column (length 30 m, internal diameter 0.25 mm, film thickness 25 μ m; VARIAN, Palo Alto, CA, USA). Oven temperature started isocratic at 70°C for 1 minute and then increased with 10°C/min up to 330°C, remaining isocratic for eight minutes. Masses were scanned at 2.5 spectra/s and mass ranges of 70 to 600 Da. For determination of retention time index, a mixture of n-alkanes ranging from ten to 36 carbon atoms was measured after each ten samples.

Data processing and quantitation was done using the Metabolite Detector software [117], which performed automated baseline correction, peak detection, peak deconvolution and peak integration. The Golm Metabolome Database [118] and the spectral library from the National Institute of Standards and Technology (NIST) were used for peak identification.

Untargeted broad-metabolite profiling in cooperation with Metanomics health GmbH

Comprehensive metabolite profiles of plasma, liver, muscle, and adipose tissue were obtained from a collaborative effort with Metanomics health GmbH (Berlin, Germany) using gas chromatography-mass spectrometry (GC-MS; Agilent 6890 GC coupled to an Agilent 5973 MS System, Agilent, Waldbronn, Germany) and liquid-chromatography-tandem mass spectrometry (LC-MS/MS; Agilent 1100 HPLC, API 4000, Applied Biosystems, Darmstadt, Germany). Proteins were removed from plasma samples by precipitation prior to collection of polar and non-polar fractions. For LC-MS/MS, both fractions were evaporated and reconstituted in appropriate solvents and measured with reversed-phase HPLC coupled to mass spectrometry. For GC-MS, the non-polar fraction was treated with methanol under acidic conditions to yield fatty acid methyl esters derived from both free fatty acids and hydrolyzed complex lipids. The polar and non-polar fractions were further derivatized with O-methylhydroxyamine hydrochloride to convert oxo-groups to O-methyloximes and subsequently with a silylating agent prior to GC-MS analysis. To account for inter- and intra-instrumental variation in GC-MS profiling, data were normalized to the median of reference samples derived from a pool formed from aliquots of all samples. Pooled reference samples were run in parallel through the whole process. Key analytical parameters determined within method development and reviewed within the present study were taken into account to specify high-quality metabolites, herein termed as semi-quantitative metabolites.

Targeted amino acid profiling via LC-MS/MS and aTRAQ™ labeling

For quantitative determination of amino acid concentrations, targeted LC-MS/MS measurements were performed using aTRAQ™ derivatization (aTRAQ reagent kit 4442671 SCIEX | 500 Old Connecticut Path, Framingham, MA 01701, USA). Tissues were ground in liquid nitrogen using pestle and mortar and 50 mg tissue was dissolved in 75 µl ice-cold methanol/water (1/1 v/v). Samples were centrifuged at 10.000 g for 10 min and supernatant was collected. Further preparation was performed according to the manufacturer's instructions. Briefly, 40 µl of plasma or tissue extract were mixed with 10 µl sulfosalicylic acid (containing norleucine as a first internal standard) to precipitate proteins and the mixture was centrifuged for 2.5 min at 10.000 g. 10 µl of the supernatant was homogenized with 40 µl labeling buffer (containing norvaline as a second internal standard) to maintain a basic pH during derivatization. Next, 10 µl from this mixture was mixed with 5 µl aTraQ reagent Δ8 (6 ¹³C carbon atoms and 2 ¹⁵N nitrogen atoms, resulting in an additional mass of 8 atomic units) for 30 min at room temperature. The derivatization reaction was stopped by addition of 5 µl hydroxylamine. The whole mixture was vacuum-dried in a vacuum concentrator (SPD111V SpeedVac™ Thermo Savant™, Germany) and subsequently mixed with internal standard containing all amino acids in the method pre-labeled with aTraQ reagent Δ0 (containing no stable-isotope labeled atoms).

Targeted acylcarnitine profiling via LC-MS/MS and butylation: method development and application to mouse samples

For the quantification of acylcarnitine species in plasma and tissues of mice, an LC-MS/MS method was developed and validated which extended the analytical panel of acylcarnitines and allowed quantitation of structural isomers derived from individual pathways of amino acid and fatty acid metabolism. The method included several new species, such as odd-numbered acylcarnitines, which are present at low concentrations. For identification of individual peaks in the chromatogram, individual acylcarnitine species were synthesized and spiked into biological samples. The method was applied to plasma and tissue samples of the three mouse models.

Here, the sample preparation, chromatographic, and mass spectrometric conditions are described as applied for the analysis of mouse samples. Furthermore, chemical synthesis of acylcarnitine species and calibration and validation of the method are described.

Analyses were performed on plasma, liver, muscle, kidney, and adipose tissue. As for the amino acid profiling procedure, tissues were ground in liquid nitrogen using pestle and mortar. Metabolites were extracted from 10 µl of plasma and 40 mg of ground tissue (wet weight). For plasma measurements, 10 µl of plasma was dissolved under ultra-sonication in 100 µl ice-cold methanol containing 1:1 diluted internal standard (ChromSystems) with deuterium-labeled amino acid and acylcarnitine species. Samples were then vacuum-dried in a vacuum concentrator (SPD111V SpeedVac™ Thermo Savant™, Germany). For tissue measurements, 40 mg of ground tissue were dissolved in 1800 µl 100% ice-cold methanol and shaken for 20 min at room temperature. Samples were subsequently centrifuged at 10.000 g for 10 minutes and supernatant extracts were transferred to a new reaction tube. For muscle and adipose tissue, with lower concentrations of acylcarnitines compared to kidney and liver tissue, 200 µl of the extracts were mixed with 20 µl ChromSystems amino acid and acylcarnitine internal standard and vacuum-dried. For liver and kidney, 200 µl of sample were mixed with 50 µl ChromSystems internal amino acid and acylcarnitine standard and vacuum-dried. Acylcarnitines were derivatized to their butyl esters as described by Gucciardi et al. [101]. Briefly, 100 µl *n*-butanol containing 5% v/v acetyl choline was added to the dried samples, incubated at 60°C for 20 minutes and subsequently evaporated to dryness. Samples were reconstituted in 100 µl (for plasma samples) or 200 µl (for tissue samples) acetonitrile/water and transferred to glass vials.

Samples were automatically injected (PAL HTC-xt, CTC analytics AG, Zwingen, Switzerland) and chromatographic separation was yielded on a Zorbax Eclipse XDB-C18 column (length 150 mm, internal diameter 3.0 mm, particle size 3.5 µm, Agilent, USA) using the Agilent 1260 Infinity Quaternary LC System. The mobile phase consisted of 0.1% formic acid, 2.5 mM ammonium acetic acid and 0.005% heptafluorobutyric acid in water (mobile phase A) or 0.1% formic acid, 2.5 mM ammonium acetic acid and 0.005% heptafluorobutyric acid in acetonitrile (mobile phase B). Mass spectrometric detection was done using the QTRAP5500 LC-MS/MS system (AB SCIEX | 500 Old Connecticut Path, Framingham, MA 01701, USA) with positive electron spray ionization and operating in multiple reaction monitoring (MRM). Peak integration and

quantification was done using Analyst 1.5[®] software (AB SCIEX | 500 Old Connecticut Path, Framingham, MA 01701, USA).

To identify individual peaks in the chromatogram, O-acylated acylcarnitines were synthesized from carnitine chloride and free fatty acids using a modified protocol from Ziegler et al. [119]. Briefly, 0.5 g of free fatty acid was incubated with 30.5 μ l thionylchloride under continuous shaking for four hours at 70°C to generate fatty acyl chlorides. Carnitine hydrochloride dissolved in trichloroacetic acid was added to the acyl chloride and incubated at 45°C for 18 hours. After cooling, the product was precipitated and washed three times in cold diethyl ether. Sodium-(s)- β -hydroxyisobutyric acid was first treated with hydrochloric acid to produce the free fatty acid, followed by evaporation of water at 90°C for 30 minutes, before incubation with thionylchloride.

Additional methods

Osmolarity measurements in urine

Osmolarity of urine samples was determined using the om-815 Osmometer (Vogel Medizintechnik, Fernwald, Germany). This osmometer determines the freezing point depression of a solution as a measure of osmolarity. The measurement was performed following the manufacturer's instructions with the use of 50 μ l urine sample.

Plasma insulin measurements using ELISA

Plasma insulin concentrations were measured via enzyme-linked immunosorbent assay (ELISA) using the Ultra Sensitive Mouse Insulin ELISA kit (Crystal Chem Inc., IL, USA). The assay was performed in a 96-well microtiter plate according to the manufacturer's instructions. Spectrometric analysis was done using the Varioskan plate reader (Thermo Scientific), giving quantitative measures of color strength.

Gene expression analyses using quantitative real-time PCR

RNA isolation and relative quantification of mRNA expression was performed as described previously with a few modifications (see [120]). After homogenization of adipose tissue, a liquid-liquid extraction with phenol-chloroform was performed. Total RNA was then extracted using the RNeasy Mini Kit (Qiagen). Purity and integrity of the RNA was assessed on the Agilent

2100 bioanalyzer (Agilent Technologies). For quantitative real-time PCR, 1 μ g RNA was transcribed into cDNA using a Reverse Transcription System from Promega. qRT-PCR analysis was performed with a LightCycler 480 (Roche). The mean of Actb, Gapdh, Hprt1 and 18S rRNA was used as the reference expression and relative quantification was carried out with the LightCycler 480 software 1.5 (Roche). Transcripts have been specified with the primers listed in Table S1.

Statistical analysis and computational data integration

Statistical analysis and computational data integration was done using the statistical programming language R. Three mouse models were studied. For every model, a corresponding wild-type group was included. Thus, in total 6 mouse groups were studied. Significant changes in metabolite concentrations or gene expression were determined as a comparison between the mouse model and the corresponding wild-type group.

For broad metabolite profiles of plasma and tissues from *ob/ob* and *db/db* mice, significance levels for metabolite concentrations were calculated by computing ANOVA models and using Student's t-statistics (unpaired and unequal variance). A significance threshold of $\alpha < 0.05$ was defined. Adjustment of *p*-values according to Benjamini and Hochberg was applied to correct for multiple testing. For untargeted GC-MS analyses of plasma and tissues of streptozotocin-treated mice, as well as for targeted amino acid and acylcarnitine profiling, differences between metabolite concentrations were assessed using unpaired two-sided Student's t-tests with unequal variance, applying a significance threshold of $\alpha < 0.05$.

Several computational data mining strategies were applied in R to integrate metabolomics data, including principal components analysis, hierarchical and *k*-means cluster analyses and pairwise Pearson's correlation analyses followed by the generation of correlation matrices and correlation networks.

To examine the grouping of individual mice according to their condition, principal components analysis to plasma and tissue samples was applied. Missing values were replaced by the mean of each variable.

Principal components analysis was also applied to identify the main metabolite groups in the plasma data sets of *ob/ob* and *db/db* mice derived from broad metabolite profiling. Five

principal components were clustered using a *k*-means clustering algorithm to identify 15 main metabolite clusters in the data set. Refinement of clustering was done using 20 times bootstrapping of the *k*-means clustering algorithm. An overall significant change of each cluster compared to wild-type animals was calculated by combining for each metabolite in the cluster its *p*-value derived from the comparison of its concentrations between knock-out and wild-type mice using the Fisher's combined probability test.

Pairwise Pearson's correlations were calculated and visualized using correlation matrices and correlation networks. To explore dominance of individual tissues on metabolite levels in plasma, measures of correlation **between** plasma and tissues were calculated. To explore regulated key components and associations between metabolites, measures of correlation **within** plasma and tissues were calculated. In addition to the base packages available in R, the packages 'FactoMineR', 'fpc', 'MADAM', 'qgraph' and 'corrplot' were used for most calculations and visualizations.

PUBLICATION 1

Metabolite profiling in plasma and tissues of ob/ob and db/db mice identifies novel markers of obesity and type 2 diabetes

Metabolomics studies have reported an increasing number of metabolites in human plasma associated with insulin resistance and type 2 diabetes. Since diabetes is often accompanied by obesity, it was the aim of the study to identify specific metabolite signatures associated with obesity and/or with type 2 diabetes. Two mouse strains, the *ob/ob* and *db/db* mice, were studied in comparison to their respective wild type strains (C57BL6 and C57BLKs). Both *ob/ob* and *db/db* mice are deficient in leptin signaling and develop severe obesity and insulin resistance. Owing to the difference in genetic background, only *db/db* mice develop β -cell failure, resulting in a relative insulin deficiency. Metabolite profiling of plasma and tissues (liver, muscle, adipose tissue) was performed using GC-MS and LC-MS and quantitative amino acid analysis via LC-MS/MS techniques.

The candidate performed the mouse studies and the tissue collection in support of technical assistance. The broad metabolite profiling was performed by Metanomics Health GmbH, Berlin. The candidate performed the quantitative LC-MS/MS amino acid profiling, data integration and statistical analysis using the statistical software environment R. This included the evaluation of statistical significances and the generation of heatmaps, principal component analysis plots, hierarchical cluster analyses and correlation networks. Gene expression analysis as well as insulin and blood glucose measurements were done by the candidate. Further contributions of the candidate included drafting, writing and revising of the manuscript, correspondence to the journal and final approval of the publication.

Giesbertz P, Padberg I, Rein D, Ecker J, Hofle AS, Spanier B, et al. Metabolite profiling in plasma and tissues of ob/ob and db/db mice identifies novel markers of obesity and type 2 diabetes. Diabetologia. 2015.

PUBLICATION 2

An LC-MS/MS method to quantify acylcarnitine species including isomeric and odd-numbered forms in plasma and tissues

Acylcarnitines are intermediates from fatty acid and amino acid oxidation, derived via the conversion of acyl-CoA by the action of carnitine transferases. They are important diagnostic markers of mitochondrial and peroxisomal oxidation disorders. Recent metabolomics studies have identified a number of acylcarnitine species associated with obesity, insulin resistance and type 2 diabetes. Quantification of acylcarnitines can be a challenge since various species occur as positional isomers and have very low concentrations. An LC-MS/MS method for the quantification of 56 acylcarnitine species was developed that allows in particular amino acid-derived positional isomers and low-abundant odd-numbered acylcarnitine species to be quantified. Identification of individual species was done via respective acylcarnitine reference substances which were synthesized via fatty acid esterification to acylcarnitines. The LC-MS/MS method was validated in plasma and liver samples from mice and showed high sensitivity, accuracy and precision. In an application to plasma and liver samples from streptozotocin-treated mice, increased concentrations of acylcarnitine species derived from branched-chain amino acid breakdown and increased levels of odd-numbered acylcarnitine species were observed. The developed method thus allows an extended quantification of acylcarnitine species from individual pathways improving the understanding of metabolite changes observed in plasma.

The candidate developed and validated the method, including chemical synthesis of acylcarnitine standards, spiking experiments and peak quantification in support of technical assistance. Furthermore, the candidate performed drafting, writing and revising of the manuscript, correspondence to the journal and final approval of the publication.

Giesbertz P, Ecker J, Haag A, Spanier B, Daniel H. An LC-MS/MS method to quantify acylcarnitine species including isomeric and odd-numbered forms in plasma and tissues. Journal of lipid research. 2015.

PUBLICATION 3

Branched-chain amino acids as biomarkers of type 2 diabetes

Elevated levels of branched-chain amino acids in plasma and urine of obese, insulin resistant, and diabetic humans have consistently been described by numerous studies. They have been proposed to serve as strong predictors of type 2 diabetes. Various mechanisms that could link branched-chain amino acid metabolism to diabetes have been proposed but the underlying mechanisms responsible for the rise in plasma BCAAs levels have not been clarified yet. A central question is whether BCAA elevations are the cause or the consequence of insulin resistance and type 2 diabetes. The review addresses recent findings on the link between BCAA, insulin action, and type 2 diabetes and discusses the role of BCAAs in altering insulin signaling in the progression of type 2 diabetes.

The candidate performed the literature search, wrote the manuscript and designed the figure.

Giesbertz P, Daniel H. Branched-chain amino acids as biomarkers in diabetes. Curr Opin Clin Nutr Metab Care. 2015.

PUBLICATION 4 (in preparation)

Signatures of acylcarnitine and acyl-CoA suggest specific regulation of mitochondrial and peroxisomal oxidation pathways in mouse models of obesity and diabetes

Obesity, insulin resistance and diabetes are characterized by changes in plasma metabolite markers of amino acid and fatty acid metabolism. Here, changes in individual metabolic routes of mitochondrial and peroxisomal amino acid and fatty acid oxidation were determined via quantification of acylcarnitine levels in plasma and tissues derived from mouse models representing different stages of obesity and diabetes. *ob/ob* and *db/db* mice as models for obesity and insulin resistance but with a different susceptibility to development of type 2 diabetes were studied as early and advanced stages of diabetes, respectively. Streptozotocin-induced insulin-deficient mice served as a model for type I diabetes or end-point stage type II diabetes with extreme hyperglycemia and ketoacidosis. A sensitive LC-MS/MS method was used to quantify up to 60 acylcarnitine species including isomers derived from individual pathways of fatty acid and amino acid oxidation. Since acylcarnitines are derived from the conversion of acyl-CoA we additionally quantified acyl-CoA species in liver and determined the correlation with the corresponding hepatic acylcarnitines. Particularly strong increases in acylcarnitine species derived from branched-chain amino acid metabolism in plasma and tissues of all mouse models were found and were most pronounced in streptozotocin-treated animals. All models also displayed increased concentrations of odd-numbered acylcarnitine species in liver while dicarboxylic acylcarnitines derived from fatty acid omega-oxidation were strongly decreased in the obese *ob/ob* and *db/db* mice. Correlations between acylcarnitine and acyl-CoA concentrations in liver were strongest for monocarboxylic metabolites, while dicarboxylic acylcarnitines like malonylcarnitine and succinylcarnitine showed no or negative correlations with their respective acyl-CoA species. In summary, alterations of metabolic profiles in specific pathways of fatty acid and amino acid oxidation were found in the mouse models and could be associated with conditions of obesity, hyperinsulinemia, and diabetes. These changes give further hints on the involvement of specific metabolic routes of mitochondrial oxidation during diabetes progression.

The candidate performed the mouse experiments, tissue collection, tissue preparation, LC-MS/MS acylcarnitine measurements and peak quantification. Acyl-CoA measurements were performed by TU Braunschweig. Statistical analysis, integration and visualization of the data were performed by the candidate using the software R. Furthermore, the candidate drafted and wrote the manuscript.

JOURNALS' PERMISSIONS TO INCLUDE ARTICLES

Article 1: Giesbertz P, Padberg I, Rein D, Ecker J, Hofle AS, Spanier B, et al. Metabolite profiling in plasma and tissues of ob/ob and db/db mice identifies novel markers of obesity and type 2 diabetes. *Diabetologia*. 2015.

-----Copyright permission of the journal: **Diabetologia**-----

Licensed content publisher	Springer
Licensed content publication	Diabetologia
Licensed content title	Metabolite profiling in plasma and tissues of ob/ob and db/db mice identifies novel markers of obesity and type 2 diabetes
Licensed content author	Pieter Giesbertz
Licensed content date	Jan 1, 2015
Volume number	58
Issue number	9
Type of Use	Thesis/Dissertation
Portion	Full text
Number of copies	10
Author of this Springer article	Yes and you are a contributor of the new work
Title of your thesis / dissertation	Plasma and tissue metabolite profiling in mouse models of obesity and diabetes
Expected completion date	Apr 2016
Estimated size(pages)	100
Total	0.00 EUR

Article 2: Giesbertz P, Ecker J, Haag A, Spanier B, Daniel H. An LC-MS/MS method to quantify acylcarnitine species including isomeric and odd-numbered forms in plasma and tissues. *Journal of lipid research*. 2015.

-----Copyright permission of the journal: **Journal of Lipid Research**-----

Copyright Permission Policy

These guidelines apply to the reuse of articles, figures, charts and photos in the **Journal of Biological Chemistry**, **Molecular & Cellular Proteomics** and the **Journal of Lipid Research**.

For authors reusing their own material:

Authors need **NOT** contact the journal to obtain rights to reuse their own material. They are automatically granted permission to do the following:

- Reuse the article in print collections of their own writing.
- Present a work orally in its entirety.
- Use an article in a thesis and/or dissertation.

- Reproduce an article for use in the author's courses. (If the author is employed by an academic institution, that institution also may reproduce the article for teaching purposes.)
- Reuse a figure, photo and/or table in future commercial and noncommercial works.
- Post a copy of the paper in PDF that you submitted via BenchPress.
 - Only authors who published their papers under the "Author's Choice" option may post the final edited PDFs created by the publisher to their own/departmental/university Web sites.
 - All authors may link to the journal site containing the final edited PDFs created by the publisher.

Please note that authors must include the following citation when using material that appeared in an ASBMB journal:

"This research was originally published in Journal Name. Author(s). Title. *Journal Name*. Year; Vol:pp-pp. © the American Society for Biochemistry and Molecular Biology."

This copyright permission is available at:

http://www.jlr.org/site/misc/Copyright_Permission.xhtml

Article 3: Giesbertz P, Daniel H. Branched-chain amino acids as biomarkers in diabetes. Curr Opin Clin Nutr Metab Care. 2015.

-Copyright permission of the journal: Current opinion in clinical nutrition & metabolic care-



RightsLink®



Title: Branched-chain amino acids as biomarkers in diabetes
Author: Pieter Giesbertz and Hannelore Daniel
Publication: Current Opinion in Clinical Nutrition and Metabolic Care
Publisher: Wolters Kluwer Health, Inc.
Date: Jan 1, 2016

Copyright © 2016, Copyright (C) 2016 Wolters Kluwer Health, Inc. All rights reserved.

LOGIN

If you're a **copyright.com** user, you can login to RightsLink using your copyright.com credentials. Already a **RightsLink** user or want to [learn more?](#)

This reuse is free of charge. No permission letter is needed from Wolters Kluwer Health, Lippincott Williams & Wilkins. We require that all authors always include a full acknowledgement. Example: AIDS: 13 November 2013 - Volume 27 - Issue 17 - p 2679-2689. Wolters Kluwer Health Lippincott Williams & Wilkins© No modifications will be permitted.



Copyright © 2015 [Copyright Clearance Center, Inc.](#) All Rights Reserved. [Privacy statement.](#) [Terms and Conditions.](#)
 Comments? We would like to hear from you. E-mail us at customer@copyright.com

DISCUSSION

Metabolomics approaches have identified over 50 plasma metabolites with changes in concentrations that are associated with different states of impaired insulin signaling and diabetes. The current PhD project was designed to improve the understanding on the origins of these metabolite markers in plasma by analyzing metabolite changes in tissues. Three different mouse models were studied which differ in their capacity to secrete insulin from β -cells and represent different stages of diabetes progression. Metabolite profiling of plasma, liver, muscle, kidney, and adipose tissue was performed by untargeted GC-MS and LC-MS analysis. Quantitative measures of amino acid and acylcarnitine levels were obtained using targeted LC-MS/MS analyses. A computational approach was used to integrate metabolomics data. Correlation measures of metabolite concentrations between plasma and tissues and within tissues were used to explore the origins of the altered metabolite concentrations observed in diabetic animals. A novel LC-MS/MS method for analyzing acylcarnitine species with improved sensitivity and coverage of > 50 entities allowed individual pathways of fatty acid and amino acid oxidation to be defined as courses for changes in plasma and tissues in insulin resistant and diabetic conditions.

Mouse models display phenotypic changes characterizing individual stages of diabetes progression in humans

Three different mouse models which differ in their capacity of β -cells to secrete insulin were studied. Table 3 and Figure S1 summarize the observed changes in body weight, plasma insulin and blood glucose levels in the three models.

Table 3. Phenotypic characteristics of the mouse models studied in this thesis.

	<i>ob/ob</i> mice	<i>db/db</i> mice	STZ-treated mice
Body weight	↑↑	↑↑	↓
Plasma insulin	↑↑	↑	↓
Blood glucose	↔	↑	↑↑

Diabetes progression

The observed phenotypic changes represent in essence what has previously been reported in literature. The *ob/ob* and *db/db* models, both impaired in leptin signaling, developed a

massive obesity. Both strains increased insulin output to compensate for an increasing insulin resistance. The difference in genetic backgrounds was described to be responsible for the different susceptibility to develop β -cell dysfunction and β -cell failure. Indeed, the *ob/ob* mice were normoglycemic suggesting a complete compensation of insulin resistance. In contrast, the *db/db* mice were hyperglycemic, indicating that the decreased insulin response of tissues was only partially compensated, in line with an only mediocre increase plasma insulin levels in these mice. In contrast to these two models of obesity-induced insulin resistance and diabetes, streptozotocin-treated animals display a strong reduction in plasma insulin levels, in accordance with a reduction in body weight and a severe hyperglycemia. With respect to the course of human diabetes development, the models may thus be categorized based on their representation of individual stages of diabetes progression as observed in humans. The *ob/ob* model represents an early prediabetic stage with obesity and insulin resistance which is completely compensated by the high insulin output. The *db/db* model is in a more advanced stage in which insulin output is increased compared to wild-type animals but not to that extent to completely compensate for insulin resistance. This state of relative insulin deficiency results in hyperglycemia. The hypoinsulinemic and hyperglycemic condition of streptozotocin-treated animals is observed in individuals with type 1 diabetes and an end-point stage of type 2 diabetes with complete pancreatic failure. This is the basis for comparison of metabolite signatures in these mouse models.

Plasma metabolite signatures in mice represent corresponding changes observed in human diabetes

Broad metabolite profiling of plasma and tissues in mice using GC-MS and LC-MS/MS identified most metabolite changes described for human diabetes. Model-specific metabolite changes were found and could be related to the specific conditions of obesity, hyperinsulinemia, hyperglycemia and insulin deficiency. Metabolite profiling data of streptozotocin-treated mice are provided in Tables S2-S5. All models displayed increases of branched-chain amino acids in plasma. These have been well described as diagnostic and prediction markers of human diabetes and metabolic disease [57, 59-61, 63, 74, 97]. The obesity and hyperinsulinemia in *ob/ob* and *db/db* mice was reflected by large increases in saturated and mono-unsaturated long-chain fatty acids (palmitic acid, palmitoleic acid, stearic acid, and oleic acid). These changes most probably result from an elevated hepatic *de novo*

lipogenesis. Whereas insulin's inhibition of hepatic gluconeogenesis via Foxo was reported to be truncated under (pre-)diabetic conditions, insulin-stimulated hepatic *de novo* lipogenesis via SREBP-1c remains intact [121]. Only in a condition of total absence of insulin signaling, as is the case for liver-specific insulin receptor knock-out (LIRKO) mice, the SREBP-1c pathway activity is decreased as well [44, 45]. A similar observation has recently been made in adipose tissue of *ob/ob* and mice fed a high-fat diet [122]. This partial insulin resistance is suggested to be responsible for the characteristic profile of hyperglycemia, hyperlipidemia, and hypercholesterolemia observed in human diabetes. Most other metabolite markers reported in human diabetes were found in mice as well, including 1,5-anhydroglucitol, 3-hydroxybutyrate, glycine, lactate, 2-hydroxybutyrate and lysophosphatidylcholine C18:2. Metabolite changes were sorted according to their appearance in either obese or diabetic models. For instance, the decrease in 1,5-anhydroglucitol, marking hyperglycemia and impaired glucose tolerance due to its competition with glucose for renal reabsorption via SGLT2, was only found in the diabetes models but not in normoglycemic *ob/ob* mice. This was similarly observed for other hyperglycemia markers like glyoxylate and fructosamine and for markers of an advanced catabolic condition like 3-hydroxybutyrate. In contrast, other metabolites, mostly lipid-related species, changed specifically only in *ob/ob* mice. Taken together, most metabolite markers known from human diabetes were also found in the mice and could here be classified as associated with obesity and/or diabetic phenotypes.

Novel metabolite markers of obesity and diabetes in plasma

Besides known markers, various new metabolites with marked changes were found in plasma, either in both *ob/ob* and *db/db* models or specifically only in *ob/ob* or *db/db* mice. Monomethyl branched fatty acids such as 16-methylheptadecanoic acid specifically increased in *db/db*, while branched-chain and odd-numbered fatty acids remained unchanged or were decreased in *ob/ob* mice. O-phosphotyrosine was also specifically increased in *db/db* mice. The origins of these changes remain unclear. O-phosphotyrosine was previously related to platelet activation [123] which is increased in hyperglycemia [124]. A number of phospholipids changed markedly in both *ob/ob* and *db/db* models for which not only the total mass but as well the individual fatty acids were determined. Changes in the phospholipid profiles of the mice were validated and confirmed in metabolite data from a study in human prediabetics [125].

A branched-chain amino acid signature observed in all three models

Despite the large differences between the models with respect to plasma insulin levels and glucose homeostasis, mice from all three models displayed increased plasma concentrations of branched-chain amino acids. The strongest increase was observed in streptozotocin-treated animals and the smallest increase was seen in *ob/ob* mice. Changes in branched-chain amino acids were already reported in the 1970s by Philip Felig in humans [60, 61] and are now considered to provide a diagnostic quality with the power to predict diabetes. However, the origin of the changes in plasma is still not known [57, 59, 74]. In recent years, the adipose tissue has been recognized as an important organ in BCAA turnover and possibly as an important determinant of plasma BCAA levels. Enzymatic activity of branched-chain aminotransferase, branched-chain keto acid dehydrogenase, as well as several downstream enzymes in BCAA-breakdown was shown to be decreased in the adipose tissue of obese and insulin resistant humans and rodent models [126-128]. In agreement with this, the strongest correlations were found between BCAA concentrations in plasma and BCAA levels in adipose tissue of the *ob/ob* and *db/db* mice. Furthermore, a reduction in transcript levels of BCKDHA was detected, coding for the α -subunit of the BCKDH complex, while transcript levels of BCAT2 remained unchanged. Next to valine, leucine, and isoleucine, the branched-chain keto acid α -ketoisocaproic acid was increased in both models. Furthermore, specifically in the *db/db* mice, 3-hydroxyisobutyric acid, a product of valine catabolism, was increased.

In contrast to the *ob/ob* and *db/db* mice, an important contribution of adipose tissue to plasma BCAA levels might not be expected in streptozotocin-treated animals, since the amount of epididymal adipose tissue in this model was reduced to almost non-detectable levels. Increased plasma BCAA levels in this model might well be the consequence of increased muscle proteolysis, due to complete lack of insulin signaling. This lack of inhibition of proteolysis by insulin increases amino acid release from muscle as demonstrated by increases of most other amino acids in the plasma of these mice and also of some amino acid breakdown products and urea. This becomes even more obvious when expressing plasma BCAA levels as ratio over the total plasma amino acid pool (Figure 4). Only for *ob/ob* and *db/db* mice an increase in this ratio is observed, which is in line with a specific increase of plasma BCAA levels in these mice, in contrast to streptozotocin-treated mice, for which proteolysis causes a general increase in circulating amino acid levels.

This suggests that the increased BCAA levels found throughout the time course of human diabetes development result from two overlapping processes with different time frames. In early stages of obesity and insulin resistance BCAA utilization in peripheral tissues, mainly in white adipose tissue, is reduced leading to higher plasma BCAA levels. As diabetes progresses and insulin signaling decreases, individuals move gradually towards a more catabolic stage with increased protein breakdown and elevated release of amino acids into plasma.

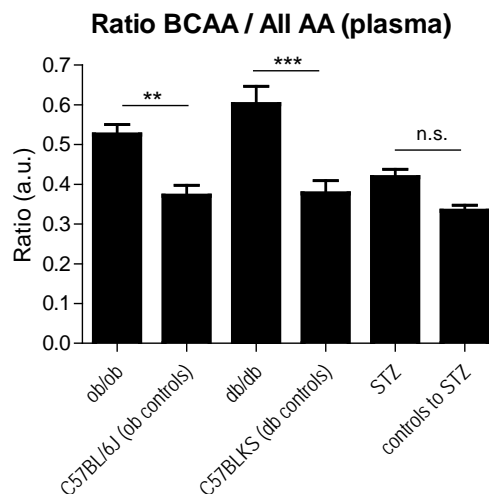


Figure 4. BCAA concentrations expressed as ratios of the total amino acid pool calculated for all six mouse groups.

White adipose tissue as important regulator of circulating BCAA levels in healthy states and insulin-resistant conditions

White adipose tissue is known as an important metabolic and endocrine organ [1, 129] which affects overall energy homeostasis via secretion of adipokines such as leptin and adiponectin. Changes in endocrine and metabolic function of white adipose tissue have been recognized as early events in obesity-induced insulin resistance and type 2 diabetes [3-5, 130]. This is thought to result from increased lipid accumulation and an increased inflammatory tone which is associated with macrophage infiltration [131, 132]. It has become obvious that the mitochondrial activity and capacity of white adipose tissue is critically involved in the pathogenesis of obesity and diabetes. Adiponectin is known as an important stimulator of mitochondrial function via the stimulation of PGC-1 α and reduced adiponectin levels in obesity are thus considered to decrease mitochondrial oxidation capacity in peripheral tissues [133]. Subcutaneous white adipose tissue from obese individuals shows a decreased activity

of mitochondrial respiratory chain complexes I–IV and a reduced overall oxidative capacity [134, 135]. In addition, a reduced mitochondrial biogenesis in subcutaneous adipose tissue of obese individuals was recently observed [136]. Furthermore, a downregulation of genes of the electron transport chain was observed in visceral fat of type 2 diabetic women [137]. These observations are supported by animal studies that show a reduction in mitochondrial activity and capacity in white adipose tissue [138, 139].

In the animal studies described here strong correlations were found between circulating BCAA concentrations and BCAA concentrations in epididymal adipose tissue in *ob/ob* and *db/db* mice. In addition, a strong reduction in the expression of BCKDHA coding for the α -subunit of the BCKDH complex was observed. This in line with previous studies in human and rodent white adipose tissue describing a reduced expression and activity of mitochondrial BCAT and total BCKD E1 α as well as an increased BCKD kinase protein expression in obesity and diabetes [126-128]. More recently, a reduced expression of BCAA catabolic genes downstream of BCKDH was reported for adipose tissue and adipocytes in conditions of increased inflammation and ER stress associated with increased expression of inflammatory cytokines such as TNF- α [140, 141]. The importance of adipose tissue in overall BCAA metabolism was demonstrated in wild-type mice in which the rate of BCAA oxidation per mg of tissue was higher in adipose tissue than in skeletal muscle [127] and recently, circulating BCAA concentrations were reported to strongly correlate with adiponectin levels [74]. In addition, adiponectin knock-out mice showed decreased BCKDH activity which could be reverted by adiponectin treatment [9]. An important link between adiponectin secretion by adipose tissue, mitochondrial oxidation capacity and circulating BCAA seems evident. Furthermore, it was recently shown that increased BCAA levels could be completely corrected by leptin treatment in type 1 diabetes [142], demonstrating a significant involvement of leptin in the metabolism of BCAA metabolism, most probably relating to hepatic BCAA metabolism. The adipose tissue thus plays both a regulatory role of BCAA metabolism in hepatic and peripheral tissues via its endocrine function and contributes to the levels of circulating BCAA via its own metabolism. Changes in adipose tissue function in obesity, insulin resistance and diabetes thus affect BCAA metabolism in multiple tissues. Next to this, quantitatively, the adipose tissue may become more important in obesity, due to the large increase in adipose tissue mass and a relative decline in skeletal muscle mass.

A novel LC-MS/MS method to quantify acylcarnitines from individual routes of amino acid and fatty acid breakdown

A drawback in almost all metabolite profiling approaches is the lack of specificity and the lack of coverage of metabolite groups from distinct pathways. This means that only in rare cases changes in metabolite concentrations can be assigned to discrete metabolic processes. As an example, the marked decrease in plasma glycine levels observed in obese and diabetic humans and in mice has been related to various metabolic processes which are well-known to change in conditions of obesity and diabetes. These include the conversion from glycine to glyoxylate by glycine transaminase [143], the utilization of glycine to restore glutathione levels during increased oxidative stress [144], the use of glycine in gluconeogenesis [76], an increased conversion of glycine and succinyl-CoA to δ -aminolevulinate [66], and the recently-reported conjugation to accumulating fatty acid oxidation intermediates resulting in the formation of acylglycines [145]. Besides this, analytical approaches are often not able to quantify distinct compounds even if they are specific intermediates of certain pathways. In diseases like diabetes, characterized by changes in multiple metabolic pathways of lipid, protein, and carbohydrate, it is important to identify metabolites specific for those pathways.

The metabolite class of acylcarnitines offers various analytical advantages (i.e. stability, specific fragmentation patterns) and addition includes a large number of metabolites that are specific to mitochondrial and peroxisomal pathways of amino acid and fatty acid oxidation (see Figure 5). With the here developed LC-MS/MS method it was aimed to quantify these specific acylcarnitine species with a focus on the quantification of short-chain isomers derived from amino acid breakdown.

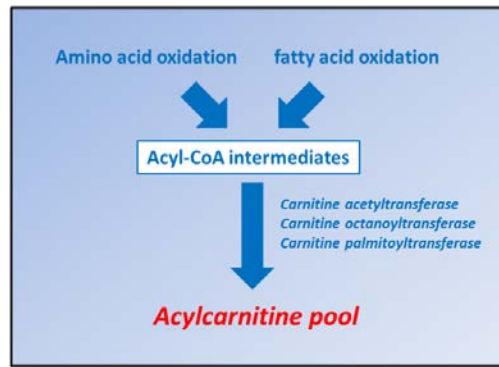


Figure 5. The acylcarnitine pool as a result of the conversion of acyl-CoA species derived from both amino acid and fatty metabolism.

The individual isomers were separated chromatographically, identified using reference compounds, and quantified individually. After validation, a total of 56 acylcarnitine species were covered by the method. This metabolite panel consists of acylcarnitines derived from amino acid breakdown, acylcarnitines with an odd-numbered carbon chain, monomethyl-branched-chain acylcarnitines, and dicarboxylic acylcarnitines. The latter metabolites are produced during microsomal and peroxisomal fatty acid breakdown processes via α - and ω -oxidation. Since these compounds appear in very low concentrations in plasma and tissues, it was essential to develop a method with high sensitivity.

Signatures of acylcarnitine and acyl-CoA give insight into altered amino acid and fatty acid oxidation in tissues

The developed LC-MS/MS acylcarnitine profiling method was applied to plasma and tissue samples from the mouse models. All mice displayed changes in concentrations of branched-chain amino acid-related acylcarnitines and these were most pronounced in plasma and tissues of streptozotocin-treated mice, but were also observed in liver and kidney samples of *ob/ob* and *db/db* mice. The corresponding CoA species increased in liver as well. Hepatic concentrations of BCAA-derived CoA and carnitine species correlated strongest. BCAA-derived acylcarnitine species were reported previously as predictors of insulin resistance and type 2 diabetes [59, 62, 67, 83].

Changes in intermediates derived from fatty acid breakdown via α -, β -, and ω -oxidation were observed as well. These changed in different directions in *ob/ob* and *db/db* mice as compared to streptozotocin-treated mice. Both *ob/ob* and *db/db* mice displayed increased plasma concentrations of stearoylcarnitine (C16:1) and oleoylcarnitine (C18:1) and increased hepatic concentrations of saturated long-chain acylcarnitines. These changes might, like the increased

fatty acid levels observed by untargeted metabolite profiling, relate to an increased SREBP-1c-dependent hepatic *de novo* lipogenesis that is associated with hyperinsulinemic states [44, 45, 121]. Furthermore, hepatic concentrations of methylmalonyl- and succinylcarnitine, derived from amino acid breakdown, were increased in *ob/ob* and *db/db* mice, whereas longer longer-chain dicarboxylic acylcarnitines such as glutarylacarnitine (C5-DC) and pimelylcarnitine (C7-DC) displayed strong decreases in liver of leptin signaling-deficient mice. This finding is in line with a proposed decreased rate in ω -oxidation, based on findings in urine of *ob/ob* mice [146] and may relate to the lack of proper leptin signaling in these mice which is known to result in a decrease of hepatic PPAR- α activity, affecting peroxisomal oxidation processes [147, 148]. In contrast, streptozotocin-treated animals displayed increased hepatic concentrations of various medium-chain dicarboxylic acylcarnitines, in line with increased excretion of adipic and suberic acid in streptozotocin-treated diabetic rats reported before [149]. However, another study in streptozotocin-treated rats could not demonstrate an increased microsomal and peroxisomal fatty acid oxidation in liver [150]. Furthermore, increased levels of odd-numbered acylcarnitine species in streptozotocin-treated animals suggest increased fatty acid α -oxidation which was previously observed in streptozotocin-treated rats [151].

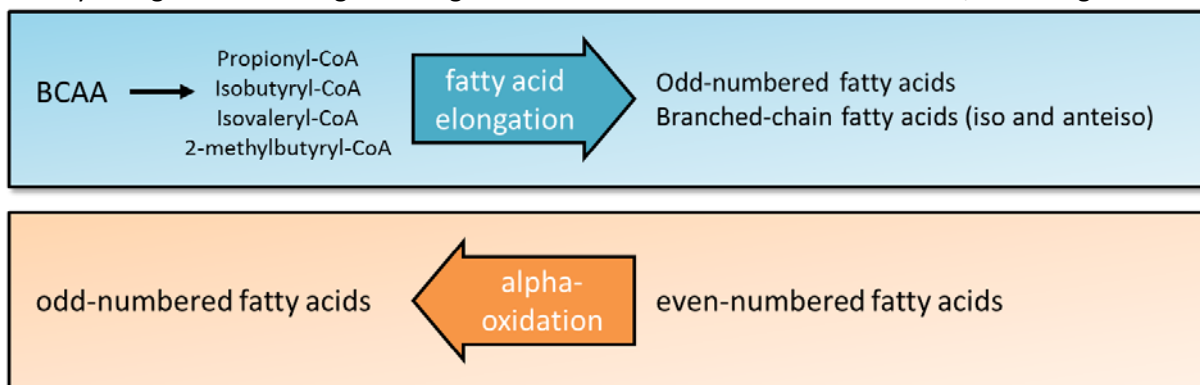
Taken together, the developed method allowed the detection of differences in the concentrations of acylcarnitine species that can be attributed to individual pathways of amino acid and fatty acid oxidation. BCAA-derived acylcarnitine species such as propionyl-, 2-methylbutyryl-, and isovalerylacarnitine increased in all models, while changes in fatty acid-derived acylcarnitine species suggest “lipid preserving” states in *ob/ob* and *db/db* models as compared to a “lipid utilizing” state in streptozotocin-treated animals.

Odd-numbered acylcarnitines as products of α -oxidation and elongation of amino acid-derived odd-numbered carbon primers

Medium- and long-chain odd-numbered molecules, both as free fatty acids and incorporated into more complex lipids, have recently been associated with insulin resistance and type 2 diabetes [58, 66, 67]. Here, increased concentrations of medium- and long-chain odd-numbered and monomethyl-branched acylcarnitines were observed in liver samples of obese and diabetic animals. Elevated odd-numbered carbon-chain (C15 and C17) levels in human plasma were associated with increased dairy intake [152], which might not be expected here,

since all mice were fed the same diet which should not contain any dairy ingredient. Endogenous production of odd-numbered carbon chains is only known to occur via peroxisomal α -oxidation of even-numbered fatty acids or alternatively via elongation of odd-numbered acyl primers (see Figure 6). Peroxisomal α -oxidation is known to be essential for the breakdown of β -methyl branched acyl-chains where β -oxidation is not possible [153]. The changes in odd-numbered acylcarnitine species in streptozotocin-treated mice are in line with a reported increase of α -oxidation in fasting state and in streptozotocin-treated diabetic rats and suggest that α -oxidation might play a particular important role in conditions of mitochondrial substrate overload in which β -oxidation is at maximal levels [151]. Although α -oxidation generates odd-numbered fatty acids, it does not provide branched carbon chains.

Figure 6. Endogenous metabolic processes generating odd-numbered carbon chains. α -oxidation is known as a peroxisomal process of fatty acid degradation in catabolic conditions shortening the fatty acid by a single carbon and generating odd-numbered carbon chains. In contrast, the elongation odd-



numbered fatty acid primers such as those derived from the breakdown of amino acids can produce both odd- and branched-chain fatty acids.

Alternatively, odd-numbered acyl chains are produced via the elongation odd-numbered and/or branched-chain acyl moieties by the fatty acid synthase complex, which was described to occur in mammalian adipose tissue [154]. Odd-numbered propionyl-CoA and branched-chain isobutyryl-, 2-methylbutyryl- and isovaleryl-CoA occur as intermediates of branched-chain amino acid breakdown and elongation of these acyl moieties by fatty acid synthase would generate longer-chain odd-numbered and iso- and anteiso-branched-chain fatty acids. Recently, adipose tissue concentrations of C15-C21 iso- and anteiso-fatty acids in obese individuals were associated with changes in BCAA breakdown and insulin sensitivity [155]. In the *ob/ob* and *db/db* mice, for which increased *de novo* lipogenesis driven by SREBP-1c was shown, increased production of odd-numbered and branched-chain fatty acids from

branched-chain amino acid-derived primers appears the most plausible explanation for the observed increases in odd-numbered acylcarnitine levels.

Impairment of the electron transport chain as a possible cause of alterations in the BCAA degradation pathways

As described above, all mouse models displayed increased concentrations of branched-chain amino acids in plasma and similarly had increased levels of BCAA-derived acylcarnitines. A decreased mitochondrial breakdown of BCAA in peripheral tissues, particularly adipose tissue, has been attributed as the major cause for elevated plasma BCAA levels [127, 128, 156]. Profiling in *ob/ob* and *db/db* mice showed that the adipose tissue metabolites showed best correlations to plasma BCAA concentrations. The observed decreased adipose tissue gene expression levels of BCKDH are in line with previous reports describing decreased protein levels and decreased activities of enzymes in the BCAA degradation pathway [127, 128, 156]. However, a modestly increased proteolysis rate caused by decreased insulin signaling could as well contribute to elevated circulating amino acid levels in later stages of diabetes progression [157]. This seems to dominate in streptozotocin-treated mice as muscle proteolysis appears especially high in this model [158].

What is of course striking is the fact that both BCAT and BCKDH expression and activities are reduced whereas BCAA-derived acyl-CoA and acylcarnitine species downstream of these enzymes are increased. This seemingly paradoxical condition in which lower enzyme activity is observed together with higher product levels requires an explanation which might be found in the electron transport chain.

Impairments in mitochondrial electron transport have been identified in type 2 diabetes and are thought to result from a reduced adiponectin signaling which results in the reduction of mitochondrial biogenesis [7] and a reduced mitochondrial capacity [8]. In addition, an increased mitochondrial supply of energy substrates can be expected, especially in insulin-deficient states like streptozotocin-treated mice, as the lack of insulin signaling results in elevated lipolysis and proteolysis rates, delivering fatty acids and amino acids to the mitochondria. Adiponectin plays a role here as well since it inhibits lipolysis and lower adiponectin levels in obesity thus further lead to increased NEFA-levels [159]. Mitochondrial

oxidation removes electrons from these substrates and transfers them to the electron carriers NADH and FADH₂. A reduced mitochondrial capacity in combination with an increased substrate supply might be major causes for a limitation of NAD⁺ and FAD leading to an increase in the ratios of NADH/NAD⁺ and FADH₂/FADH. In the streptozotocin-treated mice, this is also related to a deficiency of riboflavin [160], which might be the consequence of a higher demand of oxidized FAD as a cofactor. Riboflavin deficiency affects amino acid and fatty acid metabolism per se, since dehydrogenases in amino acid and fatty acid breakdown are dependent on FAD as cofactor [161]. In the electron transport chain, NADH and FADH₂ transfer the electrons to coenzyme Q via complex I and the electron-transferring flavoprotein (ETF). Also, the electrons generated in the oxidation of succinate to fumarate at complex II and the electrons derived from glycerol-3-phosphate via mitochondrial glycerol phosphate dehydrogenase (mGPDH) are transferred to coenzyme Q. It is thus important to realize that all electron fluxes converge at coenzyme Q (see Figure 7) and a “congestion” here would cause an upstream accumulation of substrates. It might thus not be surprising that succinylcarnitine is found as marker of glucolipotoxicity. Succinylcarnitine is derived from succinyl-CoA (and possibly also from succinate), located at the crossroads of TCA cycle, BCAA-degradation and fatty acid ω-oxidation. Furthermore, electrons from the oxidation of succinate to fumarate directly enter the electron transport chain at complex II. A reduced availability of oxidized coenzyme Q would cause a reduced electron flux from FADH₂ and a reduced oxidation rate of succinate to fumarate. The increase of all other BCAA-derived acylcarnitine and acyl-CoA species could thus simply be the result of a metabolite congestion in breakdown pathways starting at succinyl-CoA and/or succinate (see Figure 8). In the liver of streptozotocin-treated mice, this is further accompanied by an increase in N,N-dimethylglycine as a substrate of FAD-dependent dimethylglycine dehydrogenase. Also the increase of hepatic lysine and glutaric acid levels could be the result of a decreased conversion of glutaryl-CoA by FAD-dependent glutaryl-CoA dehydrogenase. Strong evidence for such a mechanism comes from a recent study in *db/db* mice that were treated with the complex I inhibitor R419 [162]. The inhibition of complex I, and thus an inhibition of electron transfer from NADH to coenzyme Q, offers an increased electron transfer from FADH₂ and complex II. Treated mice displayed an increase in the NADH/NAD⁺ ratio and a decrease in most BCAA-derived acylcarnitine species which is in

line with an increased transfer of electrons from FADH₂ to coenzyme Q and an increased oxidation of succinate to fumarate.

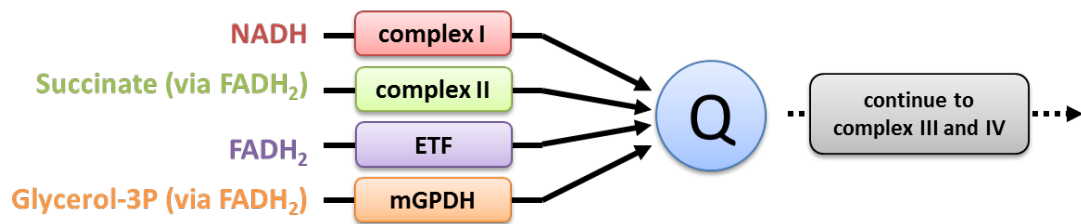


Figure 7. Electron transfer in the electron transport chain converges at coenzyme Q. ETF, electron-transferring flavoprotein; mGPDH, mitochondrial glycerol-3-phosphate dehydrogenase

The increase in BCAA intermediates found in insulin resistance and diabetic states is thus not due to an increased BCAA breakdown, but likely caused by an accumulation of downstream compounds at the electron transfer chain, with a reduction of BCKDH enzyme activity due to allosteric inhibition by its products [163]. This provides an explanation on how BCAA catabolic enzyme activity can be decreased while the intermediates in the pathway are increased. Since BCKDH is also responsible for the conversion of α -ketobutyrate to propionyl-CoA, a reduced BCKDH activity thereby also explains the observed increases in levels of α -keto-, α -hydroxy- and α -aminobutyrate. Moreover, α -hydroxybutyrate might be particularly high as the result of a general shift of the redox balance towards a reducing milieu [164]. In contrast to the increases seen for most intermediates of BCAA breakdown, a prominent decrease in plasma and most clearly in kidney was seen for 3-hydroxyisobutyrylcarnitine, which is an intermediate of valine metabolism. This decrease might be explained by the unique characteristic of valine metabolism, where, in contrast to leucine and isoleucine metabolism, a thiolase reaction converts the CoA-bound 3-hydroxyisobutyryl-CoA to 3-hydroxyisobutyrate, releasing the CoA moiety. 3-hydroxyisobutyrate can freely move over the inner mitochondrial membrane, leaving the mitochondrion and the cell to enter the plasma. From plasma, it can be taken up by liver to be used as a substrate in gluconeogenesis [165]. Increased levels of 3-hydroxyisobutyrate have been observed here in *db/db* mice and have been reported to be increased in plasma of diabetic subjects [166]. As the flux through the BCAA degradation pathway might be expected to be decreased owing to the reduced enzymatic activities of BCAA catabolic enzymes, while at the same time 3-hydroxyisobutyrate can be released, a reduced supply of 3-hydroxyisobutyrate from upstream reactions would cause 3-hydroxyisobutyrate and similarly 3-hydroxyisobutyrylcarnitine levels to decline.

In summary, it seems plausible that a reduced electron transfer in the electron transport chain causes the accumulation of succinylcarnitine and similar changes in concentrations of other BCAA-derived acylcarnitine species despite a lower flux of BCAA through the transaminase and dehydrogenase reactions. This model seems especially valid for streptozotocin-treated mice, for which most evidence is found but similar mechanisms might occur in *ob/ob* and *db/db* mice although the effects appear to be weaker.

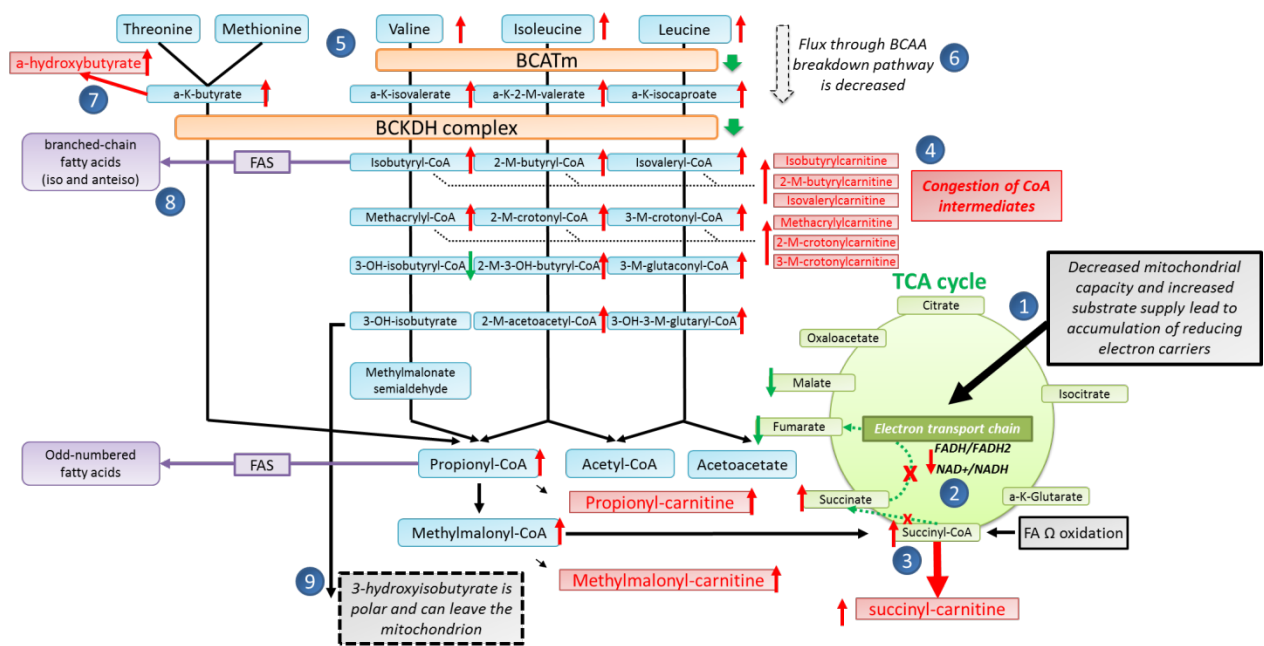


Figure 8. A model of substrate “congestion” originating at the electron transport chain.

(1) Much evidence points towards a reduced mitochondrial capacity, in combination with an increased substrate supply as the origin of a reduced electron flux through the electron transport chain. (2) A lower transfer of electrons from electron carriers causes a decrease of NAD^+/NADH and $\text{FADH}/\text{FADH}_2$ ratios and the limitation of these electron carriers in their oxidized states for reduction reactions. (3) A defective electron transfer in complex II causes a reduced conversion of succinate to fumarate and subsequently an accumulation of succinate, succinyl-CoA and succinylcarnitine. (4) The accumulation of succinyl-CoA as the end product of fatty acid ω -oxidation and BCAA oxidation could result in a congestion of intermediates resulting in the accumulation of most BCAA-derived CoA intermediates as well as the corresponding acylcarnitines. (5) Allosteric inhibition of the initial common enzymes in BCAA degradation (BCAT and BCKDH) by the accumulated products would result in a decreased activity of these enzymes. (6) A reduced activity of the rate-limiting enzymes results in a decreased pathway flux. (7) BCKDH is responsible for the conversion of α -ketobutyrate to propionyl-CoA. When BCKDH activity is reduced, α -ketobutyrate increases. A general shift of the redox balance to a reduced milieu would encourage the conversion of α -ketobutyrate to α -hydroxybutyrate. (8) Odd-numbered and branched-chain acyl-CoA species that accumulate can serve as primers in fatty acid *de novo* lipogenesis for production of long-chain odd-numbered, iso- and anteiso-monomethyl fatty acids. (9) In the breakdown pathway of valine, 3-hydroxyisobutyryl-CoA is converted to 3-hydroxyisobutyrate, releasing the CoA and allowing the 3-hydroxyisobutyrate to exit the mitochondrion. A reduced substrate supply from upstream reactions causes an intracellular decrease of 3-hydroxyisobutyryl-CoA.

CONCLUSION AND FUTURE PERSPECTIVES

The number of metabolite biomarkers that associate with human insulin resistance and diabetes is increasing steadily. However, despite all technological advances in NMR techniques and mass spectrometry, the most “robust” metabolites found in almost all studies are those known for decades. Amongst the plasma markers, branched-chain amino acids are most prominently reported. In finding the origins and causes of the increases of BCAA levels in obesity, insulin resistance and diabetes the adipose tissue was identified as the most important organ with a major contribution to BCAA turnover. With the mouse models studied here it could be made reasonable that the increase in circulating BCAA is the consequence of two main mechanisms with different impact in early and late stages of diabetes development. In early stages (i.e. in obesity), a decreased breakdown of BCAA in adipose tissue seems to be the main cause for the rise of circulating BCAA levels. In late stages, elevated proteolysis in muscle and the subsequent release of amino acids – including BCAA - into the circulation becomes the more dominant mechanism.

Next to the BCAA, most other biomarkers described in human diabetes were found in the mice studied here. Metabolite changes specific in only one or two of the models allowed a categorization of metabolite markers by associating them to obese states with normoglycemia and/or to states of hyperglycemia and increased catabolism. There is growing evidence that a decreased mitochondrial activity is the origin for changes in the plasma profiles in insulin resistance and diabetes. Data obtained here point towards an accumulation of reducing equivalents at the electron transport chain and a subsequent limitation of FAD for oxidation reactions as the plausible cause for the accumulation of various metabolites such as BCAAs, BCAA-derived intermediates, succinylcarnitine, and hydroxy-fatty acids such as α -hydroxybutyrate. It remains to be determined whether a reduced mitochondrial electron transport activity is cause or consequence of obesity and insulin resistance. A reduced mitochondrial activity, however, provides a decent explanation for a large number of the observed metabolite changes.

A number of intriguing questions remain to be answered and these relate for example to the exact origin of odd-numbered carbon chains longer than those derived from amino acids. The described mechanisms, α -oxidation and de novo synthesis/elongation from odd-numbered

primers, may well occur both and the relative contribution of both mechanisms is an interesting point of study. It also would be interesting to find the origin of dicarboxylcarnitines, especially succinylcarnitine, which has been proposed as a marker of glucolipototoxicity. In contrast to monocarboxylcarnitines, an enzyme that can convert succinyl-CoA to succinylcarnitine has not yet been found. It seems particularly valuable to employ stable-isotope labeled precursors in combination with isotopologue analysis to trace the metabolic origin of these diabetes markers.

Current metabolomics approaches are mainly untargeted and serve primarily biomarker discovery purposes. These studies produce large amounts of data in a high-throughput fashion and a big challenge is the integration of these data, requiring more intelligent computational strategies. Although the number of metabolites comprised in metabolomics approaches is growing and new biomarkers are still discovered, most studies rediscover the “knowns”. It therefore seems that the “best” diabetes biomarkers have already been found. There is currently however only one clinical test using metabolite biomarkers [81]. The benefit of metabolite markers in a clinical setting thus seems limited so far. A closer examination and association of biomarkers to more refined disease conditions could improve the identification of metabolites that can predict the transition from an insulin-resistant to a diabetic state. These biomarkers are especially valuable as they would allow defining the susceptibility of individuals to proceed from an insulin-resistant state to type 2 diabetes. It seems unlikely that BCAAs can serve this purpose as they have elevated levels throughout the course of the disease from an obese state to ketoacidosis. Furthermore, the predictive quality of many metabolite markers can be discussed, as significant correlations between metabolite concentrations and disease risk are often obtained from studies in which >2.000 individuals were used/are needed to obtain a significance level. It seems unlikely that these metabolites are suitable for the estimation of an individual’s disease risk. Moreover, many epidemiological studies in search of marker metabolites identify the same metabolites for various diseases, putting into question how selective the markers are for a certain disease and also whether analysis at the level of the individual can indeed discriminate between diseases.

Finally, comparison and interpretation of results amongst studies is only possible if a certain level of standardization is achieved and this applies to conditions of sampling, sample processing, compound identity and quantification. In this respect it is interesting to note that

most metabolomics studies do not report absolute concentrations and mainly report ratios of changes (in time course or between subcohorts) – although NMR- and MS-techniques all provide the opportunity for quantitative analysis. If marker metabolites are going to be used in diagnostics or clinical settings, quantitative analysis is a “must”.

SUMMARY

Obesity and diabetes are associated with significant changes in metabolite concentrations in plasma and urine. The present thesis describes the analysis of three mouse strains that display phenotypic changes resembling human diabetes progression. With the use of untargeted and targeted metabolomics measurements, metabolite signatures in plasma and tissues were obtained and used to explore the origins and mechanisms of plasma changes found in humans. Most metabolite markers of human plasma from obese, insulin resistant or diabetic individuals were also found in the mouse models. In addition, concentration changes in a number of novel metabolites were observed and by a comparison of metabolite profiles of obese and diabetic mice, these changes could be assigned to either an early or a more advanced stage of diabetes progression. Metabolite profiling of individual tissues and correlation analysis between plasma and tissue concentrations suggests an important role for white adipose tissue in determining plasma levels of branched-chain amino acids and derivatives which is in line with studies in humans and animal models. The development of a new LC-MS/MS method for the quantification of over 50 acylcarnitines and the application to the profiling of plasma and tissue samples revealed model-specific alterations of mitochondrial pathways of amino acid and fatty acid utilization which were related to conditions of obesity and hyperglycemia. Increases in acylcarnitines derived from branched-chain amino acid metabolism were found in all three mouse models and changes in intermediates of fatty acid oxidation pathways observed were as well. Based on metabolite signatures observed in mice and data from literature, a model was proposed by which the limited availability of oxidized cofactors for mitochondrial electron transport in the respiratory chain could lead to the accumulation of intermediates of mitochondrial oxidation pathways, especially in peripheral tissues.

In summary, with the findings from this thesis, known and new metabolite markers could be assigned to specific stages of diabetes progression, to specific tissues, and to specific pathways. This broadens our understanding on why or why not plasma metabolite changes known from human studies occur in insulin resistance and diabetes, going from pure correlations of metabolite levels and clinical conditions to a more mechanistic understanding.

ZUSAMMENFASSUNG

Bei Adipositas und Diabetes treten signifikante Veränderungen der Konzentrationen bestimmter Stoffwechselprodukte in Plasma und Urin auf. In der vorliegenden Dissertation wurden drei verschiedene Mausmodelle untersucht, die den phänotypischen Veränderungen verschiedener Stadien des Humandiabetes entsprechen. Mittels *untargeted* und *targeted metabolomics* wurden Metabolitmuster in Plasma- und in diversen Geweben identifiziert, mit dem Ziel, die zugrundeliegenden Mechanismen der Veränderungen beim Humandiabetes zu erforschen. Von den Stoffwechselprodukten, die als Plasmamarker in fettleibigen, Insulin-resistenten und diabetischen Individuen beschrieben wurden, wurde ein Großteil in den hier untersuchten Mausmodellen wiedergefunden. Zusätzlich wurde eine Reihe bislang noch nicht beschriebener Plasma-Biomarker identifiziert, die einem frühen oder einem fortgeschrittenen Diabetesstadium zugeschrieben werden konnten. Die Metabolitprofilierung einzelner Gewebe und die Korrelationsanalyse von Plasma- und Gewebkonzentrationen weisen darauf hin, dass das weiße Fettgewebe einen wichtigen Beitrag zu den Konzentrationen von verzweigt-kettigen Aminosäuren und deren Derivaten im Plasma liefert. Dieser Befund stimmt mit Erkenntnissen aus anderen Tiermodellen und aus Humanstudien überein. Im Rahmen der Dissertation wurde eine neue LC-MS/MS-Methode zur Quantifizierung von über 50 Acylcarnitinen entwickelt. Die Anwendung dieser Methode bei der Metabolitprofilierung in Plasma- und Gewebeproben zeigte Veränderungen in mitochondrialen Stoffwechselwegen von Aminosäuren und Fettsäuren auf, die mithilfe der Mausmodelle mit Fettleibigkeit und Hyperglykämie assoziiert werden konnten. In allen drei Mausmodellen wurden erhöhte Spiegel von Acylcarnitinen gefunden, welche aus verzweigt-kettigen Aminosäuren entstehen. Basierend auf den Metabolit-Signaturen in den untersuchten Mausmodellen und unter Einbeziehung von Literaturbefunden wurde ein Modell entwickelt. Dieses beschreibt, dass die begrenzte Verfügbarkeit von oxidierten Kofaktoren für den Elektronentransport in der mitochondrialen Atmungskette zu einer Anreicherung von Stoffwechsel-Intermediaten oxidativer Stoffwechselwege im Mitochondrium führt – insbesondere in peripheren Geweben.

Zusammenfassend kann festgehalten werden, dass mithilfe der Befunde aus der vorliegenden Dissertation sowohl bekannte als auch neue Biomarker identifiziert wurden, die spezifischen Stadien in der Entwicklung von Diabetes, verschiedenen Geweben und spezifischen Stoffwechselwegen zugeschrieben werden können. Die simple Korrelation von Metabolit-Veränderungen und klinischen Konditionen wird so auf eine mechanistische Ebene gehoben

und vertieft unser Verständnis der molekularen Ursachen für das Auftreten von Biomarkern in Insulinresistenz und Diabetes. Dies ist von hoher Bedeutung für die Diagnose und Therapie von Stoffwechselerkrankungen wie Diabetes oder Fettleibigkeit.

SAMENVATTING

Obesitas en diabetes worden geassocieerd met significante veranderingen in de concentraties van stoffwisselproducten in plasma en urine. Deze thesis beschrijft de studie van drie muismodellen die qua fenotypische veranderingen individuele stadia in de ontwikkeling van diabetes weerspiegelen. Met behulp van *untargeted* en *targeted metabolomics* werden metaboliëtoprofielen van plasma en weefsels bepaald. Deze werden gebruikt om de oorsprong van de veranderingen van metaboliëtoprofielen in plasma van diabetespatiënten te onderzoeken evenals de bijbehorende mechanismen. De meeste metaboliëtoprofielen die bekend zijn in plasma bij patiënten met obesitas, insulineresistentie en diabetes werden ook aangetoond in de onderzochte muismodellen. Daarnaast werden veranderingen in de concentraties van een aantal nieuwe metaboliëtoprofielen gevonden en de vergelijking van metaboliëtoprofielen in muizen met obesitas met die in muizen met diabetes maakte het mogelijk om de veranderingen toe te wijzen aan een vroeg of laat stadium in de ontwikkeling van diabetes. De metaboliëtoprofiëling van individuele weefsels en de correlatie-analyse tussen de concentraties in het plasma en in de weefsels duidde op een grote invloed van wit vetweefsel bij de bepaling van de plasmaconcentraties van vertakte aminozuren en metaboliëtoprofielen afgeleid van deze aminozuren. Dit resultaat is in overeenstemming met andere studies in mensen en diermodellen. De ontwikkeling van een nieuwe LC-MS/MS methode voor de kwantificering van meer dan 50 acylcarnitines en de toepassing van deze methode bij de metaboliëtoprofiëling van plasma- en weefselmonsters van de muismodellen bracht veranderingen in mitochondriële stoffwisselwegen van aminozuren en vetzuren aan het licht die specifiek waren voor een of meerdere modellen. Deze veranderingen werden vervolgens gerelateerd aan obesitas en hyperglycemie. Verhoogde concentraties van acylcarnitines afkomstig uit de afbraak van vertakte aminozuren werden geconstateerd in alle drie modellen. Baserend op de metaboliëtoprofielen in de muizen en literatuurstudies werd een model ontwikkeld waarbij een beperkte beschikbaarheid van geoxideerde cofactoren, nodig voor mitochondriële electronentransport in de elektronentransportketen, leidt tot de accumulatie van intermediaten bij mitochondriële oxidatie.

Samenvattend kunnen met behulp van de resultaten van deze thesis bekende en nieuwe metaboliëtoprofiëlen worden toegewezen aan specifieke stadia van diabetes, specifieke weefsels en specifieke stoffwisselwegen. De interpretatie van concentratieveranderingen in

weefsels draagt bij aan het mechanistisch begrijpen van de oorsprong van metabolietmarkers in plasma.

ABBREVIATIONS

BCAA	Branched-chain amino acids
BCAT	Branched-chain amino acid transferase
BCKDH	Branched-chain keto acid dehydrogenase
EDTA	Ethylene diamine tetraacetic acid
ELISA	Enzyme-linked immunosorbent assay
FAD	Flavin adenine dinucleotide
FOXO	Forkhead box protein O
GC-MS	Gas-chromatography coupled to mass spectrometry
HbA1c	Hemoglobin A1c
IFG	Impaired fasting glucose
IGT	Impaired glucose tolerance
IL-6	Interleukin 6
IR	Insulin resistance
LC-MS/MS	Liquid-chromatography coupled to tandem mass spectrometry
LIRKO	Liver insulin receptor knock-out
MCP-1	Monocyte chemoattractant protein
MRM	Multiple reaction monitoring
NAD ⁺	Nicotinamide adenine dinucleotide (oxidized form)
NADH	Nicotinamide adenine dinucleotide (reduced form)
PCR	Polymerase chain reaction
PI-3K	Phosphatidylinositol-3-kinase
PPAR	Peroxisome-proliferator activator receptor
RBP-4	Retinol binding protein 4
SREBP-1c	Sterol-regulator binding protein 1c
STZ	Streptozotocin
T1DM	Type 1 diabetes mellitus
T2DM	Type 2 diabetes mellitus
TNF- α	Tumor necrosis factor α
ZDF	Zucker diabetic fatty

BIBLIOGRAPHY

1. Vazquez-Vela ME, Torres N, Tovar AR. White adipose tissue as endocrine organ and its role in obesity. *Archives of medical research*. 2008;39(8):715-28.
2. Arita Y, Kihara S, Ouchi N, et al. Paradoxical decrease of an adipose-specific protein, adiponectin, in obesity. *Biochemical and biophysical research communications*. 1999;257(1):79-83.
3. Hoffstedt J, Arvidsson E, Sjolín E, et al. Adipose tissue adiponectin production and adiponectin serum concentration in human obesity and insulin resistance. *The Journal of clinical endocrinology and metabolism*. 2004;89(3):1391-6.
4. Kern PA, Di Gregorio GB, Lu T, et al. Adiponectin expression from human adipose tissue: relation to obesity, insulin resistance, and tumor necrosis factor- α expression. *Diabetes*. 2003;52(7):1779-85.
5. Lonnqvist F, Nordfors L, Jansson M, et al. Leptin secretion from adipose tissue in women. Relationship to plasma levels and gene expression. *The Journal of clinical investigation*. 1997;99(10):2398-404.
6. Haluzik M, Parizkova J, Haluzik MM. Adiponectin and its role in the obesity-induced insulin resistance and related complications. *Physiol Res*. 2004;53(2):123-9.
7. Qiao L, Kinney B, Yoo HS, et al. Adiponectin increases skeletal muscle mitochondrial biogenesis by suppressing mitogen-activated protein kinase phosphatase-1. *Diabetes*. 2012;61(6):1463-70.
8. Civitarese AE, Ukropcova B, Carling S, et al. Role of adiponectin in human skeletal muscle bioenergetics. *Cell metabolism*. 2006;4(1):75-87.
9. Lian K, Du C, Liu Y, et al. Impaired adiponectin signaling contributes to disturbed catabolism of branched-chain amino acids in diabetic mice. *Diabetes*. 2015;64(1):49-59.
10. Liu Y, Turdi S, Park T, et al. Adiponectin corrects high-fat diet-induced disturbances in muscle metabolomic profile and whole-body glucose homeostasis. *Diabetes*. 2013;62(3):743-52.
11. Buechler C, Wanninger J, Neumeier M. Adiponectin, a key adipokine in obesity related liver diseases. *World J Gastroenterol*. 2011;17(23):2801-11.
12. Myers MG, Jr., Munzberg H, Leininger GM, Leshan RL. The geometry of leptin action in the brain: more complicated than a simple ARC. *Cell metabolism*. 2009;9(2):117-23.
13. Margetic S, Gazzola C, Pegg GG, Hill RA. Leptin: a review of its peripheral actions and interactions. *International journal of obesity and related metabolic disorders : journal of the International Association for the Study of Obesity*. 2002;26(11):1407-33.
14. Banks WA, DiPalma CR, Farrell CL. Impaired transport of leptin across the blood-brain barrier in obesity. *Peptides*. 1999;20(11):1341-5.
15. El-Haschimi K, Pierroz DD, Hileman SM, et al. Two defects contribute to hypothalamic leptin resistance in mice with diet-induced obesity. *The Journal of clinical investigation*. 2000;105(12):1827-32.
16. Lahlou N, Clement K, Carel JC, et al. Soluble leptin receptor in serum of subjects with complete resistance to leptin: relation to fat mass. *Diabetes*. 2000;49(8):1347-52.
17. Lee JH, Reed DR, Price RA. Leptin resistance is associated with extreme obesity and aggregates in families. *International journal of obesity and related metabolic disorders : journal of the International Association for the Study of Obesity*. 2001;25(10):1471-3.
18. Hosoi T, Sasaki M, Miyahara T, et al. Endoplasmic reticulum stress induces leptin resistance. *Mol Pharmacol*. 2008;74(6):1610-9.
19. Muller G, Ertl J, Gerl M, Preibisch G. Leptin impairs metabolic actions of insulin in isolated rat adipocytes. *The Journal of biological chemistry*. 1997;272(16):10585-93.
20. Hotamisligil GS, Murray DL, Choy LN, Spiegelman BM. Tumor necrosis factor α inhibits signaling from the insulin receptor. *Proceedings of the National Academy of Sciences of the United States of America*. 1994;91(11):4854-8.
21. Plomgaard P, Bouzakri K, Krogh-Madsen R, et al. Tumor necrosis factor- α induces skeletal muscle insulin resistance in healthy human subjects via inhibition of Akt substrate 160 phosphorylation. *Diabetes*. 2005;54(10):2939-45.

22. Cheung AT, Wang J, Ree D, et al. Tumor necrosis factor- α induces hepatic insulin resistance in obese Zucker (fa/fa) rats via interaction of leukocyte antigen-related tyrosine phosphatase with focal adhesion kinase. *Diabetes*. 2000;49(5):810-9.
23. Yang Q, Graham TE, Mody N, et al. Serum retinol binding protein 4 contributes to insulin resistance in obesity and type 2 diabetes. *Nature*. 2005;436(7049):356-62.
24. Norseen J, Hosooka T, Hammarstedt A, et al. Retinol-binding protein 4 inhibits insulin signaling in adipocytes by inducing proinflammatory cytokines in macrophages through a c-Jun N-terminal kinase- and toll-like receptor 4-dependent and retinol-independent mechanism. *Molecular and cellular biology*. 2012;32(10):2010-9.
25. Klover PJ, Zimmers TA, Koniaris LG, Mooney RA. Chronic exposure to interleukin-6 causes hepatic insulin resistance in mice. *Diabetes*. 2003;52(11):2784-9.
26. Glund S, Deshmukh A, Long YC, et al. Interleukin-6 directly increases glucose metabolism in resting human skeletal muscle. *Diabetes*. 2007;56(6):1630-7.
27. Harman-Boehm I, Bluher M, Redel H, et al. Macrophage infiltration into omental versus subcutaneous fat across different populations: effect of regional adiposity and the comorbidities of obesity. *The Journal of clinical endocrinology and metabolism*. 2007;92(6):2240-7.
28. Kanda H, Tateya S, Tamori Y, et al. MCP-1 contributes to macrophage infiltration into adipose tissue, insulin resistance, and hepatic steatosis in obesity. *The Journal of clinical investigation*. 2006;116(6):1494-505.
29. Patsouris D, Cao JJ, Vial G, et al. Insulin resistance is associated with MCP1-mediated macrophage accumulation in skeletal muscle in mice and humans. *PloS one*. 2014;9(10):e110653.
30. Zhang HH, Halbleib M, Ahmad F, et al. Tumor necrosis factor- α stimulates lipolysis in differentiated human adipocytes through activation of extracellular signal-related kinase and elevation of intracellular cAMP. *Diabetes*. 2002;51(10):2929-35.
31. Brechtel K, Dahl DB, Machann J, et al. Fast elevation of the intramyocellular lipid content in the presence of circulating free fatty acids and hyperinsulinemia: a dynamic ¹H-MRS study. *Magn Reson Med*. 2001;45(2):179-83.
32. Pan DA, Lillioja S, Kriketos AD, et al. Skeletal muscle triglyceride levels are inversely related to insulin action. *Diabetes*. 1997;46(6):983-8.
33. Virkamaki A, Korshennikova E, Seppala-Lindroos A, et al. Intramyocellular lipid is associated with resistance to in vivo insulin actions on glucose uptake, antilipolysis, and early insulin signaling pathways in human skeletal muscle. *Diabetes*. 2001;50(10):2337-43.
34. Jacob RJ, Dziura J, Blumberg M, et al. Effects of recurrent hypoglycemia on brainstem function in diabetic BB rats: protective adaptation during acute hypoglycemia. *Diabetes*. 1999;48(1):141-5.
35. Kahn SE, Prigeon RL, McCulloch DK, et al. Quantification of the relationship between insulin sensitivity and beta-cell function in human subjects. Evidence for a hyperbolic function. *Diabetes*. 1993;42(11):1663-72.
36. Jetton TL, Lausier J, LaRock K, et al. Mechanisms of compensatory beta-cell growth in insulin-resistant rats: roles of Akt kinase. *Diabetes*. 2005;54(8):2294-304.
37. Steil GM, Trivedi N, Jonas JC, et al. Adaptation of beta-cell mass to substrate oversupply: enhanced function with normal gene expression. *American journal of physiology Endocrinology and metabolism*. 2001;280(5):E788-96.
38. Cerf ME, Chapman CS, Louw J. High-fat programming of hyperglycemia, hyperinsulinemia, insulin resistance, hyperleptinemia, and altered islet architecture in 3-month-old wistar rats. *ISRN Endocrinol*. 2012;2012:627270.
39. Haffner SM, Stern MP, Watanabe RM, Bergman RN. Relationship of insulin clearance and secretion to insulin sensitivity in non-diabetic Mexican Americans. *Eur J Clin Invest*. 1992;22(3):147-53.
40. Lorenzo C, Hanley AJ, Wagenknecht LE, et al. Relationship of insulin sensitivity, insulin secretion, and adiposity with insulin clearance in a multiethnic population: the insulin Resistance Atherosclerosis study. *Diabetes care*. 2013;36(1):101-3.

41. Kotronen A, Juurinen L, Tiikkainen M, et al. Increased liver fat, impaired insulin clearance, and hepatic and adipose tissue insulin resistance in type 2 diabetes. *Gastroenterology*. 2008;135(1):122-30.
42. Rabinowitz D, Zierler KL. Forearm metabolism in obesity and its response to intra-arterial insulin. Characterization of insulin resistance and evidence for adaptive hyperinsulinism. *The Journal of clinical investigation*. 1962;41:2173-81.
43. Shanik MH, Xu Y, Skrha J, et al. Insulin resistance and hyperinsulinemia: is hyperinsulinemia the cart or the horse? *Diabetes care*. 2008;31 Suppl 2:S262-8.
44. Biddinger SB, Hernandez-Ono A, Rask-Madsen C, et al. Hepatic insulin resistance is sufficient to produce dyslipidemia and susceptibility to atherosclerosis. *Cell metabolism*. 2008;7(2):125-34.
45. Brown MS, Goldstein JL. Selective versus total insulin resistance: a pathogenic paradox. *Cell metabolism*. 2008;7(2):95-6.
46. Semple RK, Sleight A, Murgatroyd PR, et al. Postreceptor insulin resistance contributes to human dyslipidemia and hepatic steatosis. *The Journal of clinical investigation*. 2009;119(2):315-22.
47. Raghow R, Yellaturu C, Deng X, et al. SREBPs: the crossroads of physiological and pathological lipid homeostasis. *Trends Endocrinol Metab*. 2008;19(2):65-73.
48. Abdul-Ghani MA, Tripathy D, DeFronzo RA. Contributions of beta-cell dysfunction and insulin resistance to the pathogenesis of impaired glucose tolerance and impaired fasting glucose. *Diabetes care*. 2006;29(5):1130-9.
49. Guillausseau PJ, Meas T, Virally M, et al. Abnormalities in insulin secretion in type 2 diabetes mellitus. *Diabetes Metab*. 2008;34 Suppl 2:S43-8.
50. Mulder H, Ling C. Mitochondrial dysfunction in pancreatic beta-cells in Type 2 diabetes. *Molecular and cellular endocrinology*. 2009;297(1-2):34-40.
51. Quan W, Jo EK, Lee MS. Role of pancreatic beta-cell death and inflammation in diabetes. *Diabetes Obes Metab*. 2013;15 Suppl 3:141-51.
52. Poitout V, Amyot J, Semache M, et al. Glucolipototoxicity of the pancreatic beta cell. *Biochimica et biophysica acta*. 2010;1801(3):289-98.
53. Donath MY, Boni-Schnetzler M, Ellingsgaard H, Ehses JA. Islet inflammation impairs the pancreatic beta-cell in type 2 diabetes. *Physiology (Bethesda)*. 2009;24:325-31.
54. Kajimoto Y, Kaneto H. Role of oxidative stress in pancreatic beta-cell dysfunction. *Annals of the New York Academy of Sciences*. 2004;1011:168-76.
55. Matthews DR, Hosker JP, Rudenski AS, et al. Homeostasis model assessment: insulin resistance and beta-cell function from fasting plasma glucose and insulin concentrations in man. *Diabetologia*. 1985;28(7):412-9.
56. Nolan JJ, Faerch K. Estimating insulin sensitivity and beta cell function: perspectives from the modern pandemics of obesity and type 2 diabetes. *Diabetologia*. 2012;55(11):2863-7.
57. Wang TJ, Larson MG, Vasan RS, et al. Metabolite profiles and the risk of developing diabetes. *Nature medicine*. 2011;17(4):448-53.
58. Menni C, Fauman E, Erte I, et al. Biomarkers for type 2 diabetes and impaired fasting glucose using a nontargeted metabolomics approach. *Diabetes*. 2013;62(12):4270-6.
59. Newgard CB, An J, Bain JR, et al. A branched-chain amino acid-related metabolic signature that differentiates obese and lean humans and contributes to insulin resistance. *Cell metabolism*. 2009;9(4):311-26.
60. Felig P, Marliss E, Cahill GF, Jr. Plasma amino acid levels and insulin secretion in obesity. *The New England journal of medicine*. 1969;281(15):811-6.
61. Felig P, Marliss E, Ohman JL, Cahill CF, Jr. Plasma amino acid levels in diabetic ketoacidosis. *Diabetes*. 1970;19(10):727-8.
62. Perng W, Gillman MW, Fleisch AF, et al. Metabolomic profiles and childhood obesity. *Obesity*. 2014;22(12):2570-8.
63. Wurtz P, Soinen P, Kangas AJ, et al. Branched-chain and aromatic amino acids are predictors of insulin resistance in young adults. *Diabetes care*. 2013;36(3):648-55.

64. Vannini P, Marchesini G, Forlani G, et al. Branched-chain amino acids and alanine as indices of the metabolic control in type 1 (insulin-dependent) and type 2 (non-insulin-dependent) diabetic patients. *Diabetologia*. 1982;22(3):217-9.
65. Lanza IR, Zhang S, Ward LE, et al. Quantitative metabolomics by H-NMR and LC-MS/MS confirms altered metabolic pathways in diabetes. *PLoS one*. 2010;5(5):e10538.
66. Wang-Sattler R, Yu Z, Herder C, et al. Novel biomarkers for pre-diabetes identified by metabolomics. *Molecular systems biology*. 2012;8:615.
67. Gall WE, Beebe K, Lawton KA, et al. alpha-hydroxybutyrate is an early biomarker of insulin resistance and glucose intolerance in a nondiabetic population. *PLoS one*. 2010;5(5):e10883.
68. Wang TJ, Ngo D, Psychogios N, et al. 2-Amino adipic acid is a biomarker for diabetes risk. *The Journal of clinical investigation*. 2013;123(10):4309-17.
69. Padberg I, Peter E, Gonzalez-Maldonado S, et al. A new metabolomic signature in type-2 diabetes mellitus and its pathophysiology. *PLoS one*. 2014;9(1):e85082.
70. Juraschek SP, Steffes MW, Selvin E. Associations of alternative markers of glycemia with hemoglobin A(1c) and fasting glucose. *Clinical chemistry*. 2012;58(12):1648-55.
71. Xu F, Tavintharan S, Sum CF, et al. Metabolic signature shift in type 2 diabetes mellitus revealed by mass spectrometry-based metabolomics. *The Journal of clinical endocrinology and metabolism*. 2013;98(6):E1060-5.
72. Ferrannini E, Natali A, Camastra S, et al. Early metabolic markers of the development of dysglycemia and type 2 diabetes and their physiological significance. *Diabetes*. 2013;62(5):1730-7.
73. Yamakado M, Nagao K, Imaizumi A, et al. Plasma Free Amino Acid Profiles Predict Four-Year Risk of Developing Diabetes, Metabolic Syndrome, Dyslipidemia, and Hypertension in Japanese Population. *Scientific reports*. 2015;5:11918.
74. Nakamura H, Jinzu H, Nagao K, et al. Plasma amino acid profiles are associated with insulin, C-peptide and adiponectin levels in type 2 diabetic patients. *Nutrition & diabetes*. 2014;4:e133.
75. Stancakova A, Civelek M, Saleem NK, et al. Hyperglycemia and a common variant of GCKR are associated with the levels of eight amino acids in 9,369 Finnish men. *Diabetes*. 2012;61(7):1895-902.
76. Floegel A, Stefan N, Yu Z, et al. Identification of serum metabolites associated with risk of type 2 diabetes using a targeted metabolomic approach. *Diabetes*. 2013;62(2):639-48.
77. Suhre K, Meisinger C, Doring A, et al. Metabolic footprint of diabetes: a multiplatform metabolomics study in an epidemiological setting. *PLoS one*. 2010;5(11):e13953.
78. Barber MN, Risis S, Yang C, et al. Plasma lysophosphatidylcholine levels are reduced in obesity and type 2 diabetes. *PLoS one*. 2012;7(7):e41456.
79. Crawford SO, Hoogeveen RC, Brancati FL, et al. Association of blood lactate with type 2 diabetes: the Atherosclerosis Risk in Communities Carotid MRI Study. *Int J Epidemiol*. 2010;39(6):1647-55.
80. Wurtz P, Makinen VP, Soininen P, et al. Metabolic signatures of insulin resistance in 7,098 young adults. *Diabetes*. 2012;61(6):1372-80.
81. Cobb J, Gall W, Adam KP, et al. A novel fasting blood test for insulin resistance and prediabetes. *J Diabetes Sci Technol*. 2013;7(1):100-10.
82. Tripathy D, Cobb JE, Gall W, et al. A novel insulin resistance index to monitor changes in insulin sensitivity and glucose tolerance: the ACT NOW study. *The Journal of clinical endocrinology and metabolism*. 2015;100(5):1855-62.
83. Bene J, Marton M, Mohas M, et al. Similarities in serum acylcarnitine patterns in type 1 and type 2 diabetes mellitus and in metabolic syndrome. *Ann Nutr Metab*. 2013;62(1):80-5.
84. Kotronen A, Velagapudi VR, Yetukuri L, et al. Serum saturated fatty acids containing triacylglycerols are better markers of insulin resistance than total serum triacylglycerol concentrations. *Diabetologia*. 2009;52(4):684-90.
85. Hodge AM, English DR, O'Dea K, et al. Plasma phospholipid and dietary fatty acids as predictors of type 2 diabetes: interpreting the role of linoleic acid. *The American journal of clinical nutrition*. 2007;86(1):189-97.

86. Ramsay RR, Gandour RD, van der Leij FR. Molecular enzymology of carnitine transfer and transport. *Biochimica et biophysica acta*. 2001;1546(1):21-43.
87. Ventura FV, Ijlst L, Ruiter J, et al. Carnitine palmitoyltransferase II specificity towards beta-oxidation intermediates--evidence for a reverse carnitine cycle in mitochondria. *European journal of biochemistry / FEBS*. 1998;253(3):614-8.
88. Violante S, Ijlst L, Ruiter J, et al. Substrate specificity of human carnitine acetyltransferase: Implications for fatty acid and branched-chain amino acid metabolism. *Biochimica et biophysica acta*. 2013;1832(6):773-9.
89. Jogl G, Hsiao YS, Tong L. Structure and function of carnitine acyltransferases. *Annals of the New York Academy of Sciences*. 2004;1033:17-29.
90. Hokland BM, Bremer J. Formation and excretion of branched-chain acylcarnitines and branched-chain hydroxy acids in the perfused rat kidney. *Biochimica et biophysica acta*. 1988;961(1):30-7.
91. Roe CR, Millington DS, Maltby DA. Identification of 3-methylglutaryl-carnitine. A new diagnostic metabolite of 3-hydroxy-3-methylglutaryl-coenzyme A lyase deficiency. *The Journal of clinical investigation*. 1986;77(4):1391-4.
92. Fiamoncini J, Lima TM, Hirabara SM, et al. Medium-chain dicarboxylic acylcarnitines as markers of n-3 PUFA-induced peroxisomal oxidation of fatty acids. *Mol Nutr Food Res*. 2015;59(8):1573-83.
93. Violante S, Ijlst L, Te Brinke H, et al. Carnitine palmitoyltransferase 2 and carnitine/acylcarnitine translocase are involved in the mitochondrial synthesis and export of acylcarnitines. *FASEB J*. 2013;27(5):2039-44.
94. Wu X, Huang W, Prasad PD, et al. Functional characteristics and tissue distribution pattern of organic cation transporter 2 (OCTN2), an organic cation/carnitine transporter. *The Journal of pharmacology and experimental therapeutics*. 1999;290(3):1482-92.
95. Shekhawat PS, Matern D, Strauss AW. Fetal fatty acid oxidation disorders, their effect on maternal health and neonatal outcome: impact of expanded newborn screening on their diagnosis and management. *Pediatric research*. 2005;57(5 Pt 2):78R-86R.
96. Mihalik SJ, Goodpaster BH, Kelley DE, et al. Increased levels of plasma acylcarnitines in obesity and type 2 diabetes and identification of a marker of glucolipotoxicity. *Obesity*. 2010;18(9):1695-700.
97. Batch BC, Shah SH, Newgard CB, et al. Branched chain amino acids are novel biomarkers for discrimination of metabolic wellness. *Metabolism: clinical and experimental*. 2013;62(7):961-9.
98. Adams SH, Hoppel CL, Lok KH, et al. Plasma acylcarnitine profiles suggest incomplete long-chain fatty acid beta-oxidation and altered tricarboxylic acid cycle activity in type 2 diabetic African-American women. *The Journal of nutrition*. 2009;139(6):1073-81.
99. Abdenur JE, Chamoles NA, Guinle AE, et al. Diagnosis of isovaleric acidaemia by tandem mass spectrometry: false positive result due to pivaloylcarnitine in a newborn screening programme. *Journal of inherited metabolic disease*. 1998;21(6):624-30.
100. Maeda Y, Ito T, Suzuki A, et al. Simultaneous quantification of acylcarnitine isomers containing dicarboxylic acylcarnitines in human serum and urine by high-performance liquid chromatography/electrospray ionization tandem mass spectrometry. *Rapid communications in mass spectrometry : RCM*. 2007;21(5):799-806.
101. Gucciardi A, Pirillo P, Di Gangi IM, et al. A rapid UPLC-MS/MS method for simultaneous separation of 48 acylcarnitines in dried blood spots and plasma useful as a second-tier test for expanded newborn screening. *Analytical and bioanalytical chemistry*. 2012;404(3):741-51.
102. Minkler PE, Stoll MS, Ingalls ST, et al. Quantification of carnitine and acylcarnitines in biological matrices by HPLC electrospray ionization-mass spectrometry. *Clinical chemistry*. 2008;54(9):1451-62.
103. Peng M, Fang X, Huang Y, et al. Separation and identification of underivatized plasma acylcarnitine isomers using liquid chromatography-tandem mass spectrometry for the differential diagnosis of organic acidemias and fatty acid oxidation defects. *Journal of chromatography A*. 2013;1319:97-106.
104. Srinivasan K, Ramarao P. Animal models in type 2 diabetes research: an overview. *Indian J Med Res*. 2007;125(3):451-72.

105. Tanaka T, Mochida T, Maki Y, et al. Interactive network analysis of the plasma amino acids profile in a mouse model of hyperglycemia. *Springerplus*. 2013;2(1):287.
106. Ingalls AM, Dickie MM, Snell GD. Obese, a new mutation in the house mouse. *J Hered*. 1950;41(12):317-8.
107. Hummel KP, Dickie MM, Coleman DL. Diabetes, a new mutation in the mouse. *Science*. 1966;153(3740):1127-8.
108. Zhang Y, Proenca R, Maffei M, et al. Positional cloning of the mouse obese gene and its human homologue. *Nature*. 1994;372(6505):425-32.
109. Chen H, Charlat O, Tartaglia LA, et al. Evidence that the diabetes gene encodes the leptin receptor: identification of a mutation in the leptin receptor gene in db/db mice. *Cell*. 1996;84(3):491-5.
110. Lee GH, Proenca R, Montez JM, et al. Abnormal splicing of the leptin receptor in diabetic mice. *Nature*. 1996;379(6566):632-5.
111. Naggert JK, Mu JL, Frankel W, et al. Genomic analysis of the C57BL/Ks mouse strain. *Mamm Genome*. 1995;6(2):131-3.
112. Coleman DL. Obese and diabetes: two mutant genes causing diabetes-obesity syndromes in mice. *Diabetologia*. 1978;14(3):141-8.
113. Hummel KP, Coleman DL, Lane PW. The influence of genetic background on expression of mutations at the diabetes locus in the mouse. I. C57BL-KsJ and C57BL-6J strains. *Biochem Genet*. 1972;7(1):1-13.
114. Coleman DL, Hummel KP. The influence of genetic background on the expression of the obese (Ob) gene in the mouse. *Diabetologia*. 1973;9(4):287-93.
115. Lenzen S. The mechanisms of alloxan- and streptozotocin-induced diabetes. *Diabetologia*. 2008;51(2):216-26.
116. R Development-and-Core-Team. A Language and Environment for Statistical Computing 2008 [cited 2015 8 april]. Available from: <http://www.R-project.org/>.
117. Hiller K, Hangebrauk J, Jager C, et al. MetaboliteDetector: comprehensive analysis tool for targeted and nontargeted GC/MS based metabolome analysis. *Anal Chem*. 2009;81(9):3429-39.
118. Kopka J, Schauer N, Krueger S, et al. GMD@CSB.DB: the Golm Metabolome Database. *Bioinformatics*. 2005;21(8):1635-8.
119. Ziegler HJ, Bruckner P, Binon F. O-acylation of dl-carnitine chloride. *The Journal of organic chemistry*. 1967;32(12):3989-91.
120. Ecker J, Liebisch G, Englmaier M, et al. Induction of fatty acid synthesis is a key requirement for phagocytic differentiation of human monocytes. *Proceedings of the National Academy of Sciences of the United States of America*. 2010;107(17):7817-22.
121. Shimomura I, Matsuda M, Hammer RE, et al. Decreased IRS-2 and increased SREBP-1c lead to mixed insulin resistance and sensitivity in livers of lipodystrophic and ob/ob mice. *Molecular cell*. 2000;6(1):77-86.
122. Tan SX, Fisher-Wellman KH, Fazakerley DJ, et al. Selective insulin resistance in adipocytes. *The Journal of biological chemistry*. 2015;290(18):11337-48.
123. Munoz GE, Marshall SH. Free L-phosphotyrosine activates human platelets: molecular evidence for a new signal transducer. *Cellular and molecular biology*. 1992;38(5-6):629-33.
124. Yamagishi SI, Edelstein D, Du XL, Brownlee M. Hyperglycemia potentiates collagen-induced platelet activation through mitochondrial superoxide overproduction. *Diabetes*. 2001;50(6):1491-4.
125. Hoefle AS, Bangert AM, Stamford A, et al. Metabolic responses of healthy or prediabetic adults to bovine whey protein and sodium caseinate do not differ. *The Journal of nutrition*. 2015;145(3):467-75.
126. She P, Van Horn C, Reid T, et al. Obesity-related elevations in plasma leucine are associated with alterations in enzymes involved in branched-chain amino acid metabolism. *American journal of physiology Endocrinology and metabolism*. 2007;293(6):E1552-63.

127. Herman MA, She P, Peroni OD, et al. Adipose tissue branched chain amino acid (BCAA) metabolism modulates circulating BCAA levels. *The Journal of biological chemistry*. 2010;285(15):11348-56.
128. Lackey DE, Lynch CJ, Olson KC, et al. Regulation of adipose branched-chain amino acid catabolism enzyme expression and cross-adipose amino acid flux in human obesity. *American journal of physiology Endocrinology and metabolism*. 2013;304(11):E1175-87.
129. Trayhurn P, Beattie JH. Physiological role of adipose tissue: white adipose tissue as an endocrine and secretory organ. *The Proceedings of the Nutrition Society*. 2001;60(3):329-39.
130. Cummins TD, Holden CR, Sansbury BE, et al. Metabolic remodeling of white adipose tissue in obesity. *American journal of physiology Endocrinology and metabolism*. 2014;307(3):E262-77.
131. Surmi BK, Hasty AH. Macrophage infiltration into adipose tissue: initiation, propagation and remodeling. *Future Lipidol*. 2008;3(5):545-56.
132. Zeyda M, Gollinger K, Kriehuber E, et al. Newly identified adipose tissue macrophage populations in obesity with distinct chemokine and chemokine receptor expression. *Int J Obes (Lond)*. 2010;34(12):1684-94.
133. Iwabu M, Yamauchi T, Okada-Iwabu M, et al. Adiponectin and AdipoR1 regulate PGC-1alpha and mitochondria by Ca(2+) and AMPK/SIRT1. *Nature*. 2010;464(7293):1313-9.
134. Chattopadhyay M, Guhathakurta I, Behera P, et al. Mitochondrial bioenergetics is not impaired in nonobese subjects with type 2 diabetes mellitus. *Metabolism: clinical and experimental*. 2011;60(12):1702-10.
135. Yin X, Lanza IR, Swain JM, et al. Adipocyte mitochondrial function is reduced in human obesity independent of fat cell size. *The Journal of clinical endocrinology and metabolism*. 2014;99(2):E209-16.
136. Heinonen S, Buzkova J, Muniandy M, et al. Impaired Mitochondrial Biogenesis in Adipose Tissue in Acquired Obesity. *Diabetes*. 2015;64(9):3135-45.
137. Dahlman I, Forsgren M, Sjogren A, et al. Downregulation of electron transport chain genes in visceral adipose tissue in type 2 diabetes independent of obesity and possibly involving tumor necrosis factor-alpha. *Diabetes*. 2006;55(6):1792-9.
138. Rong JX, Qiu Y, Hansen MK, et al. Adipose mitochondrial biogenesis is suppressed in db/db and high-fat diet-fed mice and improved by rosiglitazone. *Diabetes*. 2007;56(7):1751-60.
139. Choo HJ, Kim JH, Kwon OB, et al. Mitochondria are impaired in the adipocytes of type 2 diabetic mice. *Diabetologia*. 2006;49(4):784-91.
140. Serralde-Zuniga AE, Guevara-Cruz M, Tovar AR, et al. Omental adipose tissue gene expression, gene variants, branched-chain amino acids, and their relationship with metabolic syndrome and insulin resistance in humans. *Genes Nutr*. 2014;9(6):431.
141. Burrill JS, Long EK, Reilly B, et al. Inflammation and ER stress regulate branched-chain amino acid uptake and metabolism in adipocytes. *Molecular endocrinology*. 2015;29(3):411-20.
142. Wang MY, Chen L, Clark GO, et al. Leptin therapy in insulin-deficient type I diabetes. *Proceedings of the National Academy of Sciences of the United States of America*. 2010;107(11):4813-9.
143. Nikiforova VJ, Giesbertz P, Wiemer J, et al. Glyoxylate, a New Marker Metabolite of Type 2 Diabetes. *Journal of Diabetes Research*. 2014;2014:9.
144. Sekhar RV, McKay SV, Patel SG, et al. Glutathione synthesis is diminished in patients with uncontrolled diabetes and restored by dietary supplementation with cysteine and glycine. *Diabetes care*. 2011;34(1):162-7.
145. Koves TR, Ussher JR, Noland RC, et al. Mitochondrial overload and incomplete fatty acid oxidation contribute to skeletal muscle insulin resistance. *Cell metabolism*. 2008;7(1):45-56.
146. Lai RK, Goldman P. Urinary organic acid profiles in obese (ob/ob) mice: indications for the impaired omega-oxidation of fatty acids. *Metabolism: clinical and experimental*. 1992;41(1):97-105.
147. Huang J, Jia Y, Fu T, et al. Sustained activation of PPARalpha by endogenous ligands increases hepatic fatty acid oxidation and prevents obesity in ob/ob mice. *FASEB J*. 2012;26(2):628-38.

148. Liang CP, Tall AR. Transcriptional profiling reveals global defects in energy metabolism, lipoprotein, and bile acid synthesis and transport with reversal by leptin treatment in ob/ob mouse liver. *The Journal of biological chemistry*. 2001;276(52):49066-76.
149. Yoshioka K, Shimojo N, Nakanishi T, et al. Measurements of urinary adipic acid and suberic acid using high-performance liquid chromatography. *J Chromatogr B Biomed Appl*. 1994;655(2):189-93.
150. Orellana M, Valdes E, Del Villar E. Microsomal and peroxisomal fatty acid oxidation in streptozotocin diabetic rat liver. *Gen Pharmacol*. 1997;28(3):361-4.
151. Takahashi T, Takahashi H, Takeda H, Shichiri M. Alpha-oxidation of fatty acids in fasted or diabetic rats. *Diabetes research and clinical practice*. 1992;16(2):103-8.
152. Smedman AE, Gustafsson IB, Berglund LG, Vessby BO. Pentadecanoic acid in serum as a marker for intake of milk fat: relations between intake of milk fat and metabolic risk factors. *The American journal of clinical nutrition*. 1999;69(1):22-9.
153. Casteels M, Foulon V, Mannaerts GP, Van Veldhoven PP. Alpha-oxidation of 3-methyl-substituted fatty acids and its thiamine dependence. *European Journal of Biochemistry*. 2003;270(8):1619-27.
154. Horning MG, Martin DB, Karmen A, Vagelos PR. Fatty acid synthesis in adipose tissue. II. Enzymatic synthesis of branched chain and odd-numbered fatty acids. *The Journal of biological chemistry*. 1961;236:669-72.
155. Su X, Magkos F, Zhou D, et al. Adipose tissue monomethyl branched-chain fatty acids and insulin sensitivity: Effects of obesity and weight loss. *Obesity*. 2015;23(2):329-34.
156. She P, Olson KC, Kadota Y, et al. Leucine and protein metabolism in obese Zucker rats. *PloS one*. 2013;8(3):e59443.
157. Marchesini G, Forlani G, Zoli M, et al. Muscle protein breakdown in uncontrolled diabetes as assessed by urinary 3-methylhistidine excretion. *Diabetologia*. 1982;23(5):456-8.
158. Smith OL, Wong CY, Gelfand RA. Skeletal muscle proteolysis in rats with acute streptozocin-induced diabetes. *Diabetes*. 1989;38(9):1117-22.
159. Qiao L, Kinney B, Schaack J, Shao J. Adiponectin inhibits lipolysis in mouse adipocytes. *Diabetes*. 2011;60(5):1519-27.
160. Reddi AS. Riboflavin nutritional status and flavoprotein enzymes in streptozotocin-diabetic rats. *Biochimica et biophysica acta*. 1986;882(1):71-6.
161. Gregersen N. Riboflavin-responsive defects of beta-oxidation. *Journal of inherited metabolic disease*. 1985;8 Suppl 1:65-9.
162. Jenkins Y, Sun TQ, Markovtsov V, et al. AMPK activation through mitochondrial regulation results in increased substrate oxidation and improved metabolic parameters in models of diabetes. *PloS one*. 2013;8(12):e81870.
163. Boyer B, Odessey R. Kinetic characterization of branched chain ketoacid dehydrogenase. *Archives of biochemistry and biophysics*. 1991;285(1):1-7.
164. Adams SH. Emerging perspectives on essential amino acid metabolism in obesity and the insulin-resistant state. *Adv Nutr*. 2011;2(6):445-56.
165. Letto J, Brosnan ME, Brosnan JT. Valine metabolism. Gluconeogenesis from 3-hydroxyisobutyrate. *The Biochemical journal*. 1986;240(3):909-12.
166. Avogaro A, Bier DM. Contribution of 3-hydroxyisobutyrate to the measurement of 3-hydroxybutyrate in human plasma: comparison of enzymatic and gas-liquid chromatography-mass spectrometry assays in normal and in diabetic subjects. *Journal of lipid research*. 1989;30(11):1811-7.

APPENDIX

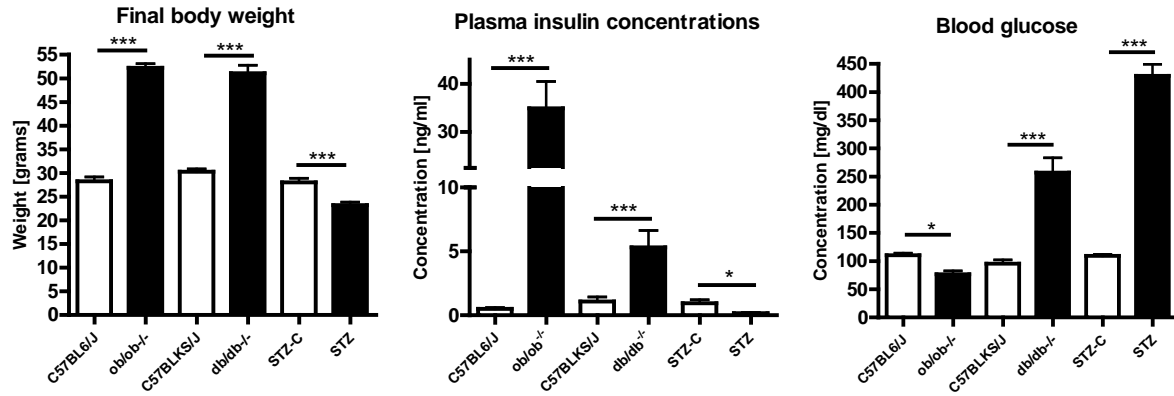


Figure S1. Body weight, plasma insulin, and blood glucose of the mice in this thesis.

Black: knock-out or treated mouse group; White: corresponding control group

Table S1. Forward and reverse primers applied to specify transcripts for quantitative real-time PCR analysis.

Gene	Forward primer	Reverse primer
Actb	5`-CTCTGGCTCCTAGCACCATGAAGA-3`	5`-GTAAAACGCAGCTCAGTAACAGTCCG-3`
Bcat2	5`-CCATATTCAAGGCTGCAGACC-3`	5`-CAGCCTTGTATTCCACTCCAC-3`
Bckdha	5`-ACCGGGAGGCAGGTGTGCT-3`	5`-GTGGAGAGGAAATGGTGACGA-3`
Bckdk	5`-CACCTTCTGAAAAGTGCCG-3`	5`-TGCACTATGGTAGGGTTGCAAC-3`
Gapdh	5`-CGCCTGGAGAAACCTGCC-3`	5`-AGCCGTATTCATTGTCATACCAGG-3`
Hprt1	5`-GTCGTGATTAGCGATGATGAACC-3`	5`-GTCTTTCAGTCCTGTCCATAATCAG-3`
Ppm1k	5`-TCTGCAGATGCAAGCCTCC-3`	5`-CCCGGCTGTCTCCAACAC-3`
18S	5`-CTTAGAGGGACAAGTGCG-3`	5`-ACGCTGAGCCAGTCAGTGTA-3`

Table S2. Plasma concentration ratios of selected metabolites for streptozotocin-treated mice compared to healthy controls derived from GC-MS measurements.

Plasma Metabolites	RATIO	TTEST
Glucose 1	3.49429278	p<0.001
Lysine	1.77188908	p<0.001
Threitol	1.96378917	p<0.001
Octadecanoic acid (C18:0)	1.38303905	p<0.005
Glycine	1.55667276	p<0.005
Leucine 1	5.27760484	p<0.005
Isoleucine 1	2.84605907	p<0.005
2-hydroxy-Pyridine	0.72376125	p<0.005
2-oxo-Isovaleric acid	0.67465239	p<0.01
Threonine	2.53398258	p<0.01
Proline	5.05687573	p<0.01
Gulose	2.66641764	p<0.01
Valine 1	2.49356599	p<0.01
Maltose	4.73068915	p<0.01
Serine	2.08454358	p<0.01
Valine 2	2.37526904	p<0.01
9,12-(Z,Z)-Octadecadienoic acid (C18:2)	1.81924244	p<0.01
Leucine 2	4.83579037	p<0.01

Ornithine	2.55846854	p<0.01
Mannose	1.48819995	p<0.05
Phosphoric acid	1.39190746	p<0.05
Glycolic acid	0.77920467	p<0.05
Indole-3-lactic acid	5.07672785	p<0.05
Isoleucine 2	4.15266498	p<0.05
Ornithine	1.96412638	p<0.05
Phenylalanine	1.82240346	p<0.05
Alanine	1.76470461	p<0.05
Glutamic acid	1.71311961	p<0.05
Tyrosine	1.6264549	p<0.05
Rhamnose	0.55619233	p<0.05
Asparagine	2.33492902	p<0.05
Cholesterol	1.13026818	p<0.05
Glucose 2	1.86062701	p<0.05
2-amino-Butanoic acid	3.84733292	p<0.05
2-hydroxy-Butanoic acid	3.82614735	p<0.05
Hexadecenoic acid (C16:1)	0.57278673	p<0.05
Laminaribiose	34.9896982	p<0.05
Pyroglutamic acid	1.6623371	p<0.05
Methionine	1.33008727	p<0.05
Lactic acid	0.76687392	p<0.05

Table S3. Hepatic concentration ratios of selected metabolites for streptozotocin-treated mice compared to healthy controls derived from GC-MS measurements.

Liver Metabolites	RATIO	TTEST
Melibiose	7.48754813	p<0.001
Glucuronic acid	3.46759881	p<0.001
2-hydroxy-Butanoic acid	2.1895122	p<0.001
N-acetyl-Glutamic acid	2.25713698	p<0.005
Lysine 1	1.46975735	p<0.005
Glutamic acid 1	2.14768778	p<0.005
N,N-dimethyl-Glycine	2.1347144	p<0.005
Urea	1.76318385	p<0.005
Glutaric acid	8.05304212	p<0.01
Lysine 2	1.7256265	p<0.01
Valine 1	2.3385964	p<0.01
Glucuronic acid	1.39484748	p<0.01
beta-Alanine	1.72388263	p<0.01
Taurine	2.40003415	p<0.05
Mannose	0.75000973	p<0.05
Glutamic acid 2	3.48278695	p<0.05
Valine 2	2.04056329	p<0.05
Glycine	0.69232756	p<0.05
Malic acid	1.48202498	p<0.05
Fumaric_acid	1.72900194	p<0.05
Proline	1.69152016	p<0.05

Threonine	1.37821651	p<0.05
Galactose	1.18899698	p<0.05
Ethanolaminophosphate	1.1915536	p<0.05
Arabinose	0.532056	p<0.05
Saccharic acid	1.33469168	p<0.05
Proline	4.77740845	p<0.05
Glycerol-3-phosphate	0.83658289	p<0.05
Phenylalanine	1.30638706	p<0.05
3-hydroxy-Butanoic acid	2.20527777	p<0.05

Table S4. Muscle concentration ratios of selected metabolites for streptozotocin-treated mice compared to healthy controls derived from GC-MS measurements.

Muscle Metabolites	RATIO	TTEST
Dehydroascorbic acid	0.40310108	p<0.001
myo-Inositol	1.95652028	p<0.001
Glycine	0.61775896	p<0.001
Pyrophosphate	2.18258826	p<0.001
Succinic acid	2.56622189	p<0.001
2-oxo-Butanoic acid	6.79201382	p<0.001
alpha-Tocopherol	2.35104106	p<0.001
Cholesterol	1.31675789	p<0.001
Glucose	4.81746623	p<0.001
Methionine	2.16225034	p<0.001
Isoleucine	3.1803998	p<0.001
Urea	1.97612958	p<0.005
Phenylalanine	2.13344309	p<0.005
Lysine	0.3894316	p<0.005
Pyruvic acid	0.44864239	p<0.005
Fumaric acid	0.4890176	p<0.01
Malic acid	0.66876946	p<0.01
9,12-(Z,Z)-Octadecadienoic acid (C18:2)	1.82181131	p<0.05
Tyrosine	1.52896281	p<0.05
Sulfuric acid	3.4939587	p<0.05
Octadecanoic acid (C18:0)	1.375115	p<0.05
9-(Z)-Octadecenoic acid (C18:1)	1.39289616	p<0.05
alpha,alpha'-D-Trehalose	0.21356543	p<0.05
Oxalic acid	0.84089083	p<0.05
Glucose-6-phosphate	1.19553799	p<0.05

Table S5. Renal concentration ratios of selected metabolites for streptozotocin-treated mice compared to healthy controls derived from GC-MS measurements.

Kidney Metabolites	RATIO	TTEST
Glycerophosphoglycerolamine	0.40494582	p<0.001
Tagatose/Psicose	3.63503993	p<0.001
9,12-(Z,Z)-Octadecadienoic acid	0.52761117	p<0.001
Glucose-6-phosphate	0.42221914	p<0.001
Cysteinesulfinic acid	0.34109038	p<0.001

Octadecanoic acid (C18:0)	0.59075854	p<0.001
Mannose/Idose/Allose/Galactose	1.98670977	p<0.001
Ethanolamine	0.48380245	p<0.001
Glucose	9.99051055	p<0.001
Fructose	4.96457652	p<0.001
Nicotinamide	0.31249227	p<0.001
sugar alcohol	0.07928176	p<0.001
Malic acid	1.6671449	p<0.001
trisaccharide phosphate	0.47297069	p<0.001
Cysteine	0.65609334	p<0.001
Glycine	0.65879082	p<0.001
Adenosine-5-monophosphate	0.75183567	p<0.005
Hypotaurine	1.80009153	p<0.005
Sulfuric acid	0.63117939	p<0.005
Inosine	0.6754349	p<0.005
Hypoxanthine	0.51527472	p<0.005
D-Glucopyranose	4.76616489	p<0.005
Adenosine-3'-monophosphoric acid	0.52252883	p<0.005
Proline	2.37311472	p<0.005
Valine	1.61339301	p<0.005
Lactic acid	1.34708396	p<0.01
Hexadecanoic acid (C16:1)	0.57378202	p<0.01
9-(Z)-Octadecenoic acid (C18:1)	0.82594121	p<0.01
Pyrophosphate	2.23691063	p<0.05
Citric acid	1.55973384	p<0.05
Ethanolaminophosphate	0.82556311	p<0.05
Glycerol	0.71949348	p<0.05
Uridine	0.72564702	p<0.05
Alanine	1.2741664	p<0.05
Threonine	2.25774514	p<0.05
Mannose-6-phosphate	1.54426988	p<0.05
Pyroglutamic acid	0.76224966	p<0.05
Fumaric acid	1.64016753	p<0.05
9-(Z)-Hexadecenoic acid (C16:1)	0.365071	p<0.05
Isoleucine	2.58896781	p<0.05
Cholesterol	0.86840501	p<0.05
Glycerol-3-phosphate	0.69430307	p<0.05

ACKNOWLEDGEMENT/DANKSAGUNG/DANKWOORD

Von Butterbrez'n und Großmüttern...

Diese Arbeit wäre nicht zustande gekommen ohne die Hilfe vieler Personen die mich während des gesamten Prozesses unterstützt haben. Insgesamt habe ich mich während meiner Doktorandenzeit sehr wohl gefühlt am Lehrstuhl und dafür möchte ich allen danken. Einige Personen haben dazu allerdings besonders beigetragen.

An erster Stelle möchte ich Frau Professor Daniel danken für ihr Vertrauen und für die Möglichkeit die Doktorarbeit am Lehrstuhl durchzuführen. Danke auch, dass Sie mir bei Publikationen geholfen haben und dass ich die Möglichkeit hatte an vielen Konferenzen teilzunehmen und mit Wissenschaftlern in Kontakt zu kommen.

Ein Dank geht auch an Dr. Britta Spanier, du warst stets für meine Fragen offen und hast immer bei meinen Überlegungen mitgedacht.

Dr. Tamara Zietek, von Dir habe ich sehr viel gelernt. Du hast mir immer geholfen, bei Korrekturen von Manuskripten, oder beim Schreiben in bestem Deutsch. Ich schätze deine Professionalität und fachliche Kompetenz sehr, ebenso wie deine Hilfsbereitschaft, deine diplomatische Art und dein Mitdenken bei Ideen. Auch neben Paperschreiben und Vortragmachen wurde es nie langweilig und so verwandelte sich das Büro auch manchmal in eine Münztauschbörse oder eine Teefabrik.

Dr. Jarlei Fiamoncini, auch du hast besonders viel zu meinem Wohlbefinden am Lehrstuhl beigetragen. Ich danke dir für die vielen Diskussionen (mit oder ohne Butterbrez'n) die zu vielen neuen Ideen geführt haben. Es bleiben schöne Erinnerungen an unseren gemeinsamen Konferenzbesuchen wie die in Boston, Barcelona und Stockholm. Deinen Umgang mit Menschen bewundere ich sehr ebenso wie die tägliche Kreativität und Spaß.

Dr. Kai Hartwig, das Themenspektrum unserer Gespräche reichte von V320 und Strich-8 bis zum Arbeitsvortschritt und zur Zukunftsplanung. Das alles hat beigetragen zu meinem Antrieb und Arbeitslust. Die spontanen Going-to-the-Grandma's-events wurden zu wichtigen Ereignissen der Woche die es möglich machten, auch kreative Abendsessions durchzuführen.

Alexander Haag, seit ich dich kenne weiß ich was exakte Arbeit ist. Ohne dich hätte ich meine massenspektrometrische Analysenwünsche niemals realisieren können. Mit dir aber, kam es zu „Breaking Bad“-artigen Synthesen, die ich nie für möglich gehalten hätte. Ich schätze dein unglaubliches Wissen sehr und es war immer ein Genuss ins Massenspektrometrie-Labor zu arbeiten, wo die Maschinen glänzten und die Arbeit von Jazz-Musik begleitet wurde.

Dr. Kurt Gedrich, meine Ideen und Vorstellungen über Berechnungen und Darstellungen in R fanden immer ein Ohr bei dir und dank deiner Hilfe konnte ich auch feinste Änderungen in Abbildungen verwirklichen.

Barbara Gelhaus, wenn es dich nicht gegeben hätte, weiß ich allerdings nicht ob unser MS-Labor nicht in Chaos versunken wäre. Ich danke dir vielmals für die gute Zusammenarbeit im Labor. Das war immer eine Freude.

Ronny Scheundel, deine zuverlässige Hilfe hat die Mausexperimenten zum Erfolg gebracht. Vielen Dank dafür.

Dr. Anja Höfle, auch du warst immer offen für wissenschaftliche Diskussionen. Diese gab es dann auch reichlich. Unsere ‚Journal Clubs‘ haben mein Wissen über Humanphysiologie und Stoffwechselwege vervielfacht.

Dr. Diogo Vasconcelos, I remember very well those evenings at which we were discussing about mTOR, glutamine, glycine, BCAAs,... And it got later and later. Hotel Lerner saved us from not getting home with empty stomachs...

Danken möchte ich auch Helene Prunkl, Irmgard Sperrer, Dr. Christine Schulze, Rosalie Morisset, Dr. Ramona Pais-Menezes, Brigitte Asafu, Cordula Hertwig und Herr Ademar Stamford. Ihr habt alle zum Erfolg beigetragen.

Pappa, mamma en Anna, auch es hie misschien verder geine get van begrip, goan ich toch in ut Limburgs euver. Ut is un fijne gedachte om te weite dat ich familie hub die mich bie dit soort processe altied zulle steune. Doaveur bin ich uch erg dankbaar. Bedank dat ger der zit en dat ich altied op uch kin røkene!

PUBLICATION LIST

- [1] **Giesbertz P**, Daniel H. Branched-chain amino acids as biomarkers of type 2 diabetes. *Curr Opin Clin Nutr Metab Care*. 2016 Jan;19(1):48-54. doi: 10.1097/MCO.0000000000000235.
- [2] **Giesbertz P**, Ecker J, Haag A, Spanier B, Daniel H. An LC-MS/MS method to quantify acylcarnitines including isomeric and odd-numbered forms in plasma and tissues. *J Lipid Res*. 2015 Oct;56(10):2029-39. doi: 10.1194/jlr.D061721. Epub 2015 Aug 3.
- [3] **Giesbertz P**, Padberg I, Rein D, Ecker J, Höfle AS, Spanier B, Daniel H. Metabolite profiling in plasma and tissues of ob/ob and db/db mice identifies novel markers of obesity and type 2 diabetes. *Diabetologia*. 2015 Sep;58(9):2133-43
- [4] Nikiforova V, **Giesbertz P**, Wiemer J, Bethan B, Looser R, Liebenberg V, Ruiz Noppinger P, Daniel H, Rein D. Glyoxylate, a new marker metabolite of type 2 diabetes. *Journal of Diabetes Research*. 2014:685204. Epub 2014 Nov 27. doi: 10.1155/2014/685204
- [5] Geillinger KE, Kuhlmann K, Eisenacher M, **Giesbertz P**, Meyer HE, Daniel H, Spanier B. Intestinal amino acid availability via PEPT-1 affects TORC1/2 signaling and the unfolded protein response. *J Proteome Res*. 2014 Aug 1;13(8):3685-92. doi: 10.1021/pr5002669
- [6] Sailer M, Dahlhoff C, **Giesbertz P**, Eidens MK, de Wit N, Rubio-Aliaga I, Boekschoten MV, Müller M, Daniel H. Increased plasma citrulline in mice marks diet-induced obesity and may predict the development of the metabolic syndrome. *PLoS One*. 2013 May 14;8(5):e63950. doi: 10.1371/journal.pone.0063950
- [7] Martin FP, Spanier B, Collino S, Montoliu I, Kolmeder C, **Giesbertz P**, Affolter M, Kussmann M, Daniel H, Kochhar S, Rezzi S. Metabotyping of *Caenorhabditis elegans* and their culture media revealed unique metabolic phenotypes associated to amino acid deficiency and insulin-like signaling. *J Proteome Res*. 2011 Mar 4;10(3):990-1003. doi: 10.1021/pr100703a
- [8] Jennen DG, Gaj S, **Giesbertz PJ**, van Delft JH, Evelo CT, Kleinjans JC. Biotransformation pathway maps in WikiPathways enable direct visualization of drug metabolism related expression changes. *Drug Discov Today*. 2010 Oct;15(19-20):851-8. doi: 10.1016/j.drudis.2010.08.002

CURRICULUM VITAE

Name Pieter Johan Giesbertz
Date of birth 24th of October 1986
Place of birth Voerendaal, Netherlands

Education

2010-Present PhD student, Lehrstuhl für Ernährungsphysiologie
Technische Universität München, Freising-Weihenstephan, Germany

2008-2010 M.Sc. in Molecular Life Sciences
Maastricht University, Netherlands

2005-2008 B.Sc. in Molecular Life Sciences
Maastricht University, Netherlands

07/2005 Graduation Lyceum Sintermeertencollege, Heerlen Netherlands

Eidesstattliche Erklärung

Ich erkläre an Eides statt, dass ich die bei der promotionsführenden Einrichtung bzw. Fakultät

Wissenschaftszentrum Weihenstephan

der TUM zur Promotionsprüfung vorgelegte Arbeit mit dem Titel:

Plasma and tissue metabolite profiling in mouse models of obesity and diabetes

in Ernährungsphysiologie

(Lehrstuhl bzw. Fachgebiet oder Klinik)

unter der Anleitung und Betreuung durch

Professor Dr. Hannelore Daniel

ohne sonstige Hilfe erstellt und bei der Abfassung nur die gemäß § 6 Abs. 6 und 7 Satz 2 angegebenen Hilfsmittel benutzt habe.

Ich habe keine Organisation eingeschaltet, die gegen Entgelt Betreuerinnen und Betreuer für die Anfertigung von Dissertationen sucht, oder die mir obliegenden Pflichten hinsichtlich der Prüfungsleistungen für mich ganz oder teilweise erledigt.

Ich habe die Dissertation in dieser oder ähnlicher Form in keinem anderen Prüfungsverfahren als Prüfungsleistung vorgelegt.

Die vollständige Dissertation wurde in veröffentlicht. Die promotionsführende Einrichtung hat der Vorveröffentlichung zugestimmt.

Ich habe den angestrebten Doktorgrad **noch nicht** erworben und bin **nicht** in einem früheren Promotionsverfahren für den angestrebten Doktorgrad endgültig gescheitert.

Ich habe bereits am bei der Fakultät für der Hochschule unter Vorlage einer Dissertation mit dem Thema die Zulassung zur Promotion beantragt mit dem Ergebnis:

Die öffentlich zugängliche Promotionsordnung der TUM ist mir bekannt, insbesondere habe ich die Bedeutung von § 28 (Nichtigkeit der Promotion) und § 29 (Entzug des Doktorgrades) zur Kenntnis genommen. Ich bin mir der Konsequenzen einer falschen Eidesstattlichen Erklärung bewusst.

Mit der Aufnahme meiner personenbezogenen Daten in die Alumni-Datei bei der TUM bin ich


einverstanden
 nicht einverstanden

München, den 28.04.2016

Peter Giesbertz
Unterschrift

Publications

Metabolite profiling in plasma and tissues of *ob/ob* and *db/db* mice identifies novel markers of obesity and type 2 diabetes

Pieter Giesbertz^{1,2}  · Inken Padberg³ · Dietrich Rein³ · Josef Ecker^{1,2} · Anja S. Höfle^{1,2} · Britta Spanier^{1,2} · Hannelore Daniel^{1,2}

Received: 12 February 2015 / Accepted: 15 May 2015 / Published online: 10 June 2015
© Springer-Verlag Berlin Heidelberg 2015

Abstract

Aims/hypothesis Metabolomics approaches in humans have identified around 40 plasma metabolites associated with insulin resistance (IR) and type 2 diabetes, which often coincide with those for obesity. We aimed to separate diabetes-associated from obesity-associated metabolite alterations in plasma and study the impact of metabolically important tissues on plasma metabolite concentrations.

Methods Two obese mouse models were studied; one exclusively with obesity (*ob/ob*) and another with type 2 diabetes (*db/db*). Both models have impaired leptin signalling as a cause for obesity, but the different genetic backgrounds determine the susceptibility to diabetes. In these mice, we profiled plasma, liver, skeletal muscle and adipose tissue via semi-quantitative GC-MS and quantitative liquid chromatography (LC)-MS/MS for a wide range of metabolites.

Results Metabolite profiling identified 24 metabolites specifically associated with diabetes but not with obesity. Among these are known markers such as 1,5-anhydro-D-sorbitol, 3-hydroxybutyrate and the recently reported marker glyoxylate. New metabolites in the diabetic model were lysine, *O*-phosphotyrosine and branched-chain fatty acids. We also

identified 33 metabolites that were similarly altered in both models, represented by branched-chain amino acids (BCAA) as well as glycine, serine, *trans*-4-hydroxyproline, and various lipid species and derivatives. Correlation analyses showed stronger associations for plasma amino acids with adipose tissue metabolites in *db/db* mice compared with *ob/ob* mice, suggesting a prominent contribution of adipose tissue to changes in plasma in a diabetic state.

Conclusions/interpretation By studying mice with metabolite signatures that resemble obesity and diabetes in humans, we have found new metabolite entities for validation in appropriate human cohorts and revealed their possible tissue of origin.

Keywords Adipose tissue · Branched-chain amino acids · Insulin resistance · Liver · Metabolomics · Muscle

Abbreviations

AAA	Aromatic amino acids
ADMA	<i>N,N</i> -dimethylarginine
BCAA	Branched-chain amino acids
BCKDH	Branched-chain keto acid dehydrogenase
FAS	Fatty acid synthase
IR	Insulin resistance
LC-MS	Liquid chromatography-MS
LPC	Lysophosphatidylcholine
PCA	Principal component analysis
SREBP	Sterol regulatory element-binding protein
TCA	Tricarboxylic acid

Electronic supplementary material The online version of this article (doi:10.1007/s00125-015-3656-y) contains peer-reviewed but unedited supplementary material, which is available to authorised users.

✉ Pieter Giesbertz
pieter.giesbertz@tum.de

¹ Department of Nutritional Physiology, Technische Universität München, Gregor-Mendel-Str. 2, 85350 Freising, Germany

² ZIEL – Institute for Food & Health, 85350 Freising, Germany

³ Metanomics Health GmbH and metanomics GmbH, Biomarker Program, Berlin, Germany

Introduction

Metabolomics studies in humans have identified plasma metabolite signatures comprising around 40 entities that associate

with the development of insulin resistance (IR) and type 2 diabetes [1]. The most discriminating metabolites are the branched-chain (BCAA) and aromatic amino acids (AAA) as well as glycine and some other amino acid degradation products. Despite the fact that the changes in plasma BCAA and glycine have already been described by Felig et al as resulting from the ‘insulin ineffectiveness characteristic of obesity’ [2], the mechanisms leading to these changes are still not known. In addition to the amino acid markers, recent profiling studies have added numerous lipid species such as odd-chain fatty acids and various triacylglycerol species to the growing list of diabetes markers (for review see [3]).

A major confounder in studies on human IR and type 2 diabetes is obesity. Although most human studies in search of diabetes-derived metabolites are corrected for BMI, it is known that obesity and diabetes have multi-level associations. In this context, it is thus relevant to ask whether the identified plasma metabolites have just a reporter status or are also causative or at least contributing to IR or type 2 diabetes development and/or progression. This, for example, has been proposed for the BCAA, which increase in concentration in the obese state and appear to contribute to IR via a crosstalk of mechanistic target of rapamycin (mTOR) and insulin signalling pathways [4]. For a separation of obesity-related from diabetes-dependent changes we here describe findings employing mouse models for both conditions with assessment of metabolite changes in plasma and in insulin-sensitive tissues such as liver, muscle and adipose tissue, which may help to identify the origins of the plasma changes.

Both *ob/ob* and *db/db* mouse models have defective leptin signalling with a lack of leptin expression in *ob/ob* mice and a leptin-receptor deficiency in *db/db* mice. Most importantly, owing to their different genetic backgrounds, they possess different susceptibilities to develop diabetes. The *ob/ob* mice on the C57BL6/J background are able to compensate for IR and develop only a mild and transient hyperglycaemia associated with pancreatic hypertrophy and hyperplasia. In contrast, pancreatic tissue of *db/db* mice on the C57BLKS/J background undergoes atrophy resulting in a decline in insulin secretion and severe hyperglycaemia [5]. Coleman and Hummel showed that the difference in the mutation of the leptin-signalling components (either hormone or receptor) plays only a minor role in the susceptibility to develop diabetes [6]. Introduction of the *ob* mutation in mice with the C57BLKS/J background revealed the same strong diabetes phenotype as in C57BLKS/J mice with the *db* mutation. The *ob/ob* model thus develops obesity and milder IR but is rather resistant to diabetes, whereas the *db/db* model develops both obesity and diabetes with loss of beta cells. We used both models with animals matched by age and sex, and fed identical diets for 12 weeks for comparative metabolite profiling. We identified various previously described marker metabolites and also new compounds which we classified as ‘caused

by obesity with normoglycaemia’ or ‘caused by diabetes with severe hyperglycaemia’.

Methods

Animals Male *db/db* mice and C57BLKS/J wild-type littermates ($n=6-10$ per group) were purchased from Charles River Laboratories (Sulzfeld, Germany). Male *ob/ob* mice and C57BL6/J wild-type littermates ($n=6-10$ per group), bred at the Research Center of Nutrition and Food Sciences (ZIEL), were obtained at the age of 5 weeks. Mice were kept on a standard-chow diet (ssniff V1534-0 R/M-H) for 3 weeks and were then placed on a chemically defined control diet (CCD; ssniff E15000-04 EF R/M Kontrolle) for 12 weeks. All mice had ad libitum access to food and water and were housed in the same open mouse facility. Body weight was determined weekly, and blood glucose was measured shortly before the end of the feeding trial. Animals were killed in a non-fasted state at an age of 20 weeks. Animal handling was conducted according with the Principles of Laboratory Care and was approved by the Veterinary Inspection Services.

Plasma and tissue collection Blood was collected into EDTA-coated tubes via cardiac puncture and centrifuged at 1,200 g and at 4°C to separate plasma. Plasma and tissues (liver, quadriceps muscle and epididymal adipose tissue) were collected, snap-frozen in liquid nitrogen, and stored at -80°C. Frozen tissues were ground prior to extraction of metabolites.

Sample preparation and metabolite profiling of mouse samples Broad metabolite profiling of plasma, liver, muscle and adipose tissue was performed using GC-MS (Agilent 6890 GC coupled to an Agilent 5973 MS System, Agilent, Waldbronn, Germany) and liquid chromatography-tandem MS (LC-MS/MS; Agilent 1100 HPLC, API 4000, Applied Biosystems, Darmstadt, Germany). In addition, for quantitative amino acid profiling of plasma, liver and muscle tissue, targeted LC-MS/MS (AB SCIEX QTrap 3200 LC-MS/MS System, AB SCIEX, Framingham, MA, USA) was applied using the aTRAQ Reagent Kit (Applied Biosystems, Darmstadt, Germany). Samples were analysed in a blinded and randomised analytical sequence design. See Electronic Supplementary Material (ESM) [Methods](#) for details on sample preparation and metabolite profiling.

Data analysis and metabolite selection Plasma metabolite concentrations in *ob/ob* and *db/db* mice were compared with their respective wild-type background and significantly changed metabolites were calculated by computing ANOVA models and using Student’s *t* statistics (unpaired and unequal variance). A significance threshold of $\alpha < 0.05$ was applied. Adjustment of *p* values according to Benjamini and

Hochberg was applied to correct for multiple testing. Metabolites were categorised based on their significance level in both mouse models or their specific change in either of the models compared with respective wild-type mice.

We used principal component analysis (PCA) to identify the major metabolite groups in the plasma data. Subsequent *k*-means clustering on the five principal components identified 15 major metabolite groups in plasma. Refinement of the clustering results was done by bootstrapping the *k*-means clustering algorithm 20 times. The overall significance of each cluster between *ob/ob* and C57BL6/J mice, and between *db/db* and C57BLKS/J mice, was determined by combining the *p* values from each metabolite derived from the comparison of concentrations between knockout and wild-type groups using Fisher's combined probability test. Finally, correlation networks for every cluster were calculated using pairwise correlations based on the metabolite concentrations in plasma and corresponding metabolite concentrations in tissues. The statistical software environment *R* was used for calculations and network visualisations [7] applying the packages 'FactoMineR', 'fpc', 'MADAM' and 'qgraph'. No animals, samples or data were excluded from the reporting.

Quantitative measurement of phospholipids in human plasma Phospholipids and sphingomyelins were measured in samples from human prediabetics and healthy controls using flow injected MS (MS/MS, QTRAP5500, AB SCIEX, Framingham, MA, USA). All participants gave written informed consent and the investigations have been approved by the ethics committee of the Technische Universität München (protocol 2436/09). See Hoefle et al [8] and ESM Methods for further details.

RNA isolation and quantitative real-time PCR analysis RNA isolation and relative quantification of mRNA expression was performed as described previously with a few modifications [9]. See ESM Methods for further details and ESM Table 1 for applied primers.

Results

Phenotypic characterisation of *ob/ob* and *db/db* mice and PCA of metabolite profiles Over 12 weeks of feeding, a dramatic weight gain was observed in both knockout mouse groups (Fig. 1a). Blood glucose concentrations were only increased in *db/db* mice (Fig. 1b) and plasma insulin levels were increased up to 35-fold in *ob/ob* mice and 2.5-fold in *db/db* mice compared with wild-type animals (Fig. 1c). Furthermore, increases in liver and adipose tissue mass and decreases in muscle mass were observed in both *ob/ob* and *db/db* mice (Fig. 1d–f).

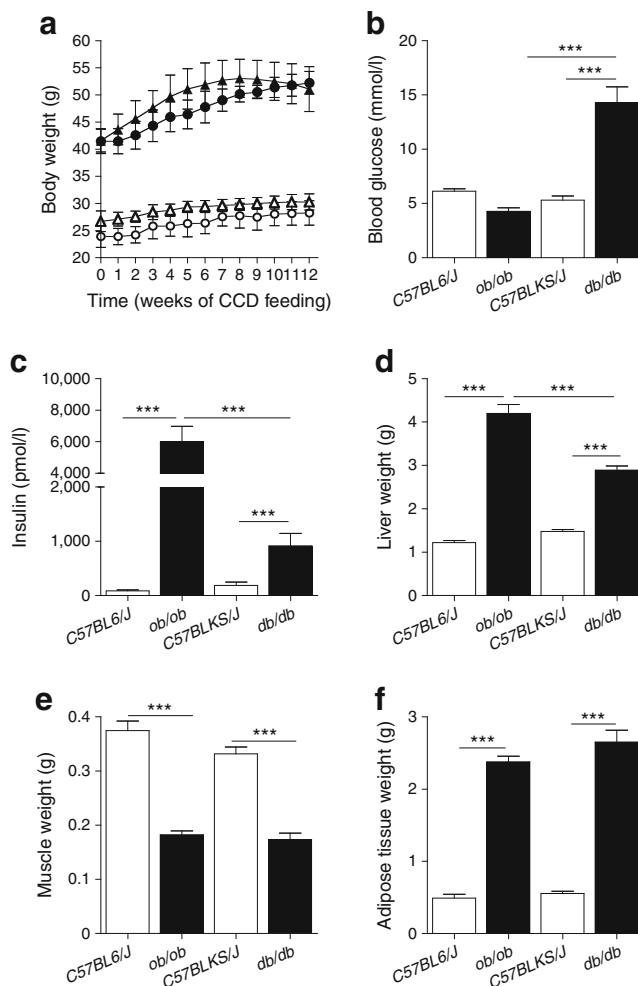


Fig. 1 Phenotypic characteristics of *ob/ob*, *db/db* and wild-type control mice. (a) Body weight development over the feeding period. White and black symbols represent wild-type and knockout mice, respectively. Circles and triangles represent C57BL6/J and C57BLKS/J mice, respectively. (b) Blood glucose concentrations of the 20-week-old animals and (c) plasma insulin concentrations at week 20. (d) Total weight of all liver lobes. (e) Total weight of left and right quadriceps muscles. (f) Total weight of left and right epididymal adipose tissue depots. Data are presented as means±SEM. ****p*<0.001

PCA of plasma and tissue metabolite profiles showed a close relationship between wild-type mice from both groups (Fig. 2), while both knockout groups separated from wild-type groups and from each other (for plasma and adipose tissue, in the first and second dimensions; and for liver, in the second dimension). Muscle tissue of wild-type strains separated in the second dimension (not shown), while knockout animals differentiated in the third dimension.

Plasma metabolite changes From the 170 metabolites quantified in plasma, 33 metabolites changed significantly in both *ob/ob* and *db/db* mice compared with respective wild-type animals (Table 1). Except for serine, changes in plasma concentrations remained significant after adjustment for multiple

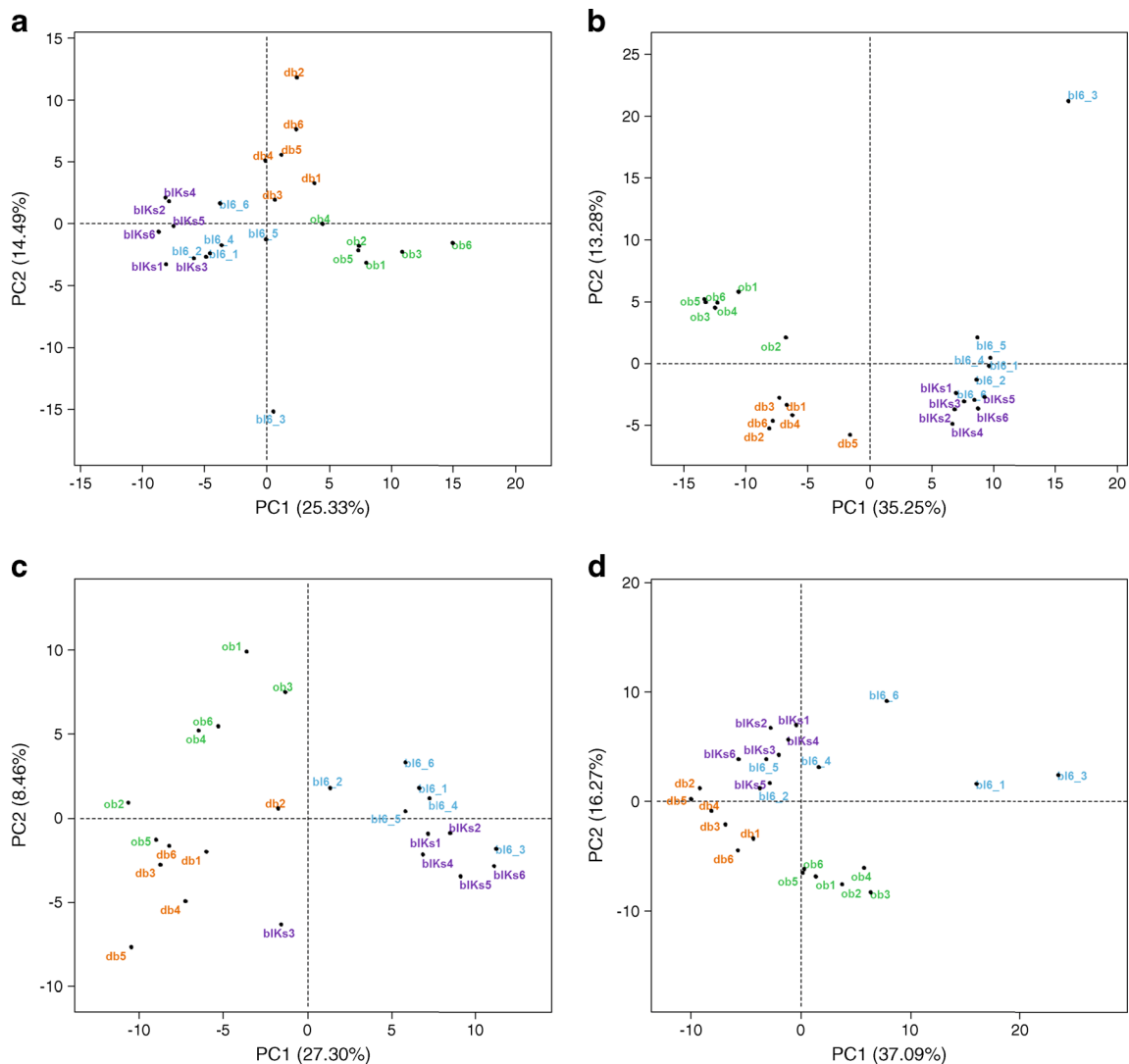


Fig. 2 PCA of metabolite profiles from plasma and tissues. **(a)** Plasma; **(b)** liver; **(c)** muscle; **(d)** adipose tissue. bl6, wild-type mice with C57BL/6J background; bIKs, wild-type mice with C57BLKS/J background; PC, principal component

testing. Prominent increases were observed for metabolites from diverse lipid classes, such as polyunsaturated fatty acids, (lyso)phosphatidylcholines, sphingomyelins and fatty alcohols as well as cholesterol and some cholesteryl ester species, while behenic acid (C22:0) was decreased. Common increases were also observed for BCAA and leucine-derived α -ketoisocaproic acid, while glycine, serine and *trans*-4-hydroxyproline levels were decreased. These metabolites thus seem to change in the early phases of IR and type 2 diabetes but mostly as a consequence of obesity.

Twenty-four metabolites changed specifically in the plasma of *db/db* mice (Table 2), of which 12 remained significant after *p* value adjustment. Besides increases in glucose, elevated levels of glyoxylate were found, which we recently described as a diabetes marker [10]. In addition, corticosterone and 18-hydroxy-11-deoxycorticosterone concentrations were markedly elevated. Specific increases were also found for the

branched-chain fatty acids 16-methylheptadecanoic acid and 3-hydroxyisobutyrate, as well as for *O*-phosphotyrosine, while lysine, arginine and lignoceric acid (C24:0) were decreased. Specific increases in *db/db* mice were also found for phospholipids containing linoleic acid. Strong trends for changes in plasma concentrations of *N,N*-dimethylarginine (ADMA) and 3-hydroxybutyrate were found, suggesting a mild ketogenic condition.

In plasma of *ob/ob* mice, 35 metabolites changed significantly (ESM Table 2). Of those, 24 remained significant after *p* value adjustment, comprising even-numbered fatty acids in unesterified forms and in ceramides, phospholipids, sphingolipids and cholesteryl esters with major increases, while triacylglycerols were reduced. Interestingly, whereas various branched-chain fatty acids were elevated in *db/db* mice, decreases of branched-chain isopalmitic acid and odd-chain C17:0 lysophosphatidylcholine were found in *ob/ob*

Table 1 Plasma metabolites significantly changed in both *ob/ob* and *db/db* mice

Metabolite	<i>ob/ob</i> vs C57BL6/J			<i>db/db</i> vs C57BLKS/J		
	Ratio <i>ob</i> :WT ^a	<i>p</i> value	Adjusted <i>p</i>	Ratio <i>db</i> :WT	<i>p</i> value	Adjusted <i>p</i>
Acyl-carriers and related						
Pantothenic acid	1.82	0.008	0.029	1.67	0.016	0.061
Amino acids, neutral						
Glycine	0.56	0.001	0.005	0.60	1.96×10 ⁻⁴	0.002
Serine	0.83	0.019	0.053	0.77	0.016	0.060
BCAA-related						
α-ketoisocaproic acid	1.44	0.029	0.077	1.97	2.08×10 ⁻⁴	0.002
Valine	1.44	9.81×10 ⁻⁵	0.001	1.58	6.16×10 ⁻⁵	0.001
Leucine	1.48	5.73×10 ⁻⁵	0.001	1.59	4.96×10 ⁻⁴	0.004
Isoleucine	1.51	1.34×10 ⁻⁵	2.47×10 ⁻⁴	1.62	0.002	0.013
Cholesterol and related						
Cholesterol, total	2.00	5.63×10 ⁻⁶	1.37×10 ⁻⁴	1.90	1.01×10 ⁻⁶	3.42×10 ⁻⁵
Cholesterol, free	1.64	3.00×10 ⁻⁴	0.003	1.51	0.002	0.012
Cholesteryl ester C20:4	1.87	0.003	0.015	1.87	0.003	0.020
Collagen metabolism						
Hydroxyproline	0.42	4.61×10 ⁻⁴	0.004	0.32	3.79×10 ⁻⁴	0.003
Dipeptides						
Anserine	0.34	0.014	0.046	0.39	0.008	0.038
Fatty acids, polyunsaturated						
Eicosapentaenoic acid (C20: <i>cis</i> [5,8,11,14,17]5)	2.81	1.49×10 ⁻⁶	8.21×10 ⁻⁵	3.24	2.67×10 ⁻⁸	4.40×10 ⁻⁶
Arachidonic acid (C20: <i>cis</i> [5,8,11,14]4)	2.87	3.83×10 ⁻⁷	3.56×10 ⁻⁵	2.34	5.47×10 ⁻⁷	3.42×10 ⁻⁵
Dihomo-γ-linolenic acid (C20: <i>cis</i> [8,11,14]3)	3.09	4.31×10 ⁻⁷	3.56×10 ⁻⁵	2.36	1.24×10 ⁻⁶	3.42×10 ⁻⁵
Fatty acids, saturated						
Stearic acid (C18:0)	2.20	3.54×10 ⁻⁶	1.21×10 ⁻⁴	2.04	1.24×10 ⁻⁶	3.42×10 ⁻⁵
Behenic acid (C22:0)	0.50	0.002	0.008	0.66	0.012	0.053
Phospholipids						
LPC (C20:4)	1.27	0.001	0.005	1.30	3.60×10 ⁻⁴	0.003
LPC (C18:1)	1.20	0.001	0.005	1.18	0.002	0.013
LPC (C18:0)	1.14	0.046	0.114	1.19	0.011	0.048
PC (C18:1,C18:2) or PC (C16:0,C20:3)	1.08	0.005	0.019	1.15	8.92×10 ⁻⁶	1.84×10 ⁻⁴
PC (C18:0,C20:4)	1.21	3.30×10 ⁻⁴	0.003	1.27	3.83×10 ⁻⁵	0.001
PC (C16:0,C16:0)	0.71	0.002	0.010	0.62	7.92×10 ⁻⁵	0.001
PC (C18:0,C20:3) or PC (C20:1,C18:2) or PC (C20:2,C18:1)	1.66	6.47×10 ⁻⁶	1.37×10 ⁻⁴	1.49	1.07×10 ⁻⁴	0.001
PC (C16:0,C20:5)	1.46	0.007	0.028	1.39	0.018	0.064
PC (C18:0,C18:1)	1.24	0.001	0.005	1.12	0.045	0.131
Glycerol phosphate, lipid fraction	2.43	2.67×10 ⁻⁵	4.41×10 ⁻⁴	1.82	2.11×10 ⁻⁴	0.002
Polyols						
1,5-Anhydrosorbitol	0.18	0.001	0.006	0.03	8.15×10 ⁻⁷	3.42×10 ⁻⁵
Redox-carrier and related						
Coenzyme Q9	7.78	6.66×10 ⁻⁶	1.37×10 ⁻⁴	3.26	0.002	0.013
Sphingomyelins						
Sphingomyelin (d18:2,C18:0)	1.53	0.001	0.005	1.46	0.002	0.013
Sphingomyelin (d18:1,C16:0)	1.21	2.09×10 ⁻⁴	0.002	1.11	0.023	0.077
Tocopherols and related						
α-Tocopherol	1.70	0.006	0.023	1.57	0.015	0.060
Triacylglycerols						
TAG (C18:2,C18:3)	0.31	0.015	0.046	0.39	0.042	0.125

^a Metabolite changes are expressed as ratios of metabolite concentrations in knockout mice compared with the respective control mice

PC, phosphatidylcholine; TAG, triacylglycerol; WT, wild-type

Table 2 Plasma metabolites significantly changed solely in *db/db* mice

Metabolite	<i>ob/ob</i> vs C57BL6/J		<i>db/db</i> vs C57BLKS/J		
	Ratio <i>ob</i> :WT ^a	<i>p</i> value	Ratio <i>db</i> :WT	<i>p</i> value	Adjusted <i>p</i>
Amino acids, neutral					
Asparagine	1.01	n.s.	0.76	0.041	0.124
Ascorbic acid and related					
Threonic acid	1.25	n.s.	1.61	0.017	0.064
BCAA metabolism					
3-Hydroxyisobutyrate	0.92	n.s.	1.64	0.020	0.067
Citrate cycle					
Succinate	0.94	n.s.	0.89	0.039	0.120
Creatine metabolism					
Creatinine	0.72	n.s.	0.64	0.037	0.117
Fatty acids, branched					
16-Methylheptadecanoic acid	0.84	n.s.	1.47	0.004	0.021
Fatty acids, polyunsaturated					
Linoleic acid (C18: <i>cis</i> [9,12]2)	0.97	n.s.	1.39	0.014	0.059
Fatty acids, saturated					
Lignoceric acid (C24:0)	0.74	n.s.	0.59	0.005	0.022
Glycolipids					
Glucose, lipid fraction	1.52	n.s.	1.69	0.045	0.131
Glycolysis/gluconeogenesis					
Glucose-6-P or fructose-6-P or myo-inositol-P	1.20	n.s.	2.15	0.004	0.021
Lactaldehyde	1.01	n.s.	0.66	0.031	0.101
Ketone bodies					
3-Hydroxybutyrate	1.19	n.s.	1.84	0.014	0.059
Lipid precursors					
Glycerol, polar fraction	1.04	n.s.	1.37	0.015	0.060
Lysine metabolism					
α -Aminoadipic acid	0.83	n.s.	0.69	0.021	0.072
Lysine	1.14	n.s.	0.66	0.002	0.013
Miscellaneous					
Glyoxylate	1.47	n.s.	6.06	6.18×10^{-5}	0.001
Monosaccharides					
Glucose or galactose or gluconic acid or mannitol	1.72	n.s.	4.81	8.06×10^{-6}	1.84×10^{-4}
Other hormones					
ADMA	1.00	n.s.	0.71	0.019	0.066
Phospholipids					
Lysophosphatidylcholine (C18:2)	0.95	n.s.	1.41	1.60×10^{-4}	0.002
PC (C16:0,C20:4) or PC (C18:2,C18:2)	1.01	n.s.	1.03	0.006	0.029
Steroids and related					
18-Hydroxy-11-deoxycorticosterone or 11-deoxycortisol	1.50	n.s.	7.18	0.002	0.013
Corticosterone	1.48	n.s.	4.93	0.004	0.022
Tyrosine metabolism					
<i>O</i> -phosphotyrosine	0.92	n.s.	1.96	0.004	0.021
Urea cycle					
Arginine	0.74	n.s.	0.59	2.49×10^{-5}	4.57×10^{-4}

^a Metabolite changes are expressed as ratios of metabolite concentrations in knockout mice compared with the respective control mice
n.s., not significant; PC, Phosphatidylcholine

mice. Specific increases of phenylalanine and tryptophan levels were also observed in *ob/ob* animals, while tryptophan

breakdown-products kynurenic acid and xanthurenic acid were reduced. In contrast, indole-3-propionic acid and

3-indoxylsulfate, arising from bacterial tryptophan breakdown [11], increased in plasma. Moreover, *ob/ob* mice displayed strong increases in ornithine and decreases in α -aminobutyrate concentrations in plasma.

Metabolite changes in liver, quadriceps muscle and epididymal adipose tissue Metabolite profiles were obtained from liver, quadriceps muscle and epididymal adipose tissue as metabolically important and insulin-dependent organs. An overview of hepatic metabolite concentration changes in *ob/ob* and *db/db* animals compared with respective wild-type animals is shown in ESM Fig. 1a,b. Metabolites from different lipid classes were dramatically increased in both models with stronger increases in *ob/ob* mice, while very-long-chain fatty acid levels were decreased (ESM Fig. 1a). Furthermore, both models displayed increased BCAA and reduced glycine and *trans*-4-hydroxyproline concentrations. Most pronounced differences in liver between *ob/ob* and *db/db* mice were found for pentoses and intermediates of the pentose phosphate pathway with increases in *db/db* mice and decreases in *ob/ob* mice (ESM Fig. 1b).

ESM Fig. 1c,d show metabolite concentration changes in muscle tissue in the two knockout mouse groups compared with the respective control mice. Both models displayed strongest elevations in free long-chain fatty acids, represented by straight-, branched- and odd-chain forms, with a more pronounced increase in the *ob/ob* group (ESM Fig. 1c). In contrast to liver tissue, no changes were observed for phospholipids. Marked differences between *ob/ob* and *db/db* groups were found for intermediates of the glycolytic chain comprising fructose-6-phosphate, fructose-1,6-diphosphate, glucose-6-phosphate and 3-phosphoglycerate, which all increased dramatically in *ob/ob* but only modestly in *db/db* mice (ESM Fig. 1d).

Adipose tissue displayed a strong decrease in levels of saturated very-long-chain fatty acids in both models (ESM Fig. 1e). Other fatty acids—in particular monounsaturated and polyunsaturated species—had increased concentrations. Furthermore, the tricarboxylic acid (TCA) cycle intermediates malate and fumarate were increased. Cholesterol showed increased concentrations in *ob/ob* mice and decreased concentrations in *db/db* mice (ESM Fig. 1f).

Identification of principal metabolite groups in plasma PCA, with subsequent clustering on principal components, identified 15 metabolite clusters in plasma. Metabolites clustered into groups with biochemical similarity or with common metabolic pathways. ESM Table 3 displays the overall significance of the clusters reached for the two knockout models as compared with wild-type mice. Five metabolite clusters displayed high significance for both knockout models (clusters 4, 8, 10, 13, 15), consisting of phospholipids, triacylglycerols, AAA and BCAA, as well as glycine,

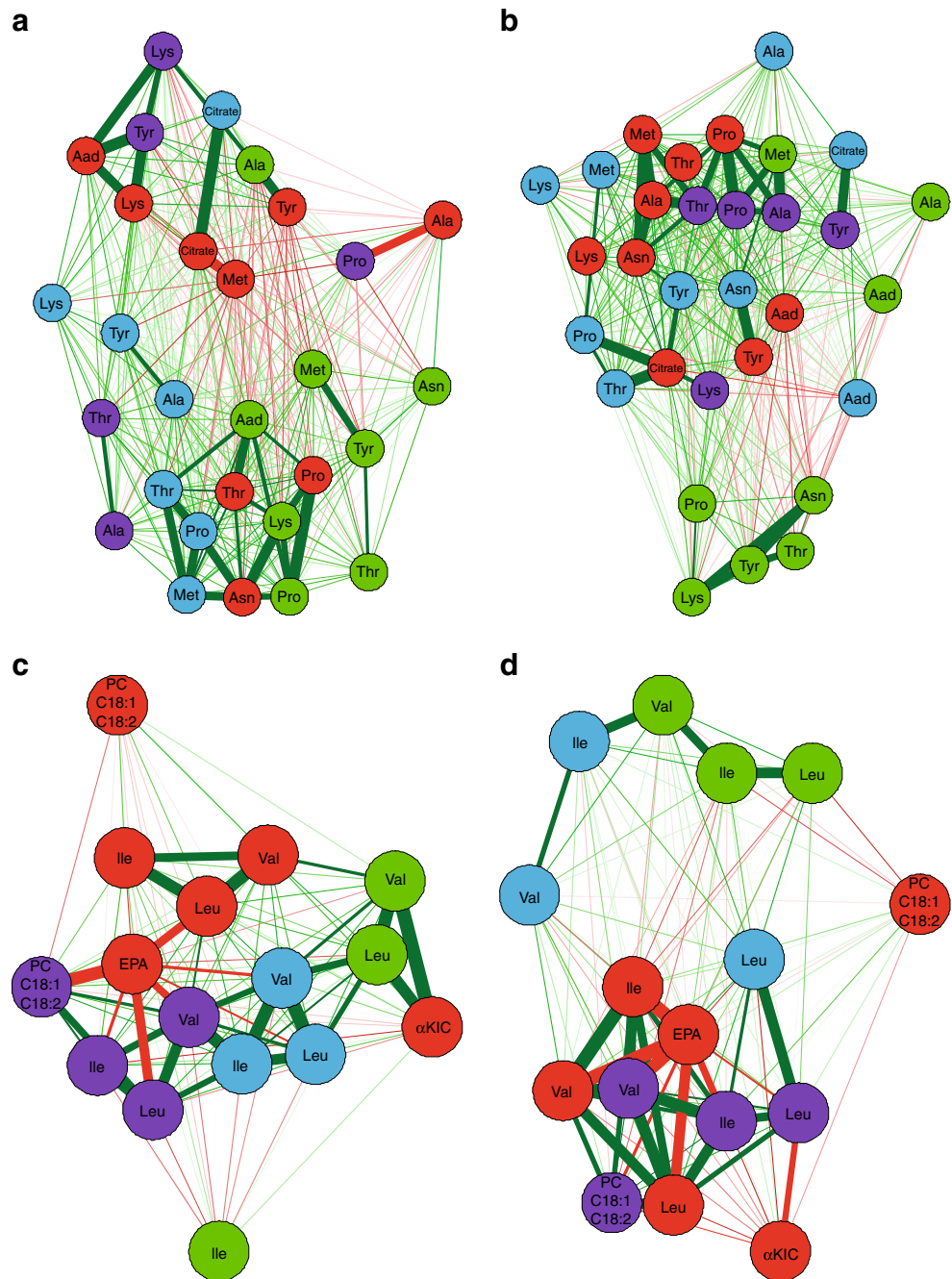
histidine and *trans*-4-hydroxyproline. Interestingly, four clusters (clusters 1, 5, 9, 11)—mainly consisting of amino acids, hexoses and catabolites—showed overall significant changes only between *db/db* and C57BLKS/J wild-type mice. Similarly, two clusters (clusters 3 and 6) showed an overall significant change only between *ob/ob* and corresponding control mice. These clusters consisted of fatty acids, TCA cycle intermediates and cholesteryl esters.

Correlation networks of plasma and tissue metabolites To explore which tissue contributes most to the changes in blood metabolites, correlation networks for every metabolite cluster between plasma and the different organs were calculated. Selected networks are displayed in Fig. 3. Clearest differences between the correlation networks of *ob/ob* and *db/db* mice were obtained for clusters 11 and 13 containing amino acids. For cluster 11, especially adipose tissue correlated strongly with plasma in the *db/db* model, while correlations with liver metabolites remained weak. In the *ob/ob* model, in contrast, liver revealed much stronger correlations. The same interdependence was observed for cluster 13, containing the BCAA. Most distinct was the network for the *db/db* model revealing strong positive correlations for BCAA between plasma and adipose tissues while correlations with liver were weak. The product of leucine transamination, α -ketoisocaproic acid, correlated negatively with adipose tissue leucine content. In contrast, in *ob/ob* mice, α -ketoisocaproic acid correlated strongest in a positive manner with liver. The observed clustering suggests an important contribution of adipose tissue to plasma amino acid concentrations in the *db/db* and far less so in the *ob/ob* model, whereas the liver appears to exert more influence in the *ob/ob* model.

Discussion

Obesity, IR and type 2 diabetes in humans cause significant changes in an array of plasma metabolites of which some have the quality to predict diabetes development in early phases [1]. In mouse models mimicking the human conditions of type 2 diabetes development, we assessed which metabolite changes associate mainly with obesity and which are specific for the diabetic state. Despite a common obesity phenotype, the mice display different impairments in glucose homeostasis and beta cell function resembling an obese phenotype with a mild IR (*ob/ob*) or a fully developed type 2 diabetes (*db/db*). By using appropriate wild-type mice as controls, we eliminated putative effects of the different genetic backgrounds. In addition to plasma, we generated metabolite profiles of liver, muscle and adipose tissue as an explorative approach which could provide indications on the origins of plasma metabolite changes. With this strategy, metabolites were identified that changed in concentrations in both the *ob/ob* and the *db/db* mice when

Fig. 3 Correlation networks of selected metabolite clusters. (**a,b**) Correlation networks for metabolite cluster 11 (see ESM Table 3) for *ob/ob* (**a**) and *db/db* (**b**) mice. (**c,d**) Correlation networks for metabolite cluster 13 for *ob/ob* (**c**) and *db/db* (**d**) mice. Node colours indicate tissue type (red, plasma; green, liver; blue, muscle; purple, adipose tissue). Green and red line colours indicate positive and negative correlations, respectively. Line thickness represents the strength of the correlation, with thicker lines indicating stronger correlations. Aad, α -amino adipic acid; EPA, eicosapentaenoic acid; KIC, α -ketoisocaproic acid; PC, principal component



compared with their respective wild-type background, and we also found metabolites that specifically mark the obese state without diabetes or the diabetic state on a background of obesity.

In addition, we compared metabolite changes in mice with alterations observed in two independent human studies comprising either prediabetic or diabetic individuals (ESM Tables 4 and 5). Prediabetic participants were defined by the WHO's criteria and diabetic patients were defined according to self-reporting, and/or type-2 diabetes medication, and/or HbA_{1c} >6.5% (47.5 mmol/mol) and fasting plasma glucose

levels >5.55 mmol/l. While parts of both studies were recently published [8, 12], we focused on novel metabolite measurements from these studies and could identify similar changes in human plasma for various known but also several yet undescribed metabolites. Interestingly, while most changes in phospholipid concentrations of prediabetic individuals were concordant with the alterations in both *ob/ob* and *db/db* mice, metabolite profiles of diabetic individuals showed strongest similarities to *db/db* mice, substantiating the discriminant power of the specific alterations observed in plasma from mice in this study.

Common alterations in lipid profiles reflect changes in de novo lipogenesis as a consequence of impaired leptin and insulin signalling Most pronounced in both models were increases in long-chain fatty acids and corresponding phospholipids, in plasma and predominantly in liver. It is well established that hepatic de novo lipogenesis is increased in obese and IR states leading to non-alcoholic fatty liver disease (NAFLD) [13]. Leptin is known to suppress stearoyl-CoA desaturase (SCD-1) which catalyses the synthesis of monounsaturated fatty acids [14]. The primary lack of leptin signalling in both mouse models may thus explain the observed increases in hepatic palmitoleic and oleic acid levels. Insulin controls de novo lipogenesis and both models are hyperinsulinaemic, which in turn affects liver as an insulin-dependent organ. Despite a developing IR, the hepatic sterol regulatory element-binding protein (SREBP)-1c signalling pathway remains insulin sensitive [15]. Increases in hepatic levels of long-chain fatty acids, polyunsaturated fatty acids and related phospholipids may well reflect changes of enzymes encoded by SREBP-1-dependent genes [16]. Remarkably, most saturated and monounsaturated fatty acids of 20–24 carbon units decreased in plasma, liver and adipose tissue, which could be a consequence of altered elongase-1 levels, the prime enzyme in the production of very-long-chain fatty acids [17]. Increased levels of isopentenyl pyrophosphate suggest enhanced hepatic cholesterol synthesis, regulated by SREBP-1a [18] and SREBP-2 [19].

Skeletal muscle also showed strong increases in concentrations of long-chain fatty acids in *ob/ob* and *db/db* mice. Although muscle tissue is not thought to significantly contribute to overall lipid production, ectopic lipid accumulation is associated with IR and NEFA in tissues, including muscle, and is thought to cause lipotoxicity and promote IR. Although increased fatty acid levels may indicate a larger supply from plasma by enhanced adipose tissue lipolysis or decreased fatty acid clearance [20, 21], increased activity of muscle-specific fatty acid synthase (FAS) might also contribute to increased levels of fatty acids [22].

Specific metabolite changes in *db/db* mice relate to hyperglycaemia and comorbidities In contrast to *ob/ob* mice, *db/db* animals are highly hyperglycaemic with only modestly elevated insulin levels, reflecting the increased susceptibility of *db/db* mice to beta cell exhaustion [5]. The *db/db* mice displayed specific changes in plasma metabolites, which were previously reported as associated with hyperglycaemia and its comorbidities. Decreased ADMA levels, related to altered endothelial functions, were reported for type 2 diabetes [23]; and low plasma levels of 1,5-anhydrosorbitol that result from competitive inhibition of reabsorption via glucose transporters in kidney by the high load of filtered glucose are also known in type 2 diabetes [24]. Furthermore, glyoxylate, recently described as a new marker for diabetes [12], was

strongly increased in plasma of *db/db* mice. Decreased creatinine concentrations reflect a reduced muscle mass [25] here showing a stronger decrease in the *db/db* model. This is associated with increased muscle catabolism causing the observed rise in plasma amino acids and elevated glucocorticoid levels. Last, the increase in plasma *O*-phosphotyrosine might relate to elevated platelet activation as a result of the hyperglycaemic state [26, 27]. Most interestingly, phosphotyrosine appeared in the same cluster with glucose and glyoxylate (see ESM Table 3).

Correlation networks and gene expression analysis suggest an increased role for adipose tissue in the *db/db* mice and for liver in *ob/ob* mice Both knockout models showed increased levels of BCAA and α -ketoisocaproic acid, the transamination product of leucine, in plasma and tissues. Leptin and insulin both contribute to the maintenance of muscle protein [16, 28]. Disturbances in leptin signalling and IR in turn increase protein degradation in muscle releasing amino acids into circulation. While most amino acids are used for hepatic gluconeogenesis, BCAA show a different fate. A significant contribution of adipose tissue to the metabolism of BCAA has become obvious in recent years. In 2007, She et al showed a decreased protein level and activity of the mitochondrial branched-chain amino acid transferase (BCAT2) and the rate-limiting branched-chain keto acid dehydrogenase (BCKDH) complex in obese rodents [29]. The networks for the BCAA cluster (cluster 13, see Fig. 3c,d) showed strong correlations between plasma and adipose tissue in the *db/db* but not in *ob/ob* mice. However, analysis of mRNA levels in adipose tissue showed similar decreases in both knockout models for *Bckdha*, the gene encoding the E1 α component of the BCKDH complex, as well as for the kinase (*Bckdk*) and for the phosphatase (*Ppm1k*) regulating BCKDH activity, while *Bcat2* remained unchanged (see ESM Fig. 2). This finding suggests that, in mice, other tissues likely contribute to the changes in BCAA levels. A recent study describes the effects of insulin on hepatic protein levels and activity of BCKDH in controlling BCAA catabolism [30]. Since *ob/ob* mice are hyperinsulinaemic, the plasma BCAA concentrations may be influenced more strongly by hepatic BCKDH in *ob/ob* mice, which is also supported by the strong correlations of plasma α -ketoisocaproic acid and hepatic BCAA in the correlation network of the *ob/ob* mice.

Changes in branched-chain fatty acids may link to BCAA-derived precursors Interestingly, plasma concentrations of odd-numbered and branched-chain fatty acids changed in different directions in the two mouse models. Whereas 16-methylheptadecanoic acid was specifically increased in *db/db* mice, *ob/ob* mice showed a decrease in C17

lysophosphatidylcholine (LPC C17:0) levels and a strong trend for a decrease for isopalmitic acid. In cohort studies, plasma levels of LPC C17:0 were recently reported to be reduced in type 2 diabetes patients [1, 31]. How odd-chain and branched-chain fatty acids link to IR and type 2 diabetes is currently not known. However, 3-hydroxyisobutyric acid, a branched short-chain fatty acid derived from valine breakdown, was specifically increased in *db/db* mice. As shown in rat epididymal adipose tissue, FAS can generate odd/branched long-chain fatty acids from propionyl-CoA and branched-chain C4- and C5-iso-acyl-CoAs as primers which are all intermediates of BCAA breakdown [32]. An aberrant availability of short-chain acyl-CoA primers for use in fatty acid synthesis could explain the changes in odd- and branched-chain fatty acid concentrations found in plasma in an insulin-resistant or diabetic state.

Conclusion We compared metabolite profiles in plasma and selected tissues of two mouse models with obesity but different stages of diabetes development. With this approach, we could define metabolites that change in the obese states and those that depend on insulin action and are associated with severe hyperglycaemia. Analysis of liver, muscle and adipose tissue revealed dominant changes in fatty acid and amino acid metabolism, with a more dominant role for adipose tissue in the diabetes model. We also identified new marker metabolites with significant changes in tissues and plasma and found similar changes for various metabolites in plasma from human prediabetic and diabetic volunteers.

Acknowledgements We thank M. Klingenspor and F. Bolze (Molecular Nutritional Medicine Unit, Technische Universität München, Freising, Germany) for *ob/ob* mice, and R. Scheundel (Nutritional Physiology Unit, Technische Universität München, Freising, Germany) for animal handling and sample collection. For fruitful discussions and comments on the manuscript, we thank colleagues from the Nutritional Physiology Unit (Technische Universität München, Freising, Germany), especially T. Zietek, J. Fiamoncini, J. Stolz and K. Gedrich.

Funding This study was financed by institutional funds of the ZIEL Research Center of Nutrition and Food Sciences.

Duality of interest The authors declare that there is no duality of interest associated with this manuscript.

Contribution statement PG, BS, and HD contributed to conception and design of the study. PG, IP and DR were responsible for the acquisition and analysis of metabolite profiling data. PG and JE were responsible for the acquisition and analysis of mRNA expression data. PG, IP, DR and ASH were responsible for acquisition of human plasma data. PG and HD drafted and wrote the manuscript. All authors contributed to critical revision of the manuscript and approved the final version. HD is the guarantor of this work.

References

- Menni C, Fauman E, Erte I et al (2013) Biomarkers for type 2 diabetes and impaired fasting glucose using a nontargeted metabolomics approach. *Diabetes* 62:4270–4276
- Felig P, Marliss E, Cahill GF Jr (1969) Plasma amino acid levels and insulin secretion in obesity. *N Engl J Med* 281:811–816
- Roberts LD, Koulman A, Griffin JL (2014) Towards metabolic biomarkers of insulin resistance and type 2 diabetes: progress from the metabolome. *Lancet Diabetes Endocrinol* 2:65–75
- Newgard CB, An J, Bain JR et al (2009) A branched-chain amino acid-related metabolic signature that differentiates obese and lean humans and contributes to insulin resistance. *Cell Metab* 9:311–326
- Coleman DL (1978) Obese and diabetes: two mutant genes causing diabetes-obesity syndromes in mice. *Diabetologia* 14:141–148
- Coleman DL, Hummel KP (1973) The influence of genetic background on the expression of the obese (*Ob*) gene in the mouse. *Diabetologia* 9:287–293
- R Development and Core Team (2008) A language and environment for statistical computing. Available from www.R-project.org, accessed 8 Apr 2015
- Hoeffle AS, Bangert AM, Stamford A et al (2015) Metabolic responses of healthy or prediabetic adults to bovine whey protein and sodium caseinate do not differ. *J Nutr* 145:467–475
- Ecker J, Liebisch G, Englmaier M, Grandl M, Robenek H, Schmitz G (2010) Induction of fatty acid synthesis is a key requirement for phagocytic differentiation of human monocytes. *Proc Natl Acad Sci U S A* 107:7817–7822
- Nikiforova VJ, Giesbertz P, Wiemer J et al (2014) Glyoxylate, a new marker metabolite of type 2 diabetes. *J Diabetes Res* 2014:9
- Devereux Woods D (1935) Indole formation by *Bacterium coli*: the breakdown of tryptophan by washed suspensions of *Bacterium coli*. *Biochem J* 29:640–648
- Padberg I, Peter E, Gonzalez-Maldonado S et al (2014) A new metabolomic signature in type-2 diabetes mellitus and its pathophysiology. *PLoS One* 9: e85082
- Kawano Y, Cohen DE (2013) Mechanisms of hepatic triglyceride accumulation in non-alcoholic fatty liver disease. *J Gastroenterol* 48:434–441
- Biddinger SB, Miyazaki M, Boucher J, Ntambi JM, Kahn CR (2006) Leptin suppresses stearoyl-CoA desaturase 1 by mechanisms independent of insulin and sterol regulatory element-binding protein-1c. *Diabetes* 55:2032–2041
- Brown MS, Goldstein JL (2008) Selective versus total insulin resistance: a pathogenic paradox. *Cell Metab* 7:95–96
- Wang Y, Botolin D, Xu J et al (2006) Regulation of hepatic fatty acid elongase and desaturase expression in diabetes and obesity. *J Lipid Res* 47:2028–2041
- Tvrđik P, Westerberg R, Silve S et al (2000) Role of a new mammalian gene family in the biosynthesis of very long chain fatty acids and sphingolipids. *J Cell Biol* 149:707–718
- Shimano H, Horton JD, Hammer RE, Shimomura I, Brown MS, Goldstein JL (1996) Overproduction of cholesterol and fatty acids causes massive liver enlargement in transgenic mice expressing truncated SREBP-1a. *J Clin Invest* 98:1575–1584
- Horton JD, Shimomura I, Brown MS, Hammer RE, Goldstein JL, Shimano H (1998) Activation of cholesterol synthesis in preference to fatty acid synthesis in liver and adipose tissue of transgenic mice overproducing sterol regulatory element-binding protein-2. *J Clin Invest* 101:2331–2339
- Bjorntorp P, Bergman H, Varnauskas E (1969) Plasma free fatty acid turnover rate in obesity. *Acta Med Scand* 185:351–356
- Frayn KN (2002) Adipose tissue as a buffer for daily lipid flux. *Diabetologia* 45:1201–1210

22. Funai K, Song H, Yin L et al (2013) Muscle lipogenesis balances insulin sensitivity and strength through calcium signaling. *J Clin Invest* 123:1229–1240
23. Paiva H, Lehtimäki T, Laakso J et al (2003) Plasma concentrations of asymmetric-dimethyl-arginine in type 2 diabetes associate with glycemic control and glomerular filtration rate but not with risk factors of vasculopathy. *Metab Clin Exp* 52:303–307
24. Akanuma Y, Morita M, Fukuzawa N, Yamanouchi T, Akanuma H (1988) Urinary excretion of 1,5-anhydro-D-glucitol accompanying glucose excretion in diabetic patients. *Diabetologia* 31:831–835
25. Baxmann AC, Ahmed MS, Marques NC et al (2008) Influence of muscle mass and physical activity on serum and urinary creatinine and serum cystatin C. *Clin J Am Soc Nephrol* 3:348–354
26. Muñoz GE, Marshall SH (1992) Free L-phosphotyrosine activates human platelets: molecular evidence for a new signal transducer. *Cell Mol Biol* 38:629–633
27. Gresele P, Marzotti S, Guglielmini G et al (2010) Hyperglycemia-induced platelet activation in type 2 diabetes is resistant to aspirin but not to a nitric oxide-donating agent. *Diabetes Care* 33:1262–1268
28. Sainz N, Rodriguez A, Catalan V et al (2009) Leptin administration favors muscle mass accretion by decreasing FoxO3a and increasing PGC-1alpha in ob/ob mice. *PLoS One* 4: e6808
29. She P, Van Horn C, Reid T, Hutson SM, Cooney RN, Lynch CJ (2007) Obesity-related elevations in plasma leucine are associated with alterations in enzymes involved in branched-chain amino acid metabolism. *Am J Physiol Endocrinol Metab* 293:E1552–E1563
30. Shin AC, Fasshauer M, Filatova N et al (2014) Brain insulin lowers circulating BCAA levels by inducing hepatic BCAA catabolism. *Cell Metab* 20:898–909
31. Wang-Sattler R, Yu Z, Herder C et al (2012) Novel biomarkers for pre-diabetes identified by metabolomics. *Mol Syst Biol* 8:615
32. Horning MG, Martin DB, Karmen A, Vagelos PR (1961) Fatty acid synthesis in adipose tissue. II. Enzymatic synthesis of branched chain and odd-numbered fatty acids. *J Biol Chem* 236:669–672

An LC-MS/MS method to quantify acylcarnitine species including isomeric and odd-numbered forms in plasma and tissues^S

Pieter Giesbertz, Josef Ecker, Alexander Haag, Britta Spanier, and Hannelore Daniel¹

Nutritional Physiology, Technische Universität München, 85350 Freising, Germany; and ZIEL Institute for Food and Health, 85350 Freising, Germany

Abstract Acylcarnitines are intermediates of fatty acid and amino acid oxidation found in tissues and body fluids. They are important diagnostic markers for inherited diseases of peroxisomal and mitochondrial oxidation processes and were recently described as biomarkers of complex diseases like the metabolic syndrome. Quantification of acylcarnitine species can become challenging because various species occur as isomers and/or have very low concentrations. Here we describe a new LC-MS/MS method for quantification of 56 acylcarnitine species with acyl-chain lengths from C2 to C18. Our method includes amino acid-derived positional isomers, like methacrylyl-carnitine (2-M-C3:1-CN) and crotonyl-carnitine (C4:1-CN), and odd-numbered carbon species, like pentadecanoyl-carnitine (C15:0-CN) and heptadecanoyl-carnitine (C17:0-CN), occurring at very low concentrations in plasma and tissues. Method validation in plasma and liver samples showed high sensitivity and excellent accuracy and precision. In an application to samples from streptozotocin-treated diabetic mice, we identified significantly increased concentrations of acylcarnitines derived from branched-chain amino acid degradation and of odd-numbered straight-chain species, recently proposed as potential biomarkers for the metabolic syndrome. **In conclusion, the LC-MS/MS method presented here allows robust quantification of isomeric acylcarnitine species and extends the palette of acylcarnitines with diagnostic potential derived from fatty acid and amino acid metabolism.**—Giesbertz, P., J. Ecker, A. Haag, B. Spanier, and H. Daniel. An LC-MS/MS method to quantify acylcarnitine species including isomeric and odd-numbered forms in plasma and tissues. *J. Lipid Res.* 2015. 56: 2029–2039.

Supplementary key words diabetes • fatty acid/oxidation • mitochondria • liver • diagnostic tools • liquid chromatography-tandem mass spectrometry

Acylcarnitines are intermediates in fatty acid and amino acid breakdown generated from the conversion of acyl-CoA species by the action of carnitine acyltransferases (1). The formation of carnitine conjugates is crucial for the

transport of activated fatty acids (acyl-CoAs) from the cytosol across the inner mitochondrial membrane into the matrix where fatty acid oxidation takes place. It has now become clear that a net efflux of acylcarnitine species from the mitochondria into the cytosol and ultimately into plasma is particularly important in situations of impaired fatty acid oxidation to prevent accumulation of potentially toxic acyl-CoA intermediates in the mitochondrion (2, 3). How acylcarnitines are released into the extracellular space is not known, but changes in plasma and/or urinary acylcarnitine profiles are used to detect disorders in fatty acid and amino acid oxidation (4). More recently, alterations in plasma acylcarnitine profiles were described as strongly associated with obesity and type 2 diabetes (5–7). A broad spectrum of short-, medium-, and long-chain acylcarnitine species is generated from multiple metabolic routes including various fatty acid and amino acid oxidation pathways. A comprehensive quantification that covers as many as possible of these entities is therefore not only important for proper clinical diagnosis of inherited enzymatic impairments, but also for basic studies of complex diseases such as the metabolic syndrome.

Acylcarnitine profiles are commonly established by direct infusion ESI-MS/MS. This technology, however, does not allow the discrimination of isomeric acylcarnitine species. Furthermore, isobaric matrix interferences can lead to an overestimation of metabolite concentrations producing false positive results, in particular, for compounds with low abundance (8). Although LC-MS/MS methods have been developed for successful separation of isomeric compounds (9–12), the identification of the exact compound in the chromatogram often remains

Abbreviations: CN, carnitine; CV, coefficient of variation; HFBA, heptafluorobutyric acid; IS, internal standard; LOD, limit of detection; LOQ, limit of quantitation; MRM, multiple reaction monitoring; STZ, streptozotocin.

¹To whom correspondence should be addressed.

e-mail: hannelore.daniel@tum.de

^SThe online version of this article (available at <http://www.jlr.org>) contains a supplement.

Manuscript received 8 July 2015 and in revised form 24 July 2015.

Published, JLR Papers in Press, August 3, 2015

DOI 10.1194/jlr.D061721

Copyright © 2015 by the American Society for Biochemistry and Molecular Biology, Inc.

This article is available online at <http://www.jlr.org>

elusive. Additionally, the abundance of many species in biological samples is often too low for robust detection and quantification.

Here we describe a robust and highly sensitive LC-MS/MS method for comprehensive quantification of an array of acylcarnitine species with a special focus on amino acid-derived intermediates, which often occur at very low concentrations and in isomeric forms. Because alterations in plasma odd-numbered fatty acids were recently shown to associate with impaired glucose tolerance and diabetes (13), we also focused on quantification of the corresponding odd-numbered acylcarnitines. The method was validated and applied to plasma and liver samples from streptozotocin (STZ)-induced insulin-deficient mice, which serve as a model of type I diabetes.

MATERIALS AND METHODS

Chemicals, solutions, reference substances, and internal standards

Ammonium acetate, *n*-butanol (99.7%), thionyl chloride, carnitine hydrochloride, formic acid (LC-MS grade), heptafluorobutyric acid (HFBA) ($\geq 99.5\%$), acetyl chloride, and acetonitrile (LC-MS grade) were purchased from Sigma-Aldrich (Taufkirchen, Germany). Water (LC-MS grade) and diethyl ether (Baker analyzed) were obtained from J. T. Baker Chemicals (Center Valley, PA). Methanol (LC-MS grade) and trichloroacetic acid were purchased from Merck (Darmstadt, Germany). The internal standard (IS) mixture containing d_9 -carnitine (0.785 pmol/ μ l), d_3 -acetyl-carnitine (0.327 pmol/ μ l), d_3 -propionyl-carnitine (0.086 pmol/ μ l), d_3 -butyryl-carnitine (0.043 pmol/ μ l), d_9 -isovaleryl-carnitine (0.039 pmol/ μ l), d_3 -hexanoyl-carnitine (0.046 pmol/ μ l), d_3 -octanoyl-carnitine (0.042 pmol/ μ l), d_3 -decanoyl-carnitine (0.046 pmol/ μ l), d_3 -dodecanoyl-carnitine (0.043 pmol/ μ l), d_3 -tetradecanoyl-carnitine (0.041 pmol/ μ l), d_3 -hexadecanoyl-carnitine (0.082 pmol/ μ l), and d_3 -octadecanoyl-carnitine (0.074 pmol/ μ l) was obtained from ChromSystems (München, Germany). The free fatty acids used for synthesis of acylcarnitines (crotonic acid, methacrylic acid, tiglic acid, dimethylacrylic acid, isobutyric acid, 2-methylbutyric acid, (S)-3-hydroxybutyric acid, (R)-3-hydroxybutyric acid, sodium-(S)- β -hydroxyisobutyric acid, 3-hydroxyisovaleric acid, *trans*-2-methylbutenoic acid, heptanoic acid, nonanoic acid, undecanoic acid, tridecanoic acid, pentadecanoic acid, heptadecanoic acid, and adipic acid) were obtained from Sigma-Aldrich. Valeryl-carnitine was acquired from LGC-Standards (Wesel, Germany), 15-methylhexadecanoic acid was obtained from Lardan (Solna, Sweden), and 3-methylglutaryl-carnitine was purchased at Avanti Polar Lipids (Alabaster, AL).

Synthesis of reference substances

O-acylated acylcarnitines were synthesized from carnitine chloride and free fatty acids using a modified protocol from Ziegler et al. (14). Briefly, the free fatty acid was incubated with thionyl chloride (15 mg free fatty acid per microliter thionyl chloride) under continuous shaking for 4 h at 70°C to generate fatty acyl chlorides. Carnitine hydrochloride dissolved in trichloroacetic acid was added to the acyl chloride and incubated at 45°C for 18 h. After cooling, the product was precipitated and washed three times in cold diethyl ether. Sodium-(s)- β -hydroxyisobutyric acid was first treated with hydrochloric acid to produce the free fatty acid, followed by evaporation of water at 90°C for 30 min, before incubation with thionyl chloride. For (S)- and (R)- β -hydroxybutyric

acid and for (S)- β -hydroxyisobutyric acid, this protocol generated a racemic mixture of both (S)- and (R)- stereoisomers.

Sample preparation and derivatization

Plasma (10 μ l) was dissolved in 100 μ l ice-cold methanol containing the IS mixture under ultra-sonication to prevent sample aggregation. Dissolved samples were evaporated to dryness in a vacuum concentrator. Tissue samples were first grounded in liquid nitrogen using pestle and mortar. Forty milligrams of tissue were then extracted using 1,800 μ l 100% ice-cold methanol and centrifuged at 10,000 g, 4°C for 10 min. IS was added to 200 μ l of the supernatant before vacuum-drying the samples.

Acylcarnitines were derivatized to their butyl esters as described by Gucciardi et al. (9). Briefly, 100 μ l *n*-butanol containing 5% v/v acetyl chloride was added to the dried samples, incubated at 60°C for 20 min at 800 rpm (Eppendorf Thermomixer Comfort; Eppendorf, Hamburg, Germany) and subsequently evaporated to dryness. Samples were reconstituted in 100 μ l (for plasma samples) or 200 μ l (for tissue samples) methanol/water and transferred to glass vials.

LC-MS/MS

The analysis was performed on a triple quadrupole QTRAP5500 LC-MS/MS system (AB Sciex, Framingham, MA), equipped with a 1200 series binary pump, a degasser, and a column oven (Agilent, Santa Clara, CA) connected to a HTC pal autosampler (CTC Analytics, Zwingen, Switzerland). A Turbo V ion spray source operating in positive ESI mode was used for ionization. The source settings were: ion spray voltage, 5,500 V; heater temperature, 600°C; source gas 1, 50 psi; source gas 2, 50 psi; curtain gas, 40 psi; and collision gas (CAD), medium.

Chromatographic separation was achieved on a Zorbax Eclipse XDB-C18 column (length 150 mm, internal diameter 3.0 mm, particle size 3.5 μ m; Agilent) at a column temperature of 50°C. Eluent A consisted of 0.1% formic acid, 2.5 mM ammonium acetate, and 0.005% HFBA in water. Eluent B consisted of 0.1% formic acid, 2.5 mM ammonium acetate, and 0.005% HFBA in acetonitrile. Gradient elution was performed with the following program: 100% A (0.5 ml/min) for 0.5 min, a linear decrease to 65% A (0.5 ml/min) for 2.5 min, hold for 3 min, a linear decrease to 40% A (0.5 ml/min) for 3.7 min, a linear decrease to 5% A (0.5 ml/min) for 1 min. Elution was then carried out at 100% B (1 ml/min) for 0.5 min, hold for 7.3 min (1.5 ml/min). Re-equilibration was finally performed at 100% A (0.5 ml/min) for 4 min. The complete running time of the program was 22 min. Analytes were measured in scheduled multiple reaction monitoring (MRM) (total scan time, 0.5 s; scan time window, 0.5 min). Quadrupoles were working at unit resolution.

Calibration and quantification

Calibration was achieved by spiking plasma and liver samples with different quantities of acylcarnitine standards. A ten-point calibration was performed by addition of increasing amounts of each standard and IS, as described in the sample preparation section. Calibration curves were constructed and fitted by linear regression without weighting. Data analysis was done using Analyst 1.5[®] software (AB Sciex).

Animal experiment and sample collection

C57BL6/N mice ($n = 10$), at an age of 12 weeks, were injected intraperitoneally with a single dose of STZ (180 mg/kg body weight dissolved in 0.1 M citric acid buffer) and mice ($n = 10$) injected intraperitoneally with citric acid buffer served as controls. All mice were fed a standard chow diet (ssniff V1534-0 R/M-H) and were not fasted prior to sampling of blood and organs. Body

weight and blood glucose levels were measured daily using tail-vein puncture. After 5 days, mice were anesthetized with isoflurane. Blood was collected into EDTA-coated tubes and was centrifuged for 10 min at 1,200 *g* and 4°C. Plasma was separated and snap-frozen in liquid nitrogen. Mice were euthanized and liver tissue was collected and immediately snap-frozen in liquid nitrogen. All samples were stored at -80°C until the day of measurement. The research was conducted in conformity with the Public Health Service policy on humane care and use of laboratory animals. All experiments were performed according to the German guidelines for animal care and were approved by the state of Bavaria (Regierung von Oberbayern) ethics committee (reference number 55.2.1-54-2532-22-11).

Statistical analysis

Levels of significance between metabolite concentrations in STZ-treated and control mice were assessed using two-sided independent Student's *t*-tests.

RESULTS

Sample extraction and derivatization

Extraction of acylcarnitine species from plasma and tissue samples was achieved using methanol and analytes were derivatized to their butyl esters. Because dicarboxylic acylcarnitines were derivatized at both carboxyl groups (see Fig. 1), we could discriminate various isobaric acylcarnitines, which have different masses as corresponding butyl esters [e.g., hydroxybutyryl-carnitine (C4-OH-CN, nonderivatized *m/z* 248, butylated *m/z* 304) and malonyl-carnitine (C3:0-DC-CN, nonderivatized *m/z* 248, butylated *m/z* 360)].

Acylcarnitine fragmentation

Mass spectrometric analysis of acylcarnitine species was performed using ESI in positive mode and product ion

spectra were acquired. Butylation of acylcarnitines (especially of dicarboxylic species) increased the ionization efficiency (data not shown). Representative fragmentation patterns for valeryl-carnitine (C5:0-CN; monocarboxylic) and 3-methylglutaryl-carnitine (C5:0-M-DC-CN; dicarboxylic) are shown in Fig. 1. Fragmentation patterns of acylcarnitines were reported to have a prominent fragment ion at *m/z* 85 in common (15). This fragment ion displayed the highest intensity in our measurements and was thus used for quantification. It is proposed to be formed due to loss of the butyl group(s) (*m/z* 56), the acyl chain [*m/z* 102 and *m/z* 146 for valeryl-carnitine (C5:0-CN) and 3-methylglutaryl-carnitine (C5:0-M-DC-CN), respectively], and the trimethylamine fragment (*m/z* 59), as initially described by Chace et al. (15) in 1997. A compilation of all acylcarnitine species covered by our method, including the corresponding MS parameters, is shown in Table 1.

Chromatographic separation and identification of isomeric acylcarnitine species

Because all acylcarnitines form a similar product ion (*m/z* 85) and many compounds are isobaric or occur as positional isomers, appropriate chromatographic separation is essential. Chromatographic separation was established using a C18-reversed phase HPLC column (length, 15 cm; internal diameter, 3.0 mm; particle size, 3.5 μm). We favored an HPLC column over an ultra-performance LC column, because larger sample volumes of complex matrices were injected. Peaks were well shaped, sharp (~0.1 min; Fig. 2), and well separated. A coelution of analyte and IS was achieved, which is important to compensate for matrix effects and varying ionization efficiencies during gradient elution (16). The addition of HFBA to the eluents as an ion-pairing reagent (17) improved peak

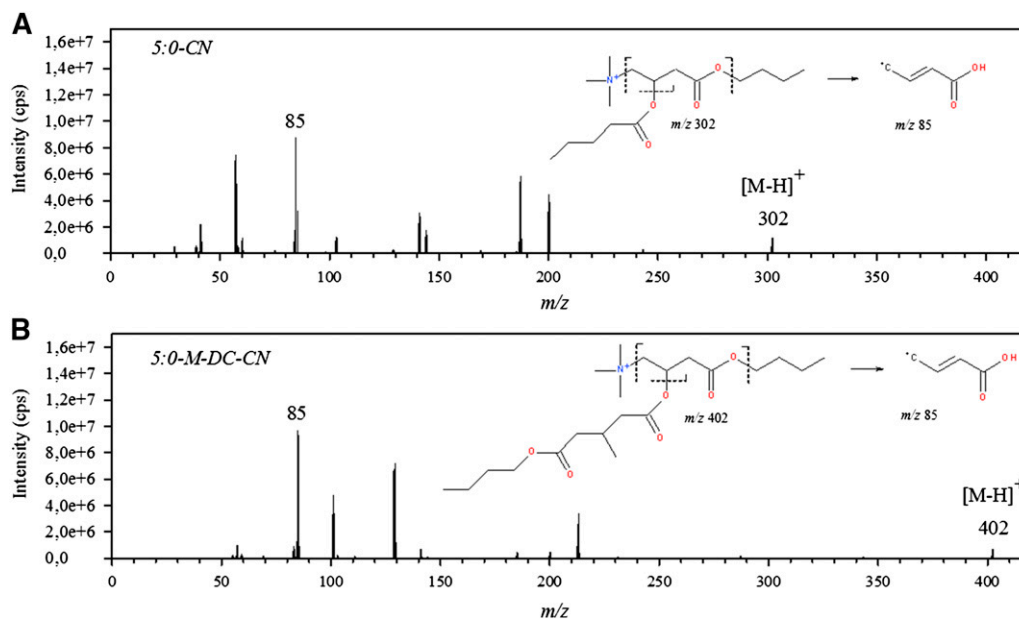


Fig. 1. Product ion spectra and proposed fragmentation patterns for valeryl-carnitine (C5:0-CN) (A) and 3-methylglutaryl-carnitine (C5-M-DC-CN) (B).

TABLE 1. MS parameters and retention times

		MRM (<i>m/z</i>)	IS	IS MRM (<i>m/z</i>)	Retention Time (min)	DP (V)	EP (V)	CE (V)	CXP (V)
Free carnitine	C0	218.1 → 85.1	d ₀ -C0	227.5 → 85.1	5.9	61	10	23	15
Hydroxypropionyl-carnitine	C3-OH	290.1 → 85.1	d ₃ -C3	277.1 → 85.1	6.1	53	10	30	15
Hydroxybutyryl-carnitine a	C4-OH a	304.1 → 85.1	d ₃ -C4	291.4 → 85.1	6.2	55	10	32	15
Hydroxybutyryl-carnitine b	C4-OH b	304.1 → 85.1	d ₃ -C4	291.4 → 85.1	6.3	55	10	32	15
3-Hydroxyisobutyryl-carnitine	2-M-C3-OH	304.1 → 85.1	d ₃ -C4	291.4 → 85.1	6.4	55	10	32	15
Acetyl-carnitine	C2	260.5 → 85.1	d ₃ -C2	263.2 → 85.1	6.4	41	10	18	15
Hydroxyvaleryl-carnitine	C5-OH	318.1 → 85.1	d ₀ -C5	311 → 85.1	6.5	58	10	33	15
Propionyl-carnitine	C3:0	274.4 → 85.1	d ₃ -C3	277.1 → 85.1	6.9	46	10	29	15
Hydroxyhexanoyl-carnitine a	C6-OH a	332.2 → 85.1	d ₃ -C6	319.2 → 85.1	7.3	61	10	35	15
Crotonyl-carnitine	C4:1	286.1 → 85.1	d ₃ -C4	291.4 → 85.1	7.3	52	10	29	15
Hydroxyhexanoyl-carnitine b	C6-OH b	332.2 → 85.1	d ₃ -C6	319.2 → 85.1	7.5	61	10	35	15
Methacrylyl-carnitine	2-M-C3:1	286.1 → 85.1	d ₃ -C4	291.4 → 85.1	7.5	52	10	29	15
Isobutyryl-carnitine	2-M-C3:0	288.2 → 85.1	d ₃ -C4	291.4 → 85.1	7.8	46	10	29	15
Butyryl-carnitine	C4:0	288.2 → 85.1	d ₃ -C4	291.4 → 85.1	8	46	10	29	15
Tiglyl-carnitine	2-M-C4:1	300.2 → 85.1	d ₀ -C5	311 → 85.1	8.2	55	10	31	15
3-Methylcrotonyl-carnitine	3-M-C4:1	300.2 → 85.1	d ₀ -C5	311 → 85.1	8.4	55	10	31	15
2-Methyl-butyl-carnitine	2-M-C4:0	302.1 → 85.1	d ₀ -C5	311 → 85.1	9.5	46	10	29	15
Isovaleryl-carnitine	3-M-C4:0	302.1 → 85.1	d ₀ -C5	311 → 85.1	9.6	46	10	29	15
Valeryl-carnitine	C5:0	302.1 → 85.1	d ₀ -C5	311 → 85.1	9.7	46	10	29	15
Fumaryl-carnitine	C4:1-DC	372.5 → 85.1	d ₅ -C5-DC	394.2 → 85.1	9.9	56	10	27	15
Malonyl-carnitine	C3-DC	360.2 → 85.1	d ₅ -C5-DC	394.2 → 85.1	10.3	55	10	32	15
Succinyl-carnitine	C4-DC	374.2 → 85.1	d ₅ -C5-DC	394.2 → 85.1	10.8	56	10	33	15
Hexanoyl-carnitine	C6:0	316.4 → 85.1	d ₃ -C6	319.2 → 85.1	10.9	56	10	27	15
Methyl-malonyl-carnitine	C3-DC-M	374.2 → 85.1	d ₅ -C5-DC	394.2 → 85.1	11.1	58	10	33	15
Glutaryl-carnitine	C5-DC	388.3 → 85.1	d ₅ -C5-DC	394.2 → 85.1	11.1	61	10	35	15
Glutaconyl-carnitine	C5:1-DC	386.3 → 85.1	d ₅ -C5-DC	394.2 → 85.1	11.2	60	10	35	15
Adipyl-carnitine	C6-DC	402.3 → 85.1	d ₅ -C5-DC	394.2 → 85.1	11.3	63	10	37	15
Methylglutaryl-carnitine	C5-M-DC	402.3 → 85.1	d ₅ -C5-DC	394.2 → 85.1	11.4	63	10	37	15
Heptanoyl-carnitine	C7:0	330.2 → 85.1	d ₃ -C6	319.2 → 85.1	11.5	60	10	30	15
Pimelyl-carnitine	C7-DC	416.3 → 85.1	d ₅ -C5-DC	394.2 → 85.1	11.7	66	10	39	15
Octanoyl-carnitine	C8:0	344.1 → 85.1	d ₃ -C8	347.4 → 85.1	11.9	66	10	33	15
Decenoyl-carnitine	C10:1	370.2 → 85.1	d ₃ -C10	375.2 → 85.1	12.1	68	10	40	15
Nonanoyl-carnitine	C9:0	358.2 → 85.1	d ₃ -C8	347.4 → 85.1	12.1	66	10	39	15
Decanoyl-carnitine	C10:0	372.2 → 85.1	d ₃ -C10	375.2 → 85.1	12.3	56	10	37	15
Iso-undecanoyl-carnitine	Iso-C11:0	386.3 → 85.1	d ₃ -C10	375.2 → 85.1	12.4	65	10	40	15
Undecanoyl-carnitine	C11:0	386.3 → 85.1	d ₃ -C10	375.2 → 85.1	12.5	65	10	40	15
Tetradecadienyl-carnitine	C14:2	424.3 → 85.1	d ₃ -C14	431.2 → 85.1	12.6	78	10	47	15
Dodecanoyl-carnitine	C12:0	400.3 → 85.1	d ₃ -C12	403.2 → 85.1	12.7	73	10	44	15
Hydroxyhexadecenyl-carnitine	C16:1-OH	470.3 → 85.1	d ₃ -C16	459.2 → 85.1	12.8	87	10	53	15
Isotridecanoyl-carnitine	Iso-C13:0	414.3 → 85.1	d ₃ -C12	403.2 → 85.1	13	80	10	45	15
Tridecanoyl-carnitine	C13:0	414.3 → 85.1	d ₃ -C12	403.2 → 85.1	13.1	80	10	45	15
Hexadecadienyl-carnitine	C16:2	452.3 → 85.1	d ₃ -C16	459.2 → 85.1	13.1	83	10	51	15
Tetradecanoyl-carnitine	C14:0	428.3 → 85.1	d ₃ -C14	431.2 → 85.1	13.4	86	10	45	15
Hydroxyhexadecanoyl-carnitine a	C16-OH a	472.3 → 85.1	d ₃ -C16	459.2 → 85.1	13.4	87	10	53	15
Hydroxyhexadecanoyl-carnitine b	C16-OH b	472.3 → 85.1	d ₃ -C16	459.2 → 85.1	13.5	87	10	53	15
Hydroxyoctadecenyl-carnitine	C18:1-OH	498.4 → 85.1	d ₃ -C18	487.5 → 85.1	13.5	92	10	57	15
Hexadecenyl-carnitine	C16:1	454.3 → 85.1	d ₃ -C16	459.2 → 85.1	13.6	84	10	51	15
Isopentadecanoyl-carnitine	iso-C15:0	442.3 → 85.1	d ₃ -C14	431.2 → 85.1	13.6	85	10	48	15
Pentadecanoyl-carnitine	C15:0	442.3 → 85.1	d ₃ -C14	431.2 → 85.1	13.7	85	10	48	15
Octadecadienyl-carnitine	C18:2	480.3 → 85.1	d ₃ -C18	487.5 → 85.1	13.7	89	10	54	15
Hexadecanoyl-carnitine	C16:0	456.5 → 85.1	d ₃ -C16	459.2 → 85.1	14.3	84	10	51	15
Octadecenyl-carnitine	C18:1	482.3 → 85.1	d ₃ -C18	487.5 → 85.1	14.3	89	10	55	15
Isoheptadecanoyl-carnitine	Iso-C17:0	470.4 → 85.1	d ₃ -C16	459.2 → 85.1	14.7	90	10	57	15
Heptadecanoyl-carnitine	C17:0	470.4 → 85.1	d ₃ -C16	459.2 → 85.1	14.8	90	10	57	15
Dodecadiolyl-carnitine	C12-DC	486.4 → 85.1	d ₅ -C5-DC	394.2 → 85.1	15.6	86	10	45	15
Octadecanoyl-carnitine	C18:0	484.4 → 85.1	d ₃ -C18	487.5 → 85.1	15.6	96	10	63	15

DP, declustering potential; EP, entrance potential; CE, collision energy; CXP, collision cell exit potential.

separation and peak sharpness. Addition of ammonium acetate enhanced ionization efficiency. Figure 2A shows a typical chromatogram (total ion count) derived from a liver sample containing acylcarnitines ranging from 0 to 18 carbon atoms. Retention times increased with the number of carbons and decreased with the number of double bonds. Because >50 mass transitions were required to quantify all metabolites, data were acquired in the scheduled MRM mode to yield more and shorter scan cycles per peak, to facilitate peak integration and data analysis.

Various acylcarnitine isomer species were expected to result from known amino acid and fatty acid breakdown pathways (18). Indeed, chromatographic separation generated multiple peaks for various *m/z* transitions [e.g., 2-methylbutyryl-carnitine (2-M-C4:0-CN), 3-methylbutyryl-carnitine (3-M-C4:0-CN), and valeryl-carnitine (C5:0-CN)]. For peak identification, matrix samples were spiked with individual acylcarnitine reference compounds as shown in Fig. 2B–D. In general, for saturated acylcarnitines, branched-chain forms elute earlier than straight-chain

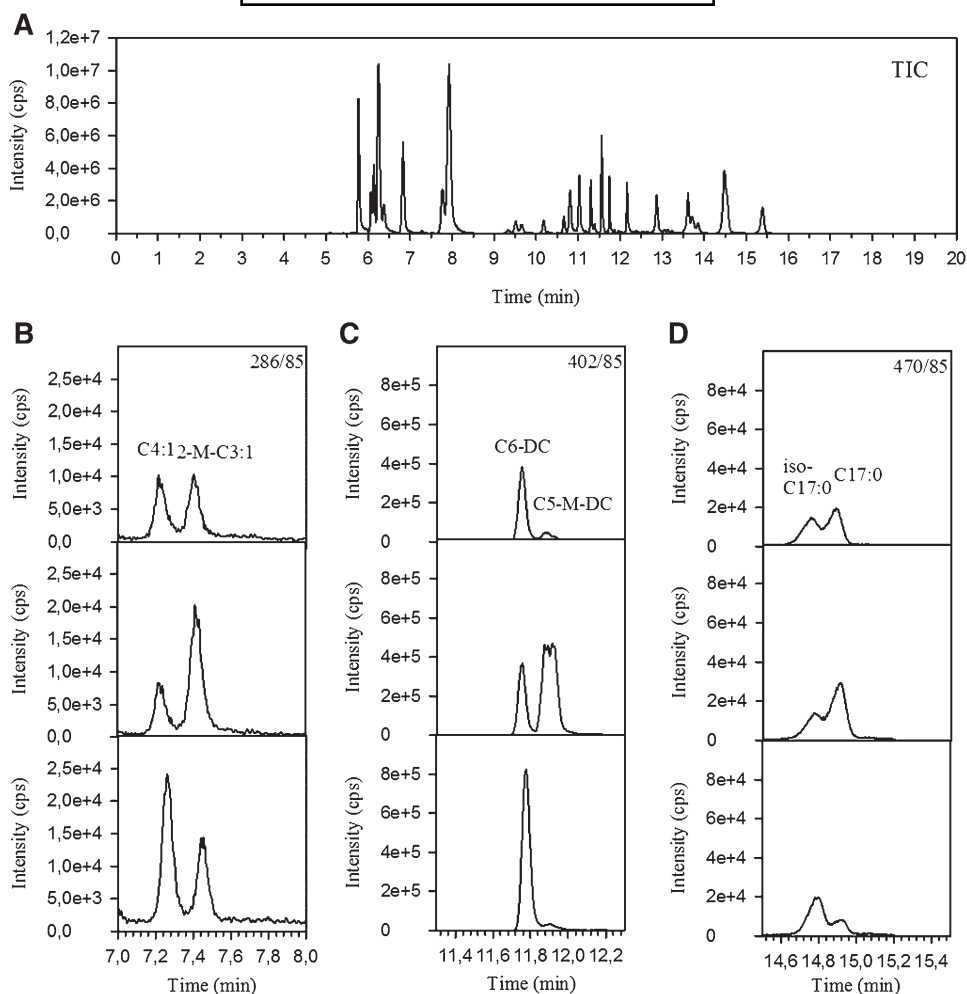


Fig. 2. Total ion count (TIC) chromatogram (A) and MRM chromatograms of exemplified spiking experiments (B–D).

forms [e.g., isobutyryl-carnitine (2-M-C3:0-CN) < butyryl-carnitine (C4:0-CN)]. This was also true for odd-numbered acylcarnitines, for which two peaks were generally found (see Fig. 2D). In contrast, for monounsaturated and dicarboxylic acylcarnitines, branched-chain forms eluted later [e.g., crotonyl-carnitine (C4:1-CN) < methacrylyl-carnitine (2-M-C3:1-CN), see Fig. 2B, C]. Furthermore, hydroxy-acylcarnitines [hydroxybutyryl-carnitine (C4-OH-CN), hydroxyhexanoyl-carnitine (C6-OH-CN), hydroxyhexadecanoyl-carnitine (C16-OH-CN)], displayed two peaks. This was in accordance with previous reports suggesting the presence of S- and R-stereoisomers (9, 11, 19).

Calibration and quantification

For quantification of metabolite concentrations and to compensate for variation in sample preparation and ionization efficiency, an acylcarnitine standard mixture containing 13 deuterium-labeled acylcarnitine species was added to the samples (Table 2). Calibration lines were generated by addition of different concentrations of acylcarnitine species to a pool of liver and plasma samples. The ratio between analyte and IS was used for quantification (“stable isotope dilution”). For those analytes without

corresponding IS, analyte-IS pairs were selected according to the closest retention times and the best accuracies for these analyte-IS allocations [e.g., nonanoyl-carnitine (C9:0-CN) to d_3 -octanoyl-carnitine (d_3 -C8:0-CN)]. For all analytes and matrices, calibration curves were linear and correlation coefficients (r^2) were greater than 0.99 (Table 2). Limits of detection (LODs) were determined as the signal-to-noise ratio of three, and limits of quantitation (LOQs) were calculated as the triple fold of the LOD and were sufficient enough for quantification of acylcarnitine species in plasma and liver samples (Table 2).

Method validation and sample stabilities

The accuracy of the method was tested in three liver and three plasma samples by spiking with acylcarnitine standards in concentrations covering the whole calibration range. Accuracies between 81 and 108% were found for the liver matrix and between 89 and 120% for the plasma matrix (Table 3), except for the lowest levels of free carnitine in liver tissues for which concentrations were overestimated. Method reproducibility was examined by determining intra- and inter-day precisions in pools of plasma and liver

TABLE 2. Calibration data

	Calibration Data (Plasma Matrix)				Calibration Data (Liver Matrix)							
	Calibration Range (pmol/ μ l)	IS (pmol/ μ l)	Slope	R ²	LOD (pmol/ μ l)	LOQ (pmol/ μ l)	Calibration Range (pmol/mg w.w.)	IS Added (pmol/mg w.w.)	Slope	Correlation Coefficient (R ²)	LOD (pmol/mg w.w.)	LOQ (pmol/mg w.w.)
C0	1.5–500	7.70	0.28	0.999	0.089	0.266	1.5–1,000	180.55	0.0088	0.990	0.275	0.824
C2	0.375–125	3.21	0.34	0.999	0.038	0.113	0.375–250	75.21	0.0099	0.999	0.074	0.222
C3	0.075–25	0.84	1.37	0.999	0.008	0.024	0.075–50	19.78	0.0389	0.999	0.003	0.008
C4	0.075–25	0.42	3.40	0.999	0.008	0.023	0.075–50	9.89	0.098	0.999	0.008	0.011
2-M-C3	0.075–25	0.42	3.49	0.999	0.007	0.021	0.075–50	9.89	0.101	0.999	0.004	0.012
C5	0.075–25	0.38	5.67	0.999	0.006	0.018	0.075–50	8.97	0.159	0.999	0.003	0.009
3-M-C4	0.075–25	0.38	5.95	0.999	0.007	0.021	0.075–50	8.97	0.158	0.999	0.003	0.009
C6	0.075–25	0.45	3.18	0.999	0.013	0.038	0.075–50	10.58	0.098	0.999	0.008	0.024
C8	0.075–25	0.41	2.27	0.997	0.006	0.020	0.075–50	9.66	0.071	0.999	0.002	0.006
C10	0.075–25	0.45	2.43	0.993	0.009	0.028	0.075–50	10.58	0.083	0.999	0.005	0.014
C12	0.15–50	0.42	2.45	0.992	0.009	0.027	0.15–100	9.89	0.093	0.999	0.004	0.012
C14	0.15–50	0.40	2.56	0.996	0.009	0.028	0.15–100	9.43	0.104	0.999	0.003	0.009
C16	0.15–50	0.80	1.80	0.998	0.002	0.007	0.15–100	18.86	0.064	0.999	0.002	0.005
C18	0.15–50	0.73	1.31	0.994	0.021	0.065	0.15–100	17.02	0.049	0.999	0.021	0.063

Calibration lines were generated by plotting the area ratios of analyte/IS against the spiked concentrations. Concentrations in liver are given per milligram of liver wet weight. w.w., wet weight.

samples (Table 4). With a few exceptions, intra- and inter-day coefficients of variation (CVs) for liver and plasma samples were below 10% for high-abundant acylcarnitines (>0.01 pmol/mg tissue; >0.01 pmol/ μ l plasma) and between 10 and 20% for low-abundant acylcarnitines. Recoveries were calculated as the difference between area ratios of prespiked samples (addition of standards before extraction) and postspiked samples (addition of standards to the methanol extract). Recoveries between 59 and 99% were found (supplementary Table 1). Matrix effects were determined by comparing the peak areas of acylcarnitine species spiked in matrix samples (three plasma and three liver samples) and corresponding amounts dissolved in methanol at two levels (supplementary Tables 2, 3). The area ratios of spiked acylcarnitine species in plasma samples ranged between 110 and 120% compared with nonmatrix samples. Area ratios of spiked acylcarnitine species in liver were between 85 and 122% compared with nonmatrix samples, with a few exceptions for short-chain species.

To assess sample stability in plasma, samples were stored at room temperature for 1 h before extraction and peak areas were compared with samples that were directly extracted. Acylcarnitines in plasma remained stable over 1 h at room temperature. For liver tissue, thawing of samples in three freeze-thaw cycles strongly affected the abundance of various analytes, but postpreparative storage of plasma and liver samples at -20°C showed a high stability of most analytes. See supplementary Table 4 for a summary on plasma and liver sample stabilities.

Method application

The developed method was applied to plasma and liver samples from STZ-treated insulin-deficient and healthy control mice. STZ causes pancreatic β -cell destruction resulting in insulin-deficient type I diabetes (20). STZ-treated animals showed very low circulating insulin levels accompanied by a dramatic weight loss and a severe increase in blood glucose levels 5 days after treatment (see supplementary Table 5).

We found that concentration ranges of acylcarnitine species in plasma and liver were in good agreement with levels reported previously (21), with highest concentrations for saturated short-chain species [acetyl-carnitine (C2:0-CN, \sim 20%), propionyl-carnitine (C3:0-CN, \sim 5%), and butyryl-carnitine (C4:0-CN, \sim 2%)] and lowest concentrations for odd-numbered medium- and long-chain species [undecanoyl-carnitine (C11:0-CN), tridecanoyl-carnitine (C13:0-CN), and pentadecanoyl-carnitine (C15:0-CN)]. Whereas almost all acylcarnitine species could be found in liver samples, the concentrations in plasma were generally far lower and a number of species (especially monounsaturated species like crotonyl- and 3-methyl-crotonyl-carnitine) could not be detected.

Comparison of acylcarnitine concentrations between diabetic and healthy mice revealed strong increases in the concentrations of various branched-chain amino acid-derived compounds in plasma and liver of diabetic mice (Fig. 3A–D). These included leucine-derived isovaleryl-carnitine (3-M-C4-CN) and 3-methylcrotonyl-carnitine (3-M-C4:1-CN) and isoleucine-derived 2-methylbutyryl-carnitine (2-M-C4-CN) and 2-methylcrotonyl-carnitine (2-M-C4:1-CN), as well as propionyl-carnitine (C3-CN) and methylmalonyl-carnitine (C3-M-DC-CN). In contrast, 3-hydroxyisobutyryl-carnitine (2-M-C3-OH-CN), which is derived from valine breakdown, showed a marked decrease, both in plasma and liver. Furthermore, elevated levels of various straight-chain odd-numbered acylcarnitines were observed in diabetic mice, most strongly in liver samples (Fig. 3E, F), whereas decreased levels were found for hexadecenoyl-carnitine (C16:1-CN) in plasma and liver and tetradecenoyl-carnitine (C14:0-CN) in liver. Supplementary Table 6 provides concentrations of all acylcarnitine species quantified in liver and plasma of healthy and diabetic mice in our study.

DISCUSSION

Acylcarnitines have recently gained considerable interest as markers for impairments in fatty acid and amino

TABLE 3. Accuracies

	Liver Spiked		Plasma Spiked	
	(pmol/mg w.w.)	Accuracy (%)	(pmol/ μ l)	Accuracy (%)
C0	30	261.8	20	119.7
	150	87.4	150	95.5
	500	89	300	97.8
C2	7.5	106.7	5	116.1
	37.5	102.7	37.5	97.7
	125	97.1	75	97.9
C3:0	1.5	104.2	1	116.3
	7.5	98.1	7.5	94.2
	25	98.7	15	97.8
C4:0	1.5	96.2	1	115.5
	7.5	101	7.5	92.2
	25	101	15	93.3
2-M-C3:0	1.5	82.9	1	120.0
	7.5	97.2	7.5	93.3
	25	96.4	15	93.9
3-M-C4:0	1.5	84.3	1	113.9
	7.5	94.3	7.5	89.5
	25	94.2	15	96.0
C5:0	1.5	84.1	1	108.3
	7.5	95.8	7.5	91.8
	25	94.1	15	97.6
C6:0	1.5	90.8	1	115.4
	7.5	100.8	7.5	102.6
	25	102	15	100.6
C8:0	1.5	90.3	1	110.1
	7.5	105	7.5	104.7
	25	107.9	15	100.9
C10:0	1.5	86.3	1	109.8
	7.5	99.3	7.5	103.6
	25	98.1	15	106.6
C12:0	3	87.2	2	108.7
	15	95.8	15	107.5
	50	96.5	30	105.7
C14:0	3	89.3	2	119.1
	15	91.7	15	109.2
	50	90	30	105.8
C16:0	3	81.7	2	112.3
	15	90.3	15	102.4
	50	92.4	30	102.1
C18:0	3	82.5	2	107.8
	15	99.6	15	106.0
	50	98.5	30	104.0

The displayed accuracy is the average of the assayed concentration (corrected by endogenous levels of plasma and liver samples) in percent of the actual spiked concentration. Concentrations in liver are given per milligram of liver wet weight. w.w., wet weight.

acid oxidation associated with the metabolic syndrome (5–7). Moreover, the metabolites were proposed to have predictive quality for disease initiation and progression (5). Various acylcarnitines occur as positional isomers and many species often appear at very low concentrations. Even though several LC-MS/MS methods have been described for quantification of isomeric acylcarnitine species (9–12), a comprehensive method that covers low-abundant species and includes odd-numbered acylcarnitines is lacking.

Here we describe a sensitive and robust method for quantification of individual isomeric acylcarnitine species, including low-abundant amino acid-derived forms (see Fig. 4). In addition, our method includes acylcarnitines with odd-numbered acyl-chain lengths, which gained increased attention recently as metabolite markers in disease states (5, 22, 23).

We applied ESI in positive mode for ionization. Collision-induced dissociation produced an intense product

ion at m/z 85 for all analytes, which was described to be a specific product ion of acylcarnitine fragmentation (15). LC with a C18-reversed phase HPLC column allowed the chromatographic separation of isomeric acylcarnitine species, and by spiking with reference compounds, we could subsequently assign the individual isomers to the respective peaks. Proper chromatographic separation is mandatory because positional isomers have similar mass transitions [e.g., crotonyl-carnitine (C4:1-CN) and methacrylyl-carnitine (2-M-C3:1-CN), m/z 286 \rightarrow m/z 85]. In addition, quantification of acylcarnitine concentrations in a direct infusion approach is challenged by potential interfering matrix components which lead to an overestimation of analyte concentrations (9). Although a separation of underivatized acylcarnitine isomers has been described (11), we applied a butylation to achieve an enhanced sensitivity, particularly for dicarboxylic acylcarnitines, as described previously (24). To further improve chromatographic separation and to enhance peak shapes, the ion pairing agent, HFBA, was added to the eluents in very low concentrations (0.005%). HFBA was favored over the stronger trifluoroacetic acid, which is more commonly used (9), because trifluoroacetic acid causes very strong ion suppression (25). We could achieve baseline separation of all acylcarnitine species including positional isomers, and all peaks were well shaped. The total running time of 22 min is in the range of other reported methods (9–11).

Calibration was performed by stable isotope dilution. A coelution of standards and available ISs was achieved, which is important for compensation of matrix effects and differences in ionization efficiency (16). LODs and LOQs were sufficient to determine analytes in plasma and/or liver (supplementary Table 6). In addition, we observed that matrix effects of liver tissue are comparable to other tissue types such as muscle, heart, or kidney tissue, and thus suggest that the method can be applied to other tissues to determine analyte concentrations in these matrices (data not shown). Importantly, extraction of increased tissue quantities (>40 mg) does not improve method performance, because this leads to increased noise and reduced signal-to-noise ratios. In general, for comparison of analyte concentrations between samples, it is recommended to extract similar quantities of tissue to reduce variation resulting from matrix effects.

To evaluate LC-MS/MS method performance, we validated our method in plasma and liver samples as described previously (26). Precisions showed CVs <15% for high-abundant metabolites and CVs <20% for low-abundant compounds. Accuracies displayed CVs of \pm 10% with a few exceptions. This is a major improvement over previously published methods, for which up to 30% variation was reported in plasma (9), or for which no measures were reported at all (11). We observed that plasma samples were stable when stored for 1 h at room temperature prior to preparation. Furthermore, most acylcarnitine species in plasma and liver showed a high postpreparative stability.

TABLE 4. Intra- and inter-day precisions

Name	Intra-day Liver (n = 5)		Inter-day Liver (n = 5)		Intra-day Plasma (n = 5)		Inter-day Plasma (n = 5)	
	Mean ± SD (pmol/mg w.w.)	CV (%)	Mean ± SD (pmol/mg w.w.)	CV (%)	Mean ± SD (pmol/μl)	CV (%)	Mean ± SD (pmol/μl)	CV (%)
C0	230.91 ± 17.61	7.6	228.47 ± 9.35	4.1	34.99 ± 3.29	9.4	33.34 ± 2.01	6.1
C3-OH	0.0098 ± 0.001	14.6	0.013 ± 0.001	13.2	—	—	—	—
C4-OH a	1.62 ± 0.099	6.1	1.71 ± 0.075	4.4	0.051 ± 0.01	12.7	0.049 ± 0.01	15.4
C4-OH b	3.89 ± 0.21	5.5	4.09 ± 0.10	2.5	0.10 ± 0.01	11.7	0.098 ± 0.01	7.8
2-M-C3-OH	0.17 ± 0.006	4.2	0.17 ± 0.009	5.5	0.062 ± 0.00	14.2	0.059 ± 0.00	8.3
C2	60.01 ± 5.23	8.7	61.26 ± 2.34	3.8	16.73 ± 1.34	8.0	15.34 ± 0.69	4.6
C5-OH	0.68 ± 0.056	8.3	0.67 ± 0.015	2.3	0.067 ± 0.00	10.6	0.067 ± 0.00	14.3
C3:0	12.73 ± 1.31	10.3	12.69 ± 0.48	3.8	0.52 ± 0.05	9.7	0.51 ± 0.04	9.7
C6-OH a	0.14 ± 0.013	9.8	0.14 ± 0.003	2.2	0.005 ± 0.00	10.4	0.005 ± 0.00	14.5
C4:1	0.0046 ± 0.000	8.4	0.0046 ± 0.000	11.5	0.003 ± 0.00	11.0	0.003 ± 0.00	11.4
C6-OH b	0.051 ± 0.004	9.3	0.051 ± 0.002	4.0	0.005 ± 0.00	12.3	0.005 ± 0.00	15.2
2-M-C3:1	0.010 ± 0.001	11.9	0.0099 ± 0.001	13.2	—	—	—	—
2-M-C3:0	1.29 ± 0.10	8.0	1.35 ± 0.094	7.0	0.16 ± 0.01	9.5	0.15 ± 0.01	10.3
C4:0	5.34 ± 0.45	8.5	5.40 ± 0.22	4.1	0.45 ± 0.04	8.9	0.43 ± 0.03	9.3
2-M-C4:1	0.011 ± 0.001	17.8	0.011 ± 0.000	7.3	0.005 ± 0.00	8.9	0.005 ± 0.00	12.9
3-M-C4:1	0.0053 ± 0.000	13.8	0.0049 ± 0.000	13.8	—	—	—	—
2-M-C4:0	0.72 ± 0.060	8.4	0.70 ± 0.026	3.8	0.054 ± 0.00	12.3	0.054 ± 0.00	12.4
3-M-C4:0	0.18 ± 0.018	10.1	0.18 ± 0.008	5.0	0.070 ± 0.00	9.7	0.070 ± 0.00	11.3
C5:0	1.56 ± 0.17	10.8	1.56 ± 0.072	4.6	0.011 ± 0.00	11.4	0.011 ± 0.00	11.0
C4:1-DC	0.024 ± 0.002	11.4	0.025 ± 0.002	12.2	0.001 ± 0.00	12.7	0.001 ± 0.00	14.2
C3-DC	4.61 ± 0.44	9.5	4.78 ± 0.23	4.7	0.039 ± 0.00	11.1	0.038 ± 0.00	11.0
C4-DC	1.51 ± 0.16	10.6	1.49 ± 0.039	2.6	0.029 ± 0.00	8.8	0.029 ± 0.00	9.3
C6:0	1.33 ± 0.13	10.0	1.31 ± 0.059	4.6	0.068 ± 0.00	10.9	0.066 ± 0.00	10.3
C3-DC-M	0.11 ± 0.010	9.6	0.11 ± 0.010	10.0	0.010 ± 0.00	18.6	0.011 ± 0.00	16.8
C5-DC	5.87 ± 0.53	9.0	5.84 ± 0.13	2.3	0.032 ± 0.00	11.7	0.030 ± 0.00	11.0
C5:1-DC	0.91 ± 0.16	17.1	0.92 ± 0.074	8.1	0.017 ± 0.00	13.2	0.020 ± 0.00	12.1
C6-DC	4.92 ± 0.53	10.9	4.81 ± 0.20	4.2	—	—	—	—
C5-M-DC	0.095 ± 0.014	15.3	0.097 ± 0.009	9.3	0.043 ± 0.00	10.7	0.039 ± 0.00	8.1
C7:0	0.19 ± 0.026	14.0	0.20 ± 0.013	6.8	0.001 ± 0.00	19.9	0.001 ± 0.00	17.0
C7-DC	2.59 ± 0.27	10.3	2.53 ± 0.10	4.1	0.011 ± 0.00	9.1	0.010 ± 0.00	10.8
C8:0	0.19 ± 0.017	8.9	0.20 ± 0.006	3.2	0.009 ± 0.00	9.0	0.008 ± 0.00	12.5
C10:1	—	—	—	—	0.004 ± 0.00	11.8	0.007 ± 0.00	19.5
C9:0	0.038 ± 0.003	10.3	0.038 ± 0.002	5.7	—	—	—	—
C10:0	0.10 ± 0.010	10.9	0.092 ± 0.008	9.2	0.010 ± 0.00	13.6	0.009 ± 0.00	14.9
Iso-C11:0	0.0094 ± 0.000	17.7	0.0086 ± 0.000	3.1	—	—	—	—
C11:0	0.0055 ± 0.000	18.6	0.0060 ± 0.001	12.7	—	—	—	—
C14:2	0.047 ± 0.002	5.1	0.044 ± 0.005	12.5	0.001 ± 0.00	10.9	0.001 ± 0.00	19.9
C12:0	0.090 ± 0.011	13.2	0.082 ± 0.002	3.1	0.015 ± 0.00	19.9	0.013 ± 0.00	19.8
C16:1-OH	0.031 ± 0.013	44.6	0.033 ± 0.004	12.5	—	—	—	—
Iso-C13:0	0.0035 ± 0.000	20.0	0.0039 ± 0.000	14.2	0.000 ± 2.37	7.9	0.000 ± 3.54	12.6
C13:0	0.0035 ± 0.000	18.4	0.0039 ± 0.000	14.2	0.001 ± 0.00	18.8	0.001 ± 0.00	16.8
C16:2	0.089 ± 0.009	10.3	0.087 ± 0.003	4.4	0.011 ± 0.00	18.4	0.010 ± 0.00	25.3
C14:0	0.22 ± 0.021	9.5	0.21 ± 0.009	4.3	0.048 ± 0.00	16.5	0.044 ± 0.00	19.6
C16-OH a	0.050 ± 0.005	10.3	0.049 ± 0.002	4.7	0.003 ± 0.00	19.0	0.010 ± 0.00	24.7
C16-OH b	0.0098 ± 0.001	13.4	0.0098 ± 0.001	11.1	0.002 ± 0.00	16.3	0.002 ± 0.00	23.7
C18:1-OH	0.11 ± 0.022	19.5	0.13 ± 0.013	10.6	—	—	—	—
C16:1	0.54 ± 0.053	10.0	0.57 ± 0.021	3.8	0.049 ± 0.00	18.9	0.045 ± 0.01	31.1
Iso-C15:0	0.011 ± 0.001	15.2	0.030 ± 0.001	3.8	0.001 ± 0.00	18.7	0.000 ± 0.00	20.0
C15:0	0.012 ± 0.000	6.5	0.011 ± 0.001	9.6	0.002 ± 0.00	15.2	0.002 ± 0.00	13.5
C18:2	1.45 ± 0.18	12.6	1.50 ± 0.049	3.3	0.051 ± 0.01	20.9	0.051 ± 0.01	38.7
C16:0	1.40 ± 0.12	8.3	1.35 ± 0.050	3.7	0.18 ± 0.03	19.5	0.17 ± 0.03	18.5
C18:1	2.67 ± 0.25	9.4	2.74 ± 0.045	1.7	0.11 ± 0.02	22.6	0.11 ± 0.03	36.9
Iso-C17:0	0.019 ± 0.001	9.8	0.018 ± 0.000	4.4	0.001 ± 0.00	16.3	0.001 ± 0.00	17.4
C17:0	0.029 ± 0.004	14.2	0.025 ± 0.001	6.9	0.001 ± 0.00	16.1	0.001 ± 0.00	14.0
C12-DC	0.0048 ± 0.000	18.2	0.0045 ± 0.001	24.1	—	—	—	—
C18:0	0.91 ± 0.081	9.0	0.93 ± 0.038	4.1	0.028 ± 0.00	17.8	0.027 ± 0.00	19.2

Intra- and inter-day precisions were assessed by calculating average concentrations and CVs from five individual plasma and liver samples. Concentrations in liver are given per milligram of liver wet weight. w.w., wet weight.

We applied our method to plasma and liver samples of STZ-treated insulin-deficient mice. STZ is selectively taken up into the pancreas and causes β-cell toxicity via alkylation, resulting in β-cell necrosis (20). STZ-treated mice showed very low circulating insulin levels paralleled by a strong increase in blood glucose and a dramatic decrease in body weight (see supplementary Table 5).

We found that, particularly, the branched-chain acylcarnitines, as intermediates of branched-chain amino acid degradation, were increased in plasma and liver, and among them, most strongly, propionyl-carnitine (C3:0-CN), 2-methylbutyryl-carnitine (2-M-C4:0-CN), and isovaleryl-carnitine (3-M-C4:0-CN), as well as 2-methylcrotonyl-carnitine (2-M-C4:1-CN) and 3-methylcrotonyl-carnitine (3-M-C4:1-CN). Interestingly,

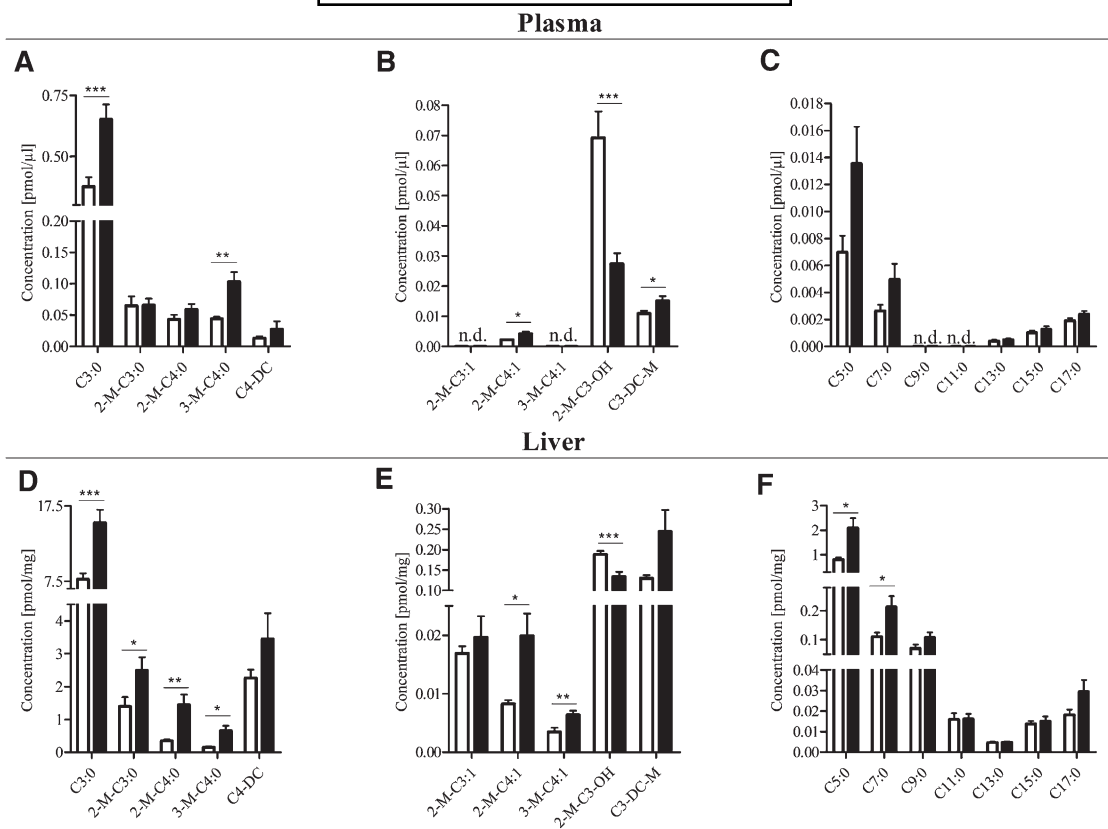


Fig. 3. Levels of acylcarnitine species in plasma and liver tissue samples obtained from STZ-treated animals and controls determined with our LC-MS/MS method. A, D: High-abundant branched-chain amino acid-derived species. B, E: Low-abundant branched-chain amino acid derived species. C, F: Odd-numbered species. Concentrations in liver are given per milligram of liver wet weight. White and black bars represent metabolite concentrations in controls and diabetic animals, respectively. * $P < 0.05$, ** $P < 0.01$, and *** $P < 0.005$.

we also detected elevated levels of the 5-carbon straight-chain valeryl-carnitine (C5:0-CN), for which the metabolic origin is obscure. Increases in plasma levels of 3-carbon-chain and 5-carbon-chain acylcarnitines derived from breakdown of branched-chain amino acids, as determined by a direct infusion MS/MS approach, were recently reported as important predictors for type 2 diabetes (5). Furthermore, while concentrations of 3-hydroxybutyryl-carnitine (C4-OH-CN) were strongly increased (by $\sim 40\%$), in diabetic mice, probably as a result of increased ketone body production (27), levels of 3-hydroxyisobutyryl-carnitine (2-M-C3-OH-CN), an intermediate in valine breakdown, displayed a strong decrease (by $\sim 50\%$) in both plasma and liver. For a correct interpretation of changes in these different pathways, it is thus necessary to include LC separation prior to MS for individual quantification of these metabolites. Similarly, while using direct infusion MS/MS, Mihalik et al. (6) reported C4-dicarboxyl-carnitine as a marker for glucolipototoxicity in type 2 diabetes, but did not discriminate between succinyl-carnitine (C4-DC-CN) and methylmalonyl-carnitine (C3-M-DC-CN), which are interconverted via methylmalonyl-CoA mutase. With our method, we found that only levels of methylmalonyl-carnitine (C3-M-DC-CN) were significantly increased in diabetic mice,

while alterations in succinyl-carnitine (C4-DC-CN) concentrations remained insignificant. Finally, we found elevated levels of several odd-numbered acylcarnitines in diabetic animals, most significantly the short-chain species, propionyl-carnitine (C3-CN), valeryl-carnitine (C5-CN), and heptanoyl-carnitine (C7-CN) in liver. Interestingly, odd-numbered fatty acids were recently proposed as potential markers of the metabolic syndrome (22). The origin and cause for these alterations in disease states is not known.

In summary, we have developed a sensitive and robust method which allows quantification of a large number of acylcarnitine species, including isomeric forms derived from a variety of metabolic pathways in amino acid and fatty acid oxidation. Compared with existing methods, we expanded the palette of analytes with novel acylcarnitine species, including low-abundant odd-numbered forms. Our LC-MS/MS method was validated in plasma and liver samples from mice and was applied to samples from STZ-treated type I diabetic mice. These mice display increased concentrations of BCAA-derived and odd-numbered acylcarnitine species, which were recently proposed as potential biomarkers for the metabolic syndrome. **66**

The authors thank Mena Eidens for excellent participation in conduction of mouse experiments and sample collection.

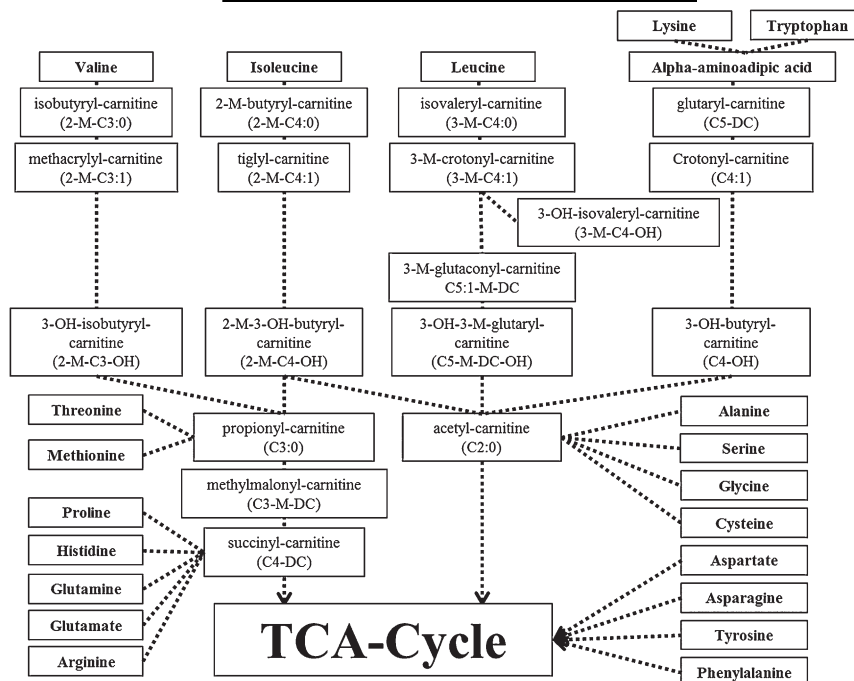


Fig. 4. Scheme displaying amino acid breakdown pathways and acylcarnitine species that can be formed from acyl-CoA intermediates.

REFERENCES

- Ramsay, R. R., R. D. Gandour, and F. R. van der Leij. 2001. Molecular enzymology of carnitine transfer and transport. *Biochim. Biophys. Acta.* **1546**: 21–43.
- Ventura, F. V., L. Ijlst, J. Ruiten, R. Ofman, C. G. Costa, C. Jakobs, M. Duran, I. Tavares de Almeida, L. L. Bieber, and R. J. Wanders. 1998. Carnitine palmitoyltransferase II specificity towards beta-oxidation intermediates—evidence for a reverse carnitine cycle in mitochondria. *Eur. J. Biochem.* **253**: 614–618.
- Violante, S., L. Ijlst, J. Ruiten, J. Koster, H. van Lenthe, M. Duran, I. T. de Almeida, R. J. Wanders, S. M. Houten, and F. V. Ventura. 2013. Substrate specificity of human carnitine acetyltransferase: Implications for fatty acid and branched-chain amino acid metabolism. *Biochim. Biophys. Acta.* **1832**: 773–779.
- Shekhawat, P. S., D. Matern, and A. W. Strauss. 2005. Fetal fatty acid oxidation disorders, their effect on maternal health and neonatal outcome: impact of expanded newborn screening on their diagnosis and management. *Pediatr. Res.* **57**: 78R–86R.
- Newgard, C. B., J. An, J. R. Bain, M. J. Muehlbauer, R. D. Stevens, L. F. Lien, A. M. Haqq, S. H. Shah, M. Arlotto, C. A. Slentz, et al. 2009. A branched-chain amino acid-related metabolic signature that differentiates obese and lean humans and contributes to insulin resistance. *Cell Metab.* **9**: 311–326.
- Mihalik, S. J., B. H. Goodpaster, D. E. Kelley, D. H. Chace, J. Vockley, F. G. Toledo, and J. P. DeLany. 2010. Increased levels of plasma acylcarnitines in obesity and type 2 diabetes and identification of a marker of glucolipototoxicity. *Obesity (Silver Spring)*. **18**: 1695–1700.
- Adams, S. H., C. L. Hoppel, K. H. Lok, L. Zhao, S. W. Wong, P. E. Minkler, D. H. Hwang, J. W. Newman, and W. T. Garvey. 2009. Plasma acylcarnitine profiles suggest incomplete long-chain fatty acid beta-oxidation and altered tricarboxylic acid cycle activity in type 2 diabetic African-American women. *J. Nutr.* **139**: 1073–1081.
- Abdenur, J. E., N. A. Chamoles, A. E. Guinle, A. B. Schenone, and A. N. Fuertes. 1998. Diagnosis of isovaleric acidemia by tandem mass spectrometry: false positive result due to pivaloylcarnitine in a newborn screening programme. *J. Inher. Metab. Dis.* **21**: 624–630.
- Gucciardi, A., P. Pirillo, I. M. Di Gangi, M. Naturale, and G. Giordano. 2012. A rapid UPLC-MS/MS method for simultaneous

- separation of 48 acylcarnitines in dried blood spots and plasma useful as a second-tier test for expanded newborn screening. *Anal. Bioanal. Chem.* **404**: 741–751.
- Maeda, Y., T. Ito, A. Suzuki, Y. Kurono, A. Ueta, K. Yokoi, S. Sumi, H. Togari, and N. Sugiyama. 2007. Simultaneous quantification of acylcarnitine isomers containing dicarboxylic acylcarnitines in human serum and urine by high-performance liquid chromatography/electrospray ionization tandem mass spectrometry. *Rapid Commun. Mass Spectrom.* **21**: 799–806.
- Peng, M., X. Fang, Y. Huang, Y. Cai, C. Liang, R. Lin, and L. Liu. 2013. Separation and identification of underivatized plasma acylcarnitine isomers using liquid chromatography-tandem mass spectrometry for the differential diagnosis of organic acidemias and fatty acid oxidation defects. *J. Chromatogr. A.* **1319**: 97–106.
- Minkler, P. E., M. S. Stoll, S. T. Ingalls, S. Yang, J. Kerner, and C. L. Hoppel. 2008. Quantification of carnitine and acylcarnitines in biological matrices by HPLC electrospray ionization-mass spectrometry. *Clin. Chem.* **54**: 1451–1462.
- Menni, C., E. Fauman, I. Erte, J. R. Perry, G. Kastemuller, S. Y. Shin, A. K. Petersen, C. Hyde, M. Psatha, K. J. Ward, et al. 2013. Biomarkers for type 2 diabetes and impaired fasting glucose using a nontargeted metabolomics approach. *Diabetes.* **62**: 4270–4276.
- Ziegler, H. J., P. Bruckner, and F. Binon. 1967. O-acylation of dl-carnitine chloride. *J. Org. Chem.* **32**: 3989–3991.
- Chace, D. H., S. L. Hillman, J. L. Van Hove, and E. W. Naylor. 1997. Rapid diagnosis of MCAD deficiency: quantitative analysis of octanoylcarnitine and other acylcarnitines in newborn blood spots by tandem mass spectrometry. *Clin. Chem.* **43**: 2106–2113.
- Ecker, J. 2012. Profiling eicosanoids and phospholipids using LC-MS/MS: principles and recent applications. *J. Sep. Sci.* **35**: 1227–1235.
- Frolov, A., and R. Hoffmann. 2008. Separation of Amadori peptides from their unmodified analogs by ion-pairing RP-HPLC with heptafluorobutyric acid as ion-pair reagent. *Anal. Bioanal. Chem.* **392**: 1209–1214.
- Schooneman, M. G., F. M. Vaz, S. M. Houten, and M. R. Soeters. 2013. Acylcarnitines: reflecting or inflicting insulin resistance? *Diabetes.* **62**: 1–8.
- Soeters, M. R., M. J. Serlie, H. P. Sauerwein, M. Duran, J. P. Ruiten, W. Kulik, M. T. Ackermans, P. E. Minkler, C. L. Hoppel, R. J. Wanders,

- et al. 2012. Characterization of D-3-hydroxybutyrylcarnitine (keto-carnitine): an identified ketosis-induced metabolite. *Metabolism*. **61**: 966–973.
20. Lenzen, S. 2008. The mechanisms of alloxan- and streptozotocin-induced diabetes. *Diabetologia*. **51**: 216–226.
21. Primassin, S., F. Ter Veld, E. Mayatepek, and U. Spiekerkoetter. 2008. Carnitine supplementation induces acylcarnitine production in tissues of very long-chain acyl-CoA dehydrogenase-deficient mice, without replenishing low free carnitine. *Pediatr. Res.* **63**: 632–637.
22. Wang-Sattler, R., Z. Yu, C. Herder, A. C. Messias, A. Floegel, Y. He, K. Heim, M. Campillos, C. Holzapfel, B. Thorand, et al. 2012. Novel biomarkers for pre-diabetes identified by metabolomics. *Mol. Syst. Biol.* **8**: 615.
23. Fiehn, O., W. T. Garvey, J. W. Newman, K. H. Lok, C. L. Hoppel, and S. H. Adams. 2010. Plasma metabolomic profiles reflective of glucose homeostasis in non-diabetic and type 2 diabetic obese African-American women. *PLoS One*. **5**: e15234.
24. De Jesús, V. R., D. H. Chace, T. H. Lim, J. V. Mei, and W. H. Hannon. 2010. Comparison of amino acids and acylcarnitines assay methods used in newborn screening assays by tandem mass spectrometry. *Clin. Chim. Acta*. **411**: 684–689.
25. Annesley, T. M. 2003. Ion suppression in mass spectrometry. *Clin. Chem.* **49**: 1041–1044.
26. Sterz, K., G. Scherer, and J. Ecker. 2012. A simple and robust UPLC-SRM/MS method to quantify urinary eicosanoids. *J. Lipid Res.* **53**: 1026–1036.
27. Blackshear, P. J., and K. G. Alberti. 1974. Experimental diabetic ketoacidosis. Sequential changes of metabolic intermediates in blood, liver, cerebrospinal fluid and brain after acute insulin deprivation in the streptozotocin-diabetic rat. *Biochem. J.* **138**: 107–117.



Branched-chain amino acids as biomarkers in diabetes

Pieter Giesbertz and Hannelore Daniel

Purpose of review

Numerous human studies have consistently demonstrated that concentrations of branched-chain amino acids (BCAAs) in plasma and urine are associated with insulin resistance and have the quality to predict diabetes development. However, it is not known how altered BCAA levels link to insulin action and diabetes. This review addresses some recent findings in BCAA metabolism and discusses their role as reporter molecules of insulin sensitivity and diabetes and their possible contribution to disease progression.

Recent findings

Changes in plasma and urine levels result mainly from altered metabolism in tissues and recent studies have thus focused on organ-specific changes in BCAA handling using animal models and human tissue samples. A decreased mitochondrial oxidation has been demonstrated in peripheral tissues and that was shown to be associated with an increased inflammatory tone and changes in adipokine levels (adiponectin and leptin). These changes appear already before insulin resistance is established. Key findings demonstrating the discordance between changes in BCAA and insulin resistance are derived from studies using insulin sensitizers and from data collected in patients undergoing Roux-en-Y bypass bariatric surgery. Intermediates derived from BCAA breakdown rather than BCAA itself were recently proposed to contribute to the development of insulin resistance and studies now explore the biomarker qualities of these metabolites.

Summary

Understanding the mechanisms and putative causalities in the alterations in BCAA levels as found in obesity, metabolic syndrome and diabetes is crucial for any intervention options but also for the use of BCAA and derivatives as biomarkers in clinical routine.

Keywords

biomarkers, branched-chain amino acids, diabetes, impaired mitochondrial oxidation, insulin resistance

INTRODUCTION

In the early 1970s, elevated plasma concentrations of branched-chain amino acids (BCAAs) leucine, valine, and isoleucine in patients with impaired insulin signalling were first described [1,2]. During the last 5 years, an overwhelming number of publications have consistently demonstrated increased plasma BCAA levels related to obesity, insulin resistance, and diabetes in large prospective and cross-sectional human studies [3–5,6^{***},7]. For type 2 diabetes (T2DM), BCAA levels are now considered as predictive markers of disease development [8–10]. Evidence that BCAAs may not only have a ‘reporter quality’ but may as well contribute to the development of insulin resistance and T2DM comes from animal and cell culture studies proposing a persistent activation of the mammalian target of rapamycin complex 1 (mTORC1) [3,11]. The relationship of

BCAAs and insulin resistance is further supported by the dramatic reduction in circulating BCAA levels in patients undergoing Roux-en-Y gastric bypass surgery, coinciding with improvements in insulin sensitivity, glucose homeostasis, and overall health [12]. Together with these proposed biomarker qualities, new methods such as capillary electrophoresis allowing separation and quantification of BCAAs in no more than 3 min [13] may bring BCAA analysis into the clinical routine.

Nutritional Physiology, Technische Universität München, Germany

Correspondence to Pieter Giesbertz, Nutritional Physiology, Technische Universität München, Gregor-Mendel-Str. 2 85350, Freising, Germany.
Tel: +49 8161 713553; fax: +49 8161 713999;
e-mail: pieter.giesbertz@tum.de

Curr Opin Clin Nutr Metab Care 2016, 19:48–54

DOI:10.1097/MCO.0000000000000235

KEY POINTS

- Despite an overall consistency of results showing strong correlations of circulating BCAAs and insulin sensitivity, effects are stronger in men and variations related to age and ethnicity have been observed.
- Increases in circulating and urinary BCAAs were shown to relate to changes in hormone/cytokine secretion and mitochondrial utilization in peripheral tissues.
- Impaired mitochondrial oxidation appears to be the prime cause for increases in BCAAs, independent of established insulin resistance.
- Studies suggest that intermediates, such as branched-chain keto acids, branched-chain fatty acids, and various acylcarnitines of BCAA oxidation may induce insulin resistance. Various intermediates have as well been proposed to serve as biomarkers that reflect insulin resistance and could predict diabetes.
- A supplementation of BCAAs might be beneficial or harmful in diabetes, depending on disease state.

The review discusses recent findings on mammalian BCAA metabolism and the role of BCAAs and their breakdown products as biomarkers of insulin resistance and diabetes, including variations because of age, sex, and ethnicity. By expanding the review to research in cells and experimental animals, we discuss how BCAAs on a mechanistic basis may contribute to the development of insulin resistance and T2DM.

ELEVATIONS OF BRANCHED-CHAIN AMINO ACID CONCENTRATIONS IN PLASMA AND URINE MARK STATES OF IMPAIRED INSULIN SIGNALLING

A large number of metabolomics approaches have identified characteristic metabolite profiles associated with insulin resistance and diabetic conditions and the metabolites changing most robustly in plasma [3,4,7–10] and urine [5] are the BCAAs. This reproduces and extends the findings of Philip Felig in the early 1970s describing elevations in plasma BCAA levels associated with impaired insulin signalling [1,2]. Despite an overall consistency in reports describing elevated BCAA levels in states of insulin resistance and diabetes, effect sizes are quite different and seem to depend on age, sex and ethnicity. In general, men appear to display stronger correlations [14,15] and this was recently proposed to originate from variations in the catabolic activity of liver [16]. Findings on differences between young and adult volunteers in the relationship of BCAA levels and insulin resistance [17,18] could not be observed in

two more recent studies [10,19]. Although studies in Asian subpopulations suggest that BCAAs are suitable for diagnosis and prediction of insulin resistance and T2DM in these ethnic groups [9,20[■],21,22], a recent study in American-Indians could not observe predictive quality of BCAAs for development of T2DM [23].

Altered systemic BCAA levels have been found to associate with various clinical parameters for insulin resistance and glucose homeostasis, such as BMI, waist circumference, homeostasis model assessment for insulin resistance (HOMA-IR), haemoglobin A1c, and fasting blood glucose. A recent study in almost 3000 volunteers found the strongest correlations amongst various parameters between plasma BCAA levels and visceral fat area, HOMA-IR, fasting insulin levels, and measures of obesity [9]. A strong positive correlation of BCAA levels and HOMA-IR was also found in healthy Japanese study participants [22] and in T2DM patients whereas negative correlations were found between BCAA and adiponectin concentrations [6[■]].

ORGAN-SPECIFIC AND INTERORGAN CHANGES IN BRANCHED-CHAIN AMINO ACID METABOLISM IN STATES OF INSULIN RESISTANCE AND TYPE 2 DIABETES

There is currently a lack of understanding by which mechanism changes in BCAA levels link to insulin resistance and T2DM. However, an important role for the adipose tissue in BCAA metabolism has become evident. Expansion of adipose tissue, accompanied by altered hormone and cytokine secretion, an enhanced inflammatory tone, and the invasion of macrophages have been recognized as early events in obesity-induced insulin resistance [24]. Studies in human and rodent adipose tissue have demonstrated reduced expression and activity of mitochondrial branched-chain aminotransferase (BCATm) and branched-chain keto acid dehydrogenase (BCKDH) in obese and diabetic conditions [25–28]. These are the first two enzymes by which all three amino acids are transaminated and thereafter decarboxylated and dehydrated. More recently, a reduced expression of BCAA catabolic genes downstream of BCKDH was shown, associated with increased expression of inflammatory cytokines such as TNF α [29]. A decreased degradation of radiolabeled [14C]-leucine in adipocytes treated with proinflammatory cytokines supports the concept that mitochondrial BCAA breakdown in adipose tissue is markedly impaired in an inflammatory state [30[■]]. These findings match with studies comparing lean humans and obese humans classified as metabolically healthy obese

and metabolically unhealthy obese individuals. The metabolically healthy obese individuals were characterized by preserved insulin sensitivity, reduced inflammatory status, and a normal plasma lipid profile compared with metabolically unhealthy patients. However, the increase in circulating BCAA concentrations and the decrease in expression of most BCAA catabolic genes in subcutaneous adipose tissue was similar in metabolically healthy and unhealthy obese individuals [31]. This suggests that part of the observed changes in circulating BCAAs – despite their strong correlation with insulin resistance – originates from a decreased mitochondrial oxidation rate occurring independent of insulin resistance. This might also be concluded from insulin-sensitizer studies. Whereas a study using thiazolidinediones as insulin sensitizer revealed that changes in adipose tissue expression of genes in BCAA degradation correlated positively with insulin sensitivity [32], a recent study employing a combination of thiazolidinediones and metformin failed to observe an expected decrease in systemic BCAA levels, despite increased insulin sensitivity [33^{***}]. Nevertheless, the downregulation of almost all genes in the BCAA degradation pathway in both visceral and subcutaneous adipose tissue was shown to be exacerbated in obese individuals with T2DM as compared with equally obese individuals with abnormal glucose tolerance [34].

Evidence for a decreased mitochondrial BCAA oxidation also comes from recent research in mice lacking adiponectin. When these mice were fed a high-fat diet, a decreased BCKDH activity in muscle was observed, which could be corrected upon adiponectin treatment [35^{***}]. This was shown to occur partially via a mechanism depending on AMP-activated protein kinase (AMPK) and involving BCKDH kinase and BCKDH phosphatase, which reversibly modify BCKDH activity via phosphorylation and dephosphorylation, respectively. A critical role of adiponectin was also suggested by findings from an observational study in humans showing strong negative correlations between plasma BCAAs and adiponectin levels [6^{***}]. A key regulator of mitochondrial metabolism, the transcription factor peroxisome proliferator-activated receptor gamma coactivator 1 alpha (PGC-1 α), was shown to regulate the expression of enzymes in BCAA metabolism. In skeletal muscle overexpressing PGC-1 α , expression levels of BCATm and BCKDH increased, whereas BCKDH kinase remained unchanged [36] and BCAA levels in muscle tissue decreased [37^{***}]. Effects of adiponectin signalling via the adiponectin receptor and PGC-1 α as a downstream target [38] suggest that the effects of adiponectin may be mediated by PGC-1 α .

Whereas a reduced mitochondrial degradation of BCAA in peripheral tissues in an insulin resistant state has been consistently observed, the role of the liver in overall BCAA homeostasis remains to be defined. Studies employing genetic models of obesity and diabetes, such as *ob/ob* mice, Zucker diabetic fatty rats, and obese Zucker rats, all describe a decreased hepatic BCKDH activity and increased circulating BCAA levels [26,39]. Studies in rodent models of diet-induced obesity, in contrast, reported increased hepatic BCKDH activities and near to normal plasma BCAA levels [40,41]. It is suggested that this increased BCKDH activity in liver in diet-induced obesity may represent a compensatory mechanism for the reduced activity in peripheral tissues. In support of this, it was recently shown that hepatic BCKDH activity is stimulated by insulin-dependent hypothalamic signalling leading to a reduction in circulating BCAA levels [16]. The fact that the genetic mouse models showing decreased hepatic BCKDH levels are either leptin deficient or leptin resistant in an early stage of disease suggests that impaired adipokine signalling (leptin versus adiponectin) is a key element in the obesity-driven changes in circulating BCAA levels [16] and that these effects might occur earlier as well as partially independent from any changes in insulin sensitivity. However, it can be easily anticipated that insulin has an effect on systemic BCAA as well by its inhibitory effect of protein breakdown and thus a reduced release of amino acid into circulation [42]. With a reduced sensitivity of tissues to insulin, a slightly but constitutively increased protein breakdown and thus amino acid release into circulation may as well contribute to the elevated BCAA levels in insulin resistance and diabetic conditions. This impaired response to insulin may also explain the observed retarded changes in circulating BCAA to return to fasting levels when an oral glucose tolerance test is performed in volunteers of poor metabolic health [43–45]. The proposed insulin-dependent and independent mechanisms by which BCAA levels are affected are not mutually exclusive.

BCAAS AND INTERMEDIATES OF BRANCHED-CHAIN AMINO ACID BREAKDOWN AS CONTRIBUTORS TO INSULIN RESISTANCE AND TYPE 2 DIABETES

The studies described above suggest that altered systemic BCAA levels originate likely from impaired protein homeostasis and reduced mitochondrial oxidation in peripheral tissues. Evidence that BCAAs may not only serve as ‘reporters’ of insulin resistance and T2DM but may also be causative or at least

contribute to disease development comes from a study on rats. In this study, a BCAA supplementation in animals fed a high-fat diet was reported to cause a similar degree of insulin resistance compared to animals fed a high-fat diet only, despite a reduced food intake and a reduction in weight gain [3]. This observation is extended by a recent human study showing that a supplementation with essential amino acids decreased glucose infusion rates needed to maintain euglycemia at different levels of insulin infusion. This suggests that these amino acids decreased peripheral insulin sensitivity [46]. This however could not be confirmed in another recent study with an acute elevation of plasma BCAA concentrations in young healthy volunteers, which failed to affect insulin-dependent glucose disposal [47^{*}]. A difference between both studies is that the first study provides other essential amino acids on top of the BCAAs, which by sharing and competing for common uptake pathways into cells may alter insulin-mediated intracellular response pathways. Mechanistic studies in cell cultures and rodent models suggest a role for BCAAs – especially of leucine – to promote insulin resistance via a stimulation of mTORC1 and S6 kinase and phosphorylation of the insulin receptor substrates 1 and 2 [3,11,48]. In support of this, it was recently shown that deprivation of individual BCAAs in mice and in cell lines could improve insulin sensitivity, involving both mTORC1/S6K and AMPK signalling pathways [11]. BCATm knock-out mice, which have markedly increased plasma BCAA levels [49,50] show a tissue-specific BCAA activation of mTOR and display increased insulin sensitivity. These findings suggest that elevated plasma BCAAs per se are not harmful, but that BCAA-derived intermediates are likely to be responsible for the effects. This is also suggested by a study in overweight individuals submitted to a 6-month exercise program that successfully increased insulin sensitivity without changes in plasma BCAA levels when compared with untrained volunteers but with differences in some BCAA intermediates conjugated to glycine and carnitine [51]. Additional evidence that BCAA degradation products and in particular the keto acids can induce mitochondrial dysfunction is derived from studies in rat brain [52].

Paradoxically, results from some studies suggest that BCAAs should have ameliorating effects on diabetes progression. BCAAs were shown to increase muscle protein synthesis in healthy individuals and ameliorate liver pathologies [46,53,54]. Leucine administered directly into the brain was shown to induce hypothalamic satiety signalling, which could improve weight loss and secondarily improve insulin sensitivity. However, these central effects of

leucine were not consistently observed (for a recent review see [55]). Another direct target organ of BCAAs is β -cells. All three BCAAs, but especially leucine, were shown to be insulinotropic and capable to lower blood glucose levels in humans [56]. The beneficial effects of milk proteins, especially whey, on glucose homeostasis in diabetes are suggested to be at least partly a consequence of the high BCAA content in whey [57]. A recent study in streptozotocin-induced insulin deficient rats reports that BCAAs can reduce oxidative stress in pancreatic islets and ameliorate β -cell dysfunction, involving c-Jun N-terminal kinase, protein kinase D1 and pancreatic/duodenal homeobox-1 [58^{*}]. However, the BCAA dose of 1.25 g/kg/day used in this rat study would translate into a dose in humans far exceeding leucine tolerance levels in humans [59]. It appears thus that health effects of a BCAA supplementation on insulin resistance and T2DM may depend on the disease stage. Whereas supplementing BCAA in healthy individuals does not cause any harm by a rapid oxidation with functional mitochondrial machinery, in obese individuals, or in animals fed with a high-fat diet BCAA supplementation appears to cause metabolic disturbances by a substrate overload of mitochondria and impaired amino acid oxidation. In a diabetic stage with β -cell dysfunction, effects of BCAAs on the β -cell might be beneficial to ameliorate dysglycemia.

DEGRADATION PRODUCTS OF BRANCHED-CHAIN AMINO ACIDS AS MARKERS FOR INSULIN RESISTANCE AND DIABETES

Recent metabolomics studies in search of new diabetes markers reported changes in plasma levels of BCAA-derived branched-chain keto acids [7,42] and short branched-chain fatty acids as new entities [5]. Newgard *et al.* demonstrated that odd numbered 3 and 5-carbon acylcarnitines – which are likely products of BCAA catabolism – have a predictive power for diabetes development [3]. Acylcarnitines appear in plasma and urine and have gained interest as robust and easily measurable metabolites marking conditions of impaired mitochondrial oxidation. Various acylcarnitines derived from BCAA breakdown could be associated with insulin resistance and T2DM in recent studies [16,19,60]. Particularly strong evidence was found for succinyl-carnitine as a marker for glucolipototoxicity as an intermediate at the crossroads of tricarboxylic acid cycle, respiratory chain, and BCAA breakdown [60]. We recently described a new LC-MS/MS method allowing the analysis of an extended palette of acylcarnitines including those

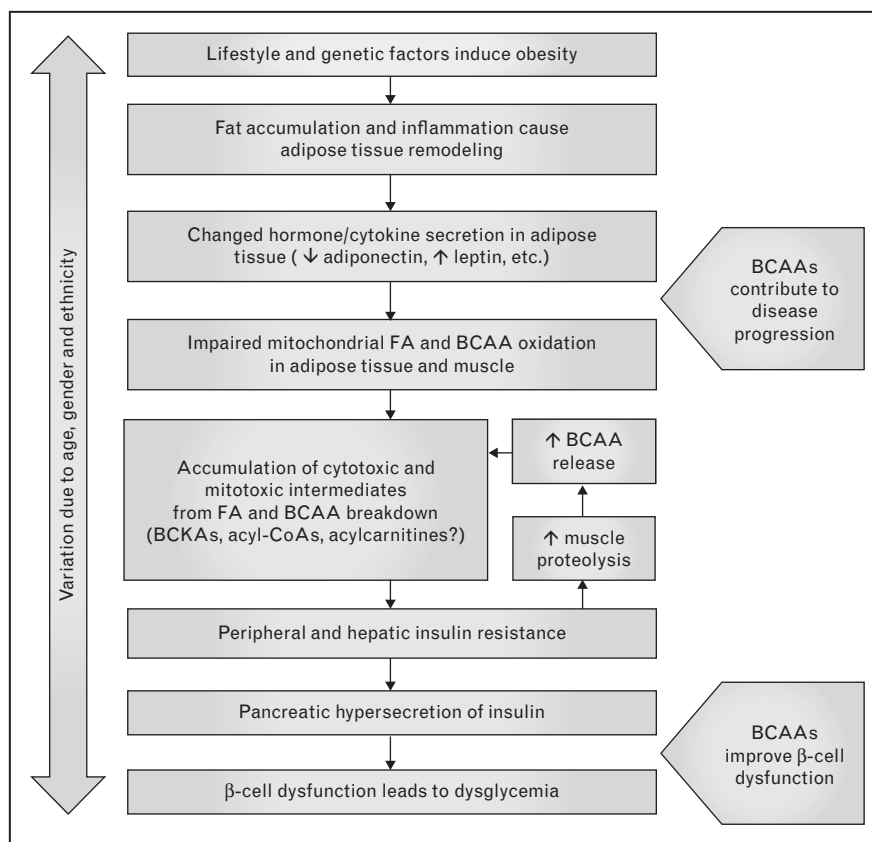


FIGURE 1. A proposed aetiology of increased BCAA levels in insulin resistance and T2DM that includes novel findings. The adipose tissue in obese state is characterized by an accumulation of fat, an increased proinflammatory state, and changes in hormone and cytokine secretion, which are proposed to be the basis for an impaired mitochondrial function in peripheral tissues. Incomplete oxidation of branched-chain amino acids results in the accumulation of toxic intermediates, which interfere with insulin signalling. Impaired insulin signalling in muscle causes an increased proteolysis, leading to a further release of BCAAs in the circulation and a further supply of substrates for mitochondrial oxidation. A supplementation of BCAAs at this time point of the disease might be toxic, since it further provides a substrate supply to the mitochondria. Pancreatic β cells respond to insulin resistance by increasing insulin secretion, up to the point of β -cell exhaustion. At this stage, BCAA supplementation might improve glucose homeostasis by ameliorating β -cell toxicity. Lastly, the role of BCAAs in this disease pathology seems to vary depending on age, gender, and ethnicity.

derived from BCAA catabolism [61]. Recently, acyl-CoA species of BCAA breakdown were determined as well [16]. Additional new biomarkers related to BCAA catabolism are long-chain monomethyl and odd-numbered fatty acids. They could originate from an odd-chain starter CoA with chain elongation in the fatty acid synthase complex. Our work in leptin-deficient mice [28] and other studies in adipose tissue with decreased BCKDH activity [62[□]] revealed decreased levels of monomethyl fatty acids. Whether these derivatives of BCAA breakdown better reflect the different states of obesity, insulin resistance, and T2DM than the BCAAs needs to be further studied. A disadvantage of these new marker metabolites as compared with BCAAs is the lower plasma and tissue concentrations of several species, resulting in higher

analytical variation; with some compounds also having lower stability.

SUMMARY

A synopsis of the current status in understanding why BCAAs and their intermediates serve as biomarkers of the metabolic syndrome and T2DM and how they could contribute to disease progression is depicted in Figure 1. It builds on the findings that early changes in adipose tissue increasing the proinflammatory tone cause a reduced peripheral BCAA catabolic activity. There is growing evidence that reduced adiponectin secretion in obese states affects in an autocrine and paracrine manner the oxidation of BCAA in adipose tissue and muscle. Based on the need to oxidize larger quantities of

amino acids provided by the high protein intake in modern diets, this reduced capacity of BCAA catabolism in adipose and muscle tissues may be the prime cause of the elevated plasma levels and this can occur before the establishment of insulin resistance. Evidence for this comes from a study in metabolically healthy obese individuals, which have preserved insulin sensitivity but already display increased circulating BCAAs. A further discordance between BCAA changes and insulin resistance can be observed in studies using insulin sensitizers and in patients undergoing Roux-en-Y bypass surgery. However, when insulin resistance is developing – to which intermediates of fatty acid and BCAA breakdown could contribute – a reduced inhibition of proteolysis by insulin in muscle would further elevate plasma BCAA levels. Under those conditions, a supplementation of BCAAs appears particularly detrimental as it further increases the substrate load for mitochondrial oxidation. With progressing pancreatic dysfunction and lack of insulin secretion a further increase in extracellular BCAA pools by increased proteolysis would occur but here higher BCAA levels as well as BCAA supplementation could be beneficial by their insulinotropic effects that could improve glucose homeostasis.

Acknowledgements

None.

Financial support and sponsorship

None.

Conflicts of interest

There are no conflicts of interest.

REFERENCES AND RECOMMENDED READING

Papers of particular interest, published within the annual period of review, have been highlighted as:

- of special interest
- of outstanding interest

1. Felig P, Marliss E, Cahill GF Jr. Plasma amino acid levels and insulin secretion in obesity. *N Engl J Med* 1969; 281:811–816.
 2. Felig P, Marliss E, Ohman JL, Cahill CF Jr. Plasma amino acid levels in diabetic ketoacidosis. *Diabetes* 1970; 19:727–728.
 3. Newgard CB, An J, Bain JR, *et al.* A branched-chain amino acid-related metabolic signature that differentiates obese and lean humans and contributes to insulin resistance. *Cell Metab* 2009; 9:311–326.
 4. Batch BC, Shah SH, Newgard CB, *et al.* Branched chain amino acids are novel biomarkers for discrimination of metabolic wellness. *Metabolism* 2013; 62:961–969.
 5. Younsri NA, Mook-Kanamori DO, Selim MM, *et al.* A systems view of type 2 diabetes-associated metabolic perturbations in saliva, blood and urine at different timescales of glycaemic control. *Diabetologia* 2015; 58:1855–1867.
 6. Nakamura H, Jinzu H, Nagao K, *et al.* Plasma amino acid profiles are associated with insulin, C-peptide and adiponectin levels in type 2 diabetic patients. *Nutr Diabetes* 2014; 4:e133.
- This study examines in a structured manner the correlations between circulating amino acids and clinical parameters of insulin and glucose for 51 Japanese patients. Results show that branched-chain amino acid levels correlate positively with insulin-related parameters and negatively with adiponectin.
7. Menni C, Fauman E, Erte I, *et al.* Biomarkers for type 2 diabetes and impaired fasting glucose using a nontargeted metabolomics approach. *Diabetes* 2013; 62:4270–4276.
 8. Wang TJ, Larson MG, Vasan RS, *et al.* Metabolite profiles and the risk of developing diabetes. *Nat Med* 2011; 17:448–453.
 9. Yamakado M, Nagao K, Imaizumi A, *et al.* Plasma free amino acid profiles predict four-year risk of developing diabetes, metabolic syndrome, dyslipidemia, and hypertension in Japanese population. *Sci Rep* 2015; 5:11918.
 10. McCormack SE, Shaham O, McCarthy MA, *et al.* Circulating branched-chain amino acid concentrations are associated with obesity and future insulin resistance in children and adolescents. *Pediatr Obes* 2013; 8:52–61.
 11. Xiao F, Yu J, Guo Y, *et al.* Effects of individual branched-chain amino acids deprivation on insulin sensitivity and glucose metabolism in mice. *Metabolism* 2014; 63:841–850.
 12. Arora T, Velagapudi V, Pournaras DJ, *et al.* Roux-en-y gastric bypass surgery induces early plasma metabolomic and lipidomic alterations in humans associated with diabetes remission. *PLoS one* 2015; 10:e0126401.
 13. Tuma P, Gojda J. Rapid determination of branched chain amino acids in human blood plasma by pressure-assisted capillary electrophoresis with contactless conductivity detection. *Electrophoresis* 2015; 36:1969–1975.
 14. Newbern D, Gumus Balikcioglu P, Balikcioglu M, *et al.* Sex differences in biomarkers associated with insulin resistance in obese adolescents: metabolomic profiling and principal components analysis. *J Clin Endocrinol Metab* 2014; 99:4730–4739.
 15. Xie G, Ma X, Zhao A, *et al.* The metabolite profiles of the obese population are gender-dependent. *J Proteome Res* 2014; 13:4062–4073.
 16. Shin AC, Fasshauer M, Filatova N, *et al.* Brain insulin lowers circulating BCAA levels by inducing hepatic BCAA catabolism. *Cell Metab* 2014; 20:898–909.
 17. Michaliszyn SF, Sjaarda LA, Mihalik SJ, *et al.* Metabolomic profiling of amino acids and beta-cell function relative to insulin sensitivity in youth. *J Clin Endocrinol Metab* 2012; 97:E2119–E2124.
 18. Mihalik SJ, Michaliszyn SF, de las Heras J, *et al.* Metabolomic profiling of fatty acid and amino acid metabolism in youth with obesity and type 2 diabetes: evidence for enhanced mitochondrial oxidation. *Diabetes Care* 2012; 35:605–611.
 19. Perng W, Gillman MW, Fleisch AF, *et al.* Metabolomic profiles and childhood obesity. *Obesity* 2014; 22:2570–2578.
 20. Tillin T, Hughes AD, Wang Q, *et al.* Diabetes risk and amino acid profiles: cross-sectional and prospective analyses of ethnicity, amino acids and diabetes in a South Asian and European cohort from the SABRE (Southall And Brent REvisited) study. *Diabetologia* 2015; 58:968–979.
- This study examined correlations of amino acids and parameters of obesity, insulin resistance and diabetes, comparing South Asian and European cohorts. Variations in the association between BCAAs and obesity or diabetes were observed.
21. Tai ES, Tan ML, Stevens RD, *et al.* Insulin resistance is associated with a metabolic profile of altered protein metabolism in Chinese and Asian-Indian men. *Diabetologia* 2010; 53:757–767.
 22. Yamada C, Kondo M, Kishimoto N, *et al.* Association between insulin resistance and plasma amino acid profile in nondiabetic Japanese subjects. *J Diabetes Investig* 2015; 6:408–415.
 23. Zhao J, Zhu Y, Hyun N, *et al.* Novel metabolic markers for the risk of diabetes development in American Indians. *Diabetes Care* 2015; 38:220–227.
 24. Cummins TD, Holden CR, Sansbury BE, *et al.* Metabolic remodeling of white adipose tissue in obesity. *Am J Physiol Endocrinol Metab* 2014; 307:E262–E277.
 25. Herman MA, She P, Peroni OD, *et al.* Adipose tissue branched chain amino acid (BCAA) metabolism modulates circulating BCAA levels. *J Biol Chem* 2010; 285:11348–11356.
 26. She P, Van Horn C, Reid T, *et al.* Obesity-related elevations in plasma leucine are associated with alterations in enzymes involved in branched-chain amino acid metabolism. *Am J Physiol Endocrinol Metab* 2007; 293:E1552–E1563.
 27. Lackey DE, Lynch CJ, Olson KC, *et al.* Regulation of adipose branched-chain amino acid catabolism enzyme expression and cross-adipose amino acid flux in human obesity. *Am J Physiol Endocrinol Metab* 2013; 304:E1175–E1187.
 28. Giesbertz P, Padberg I, Rein D, *et al.* Metabolite profiling in plasma and tissues of ob/ob and db/db mice identifies novel markers of obesity and type 2 diabetes. *Diabetologia* 2015; 58:2133–2143.
 29. Serralde-Zuniga AE, Guevara-Cruz M, Tovar AR, *et al.* Omental adipose tissue gene expression, gene variants, branched-chain amino acids, and their relationship with metabolic syndrome and insulin resistance in humans. *Genes Nutr* 2014; 9:431.
 30. Burrill JS, Long EK, Reilly B, *et al.* Inflammation and ER stress regulate branched-chain amino acid uptake and metabolism in adipocytes. *Mol Endocrinol* 2015; 29:411–420.
- Adipocytes treated with TNF α were shown to have decreased uptake and conversion of BCAAs. This underlines the role of inflammation on BCAA metabolism in adipocytes.
31. Badoud F, Lam KP, DiBattista A, *et al.* Serum and adipose tissue amino acid homeostasis in the metabolically healthy obese. *J Proteome Res* 2014; 13:3455–3466.
 32. Rasouli N, Kern PA, Elbein SC, *et al.* Improved insulin sensitivity after treatment with PPAR γ and PPAR α ligands is mediated by genetically modulated transcripts. *Pharmacogenet Genomics* 2012; 22:484–497.

33. Irving BA, Carter RE, Soop M, *et al.* Effect of insulin sensitizer therapy on amino acids and their metabolites. *Metabolism* 2015; 64:720–728. The effects of insulin sensitizing with pioglitazone and metformin on plasma amino acid concentrations were studied. The study reported that despite increased sensitivity BCAAs do not decrease, providing evidence for a discordance of BCAA levels and insulin sensitivity.
34. Dharuri H, t Hoen PA, van Klinden JB, *et al.* Downregulation of the acetyl-CoA metabolic network in adipose tissue of obese diabetic individuals and recovery after weight loss. *Diabetologia* 2014; 57:2384–2392.
35. Lian K, Du C, Liu Y, *et al.* Impaired adiponectin signaling contributes to disturbed catabolism of branched-chain amino acids in diabetic mice. *Diabetes* 2015; 64:49–59. In adiponectin knock-out mice, branched-chain keto acid dehydrogenase decreased, whereas this was reverted by adiponectin administration. Branched-chain amino acid concentrations changed accordingly. This study provides strong evidence for the regulatory role of adiponectin on BCAA metabolism.
36. Hatazawa Y, Tadaishi M, Nagaïke Y, *et al.* PGC-1 α -mediated branched-chain amino acid metabolism in the skeletal muscle. *PLoS one* 2014; 9:e91006.
37. Hatazawa Y, Senoo N, Tadaishi M, *et al.* Metabolomic analysis of the skeletal muscle of mice overexpressing PGC-1 α . *PLoS one* 2015; 10:e0129084. This study provides evidence that PGC-1 α is a regulator of BCAA metabolism by showing that skeletal muscle overexpressing PGC-1 α displays decreased BCAA levels.
38. Iwabu M, Yamauchi T, Okada-Iwabu M, *et al.* Adiponectin and AdipoR1 regulate PGC-1 α and mitochondria by Ca(2+) and AMPK/SIRT1. *Nature* 2010; 464:1313–1319.
39. Doisaki M, Katano Y, Nakano I, *et al.* Regulation of hepatic branched-chain alpha-keto acid dehydrogenase kinase in a rat model for type 2 diabetes mellitus at different stages of the disease. *Biochem Biophys Res Commun* 2010; 393:303–307.
40. Kadota Y, Toyoda T, Kitaura Y, *et al.* Regulation of hepatic branched-chain alpha-ketoacid dehydrogenase complex in rats fed a high-fat diet. *Obes Res Clin Pract* 2013; 7:e439–e444.
41. Sailer M, Dahlhoff C, Giesbertz P, *et al.* Increased plasma citrulline in mice marks diet-induced obesity and may predict the development of the metabolic syndrome. *PLoS one* 2013; 8:e63950.
42. She P, Olson KC, Kadota Y, *et al.* Leucine and protein metabolism in obese Zucker rats. *PLoS one* 2013; 8:e59443.
43. Padberg I, Peter E, Gonzalez-Maldonado S, *et al.* A new metabolomic signature in type-2 diabetes mellitus and its pathophysiology. *PLoS one* 2014; 9:e85082.
44. Kuehnbaum NL, Gillen JB, Gibala MJ, Britz-McKibbin P. Personalized metabolomics for predicting glucose tolerance changes in sedentary women after high-intensity interval training. *Sci Rep* 2014; 4:6166.
45. Liu L, Feng R, Guo F, *et al.* Targeted metabolomic analysis reveals the association between the postprandial change in palmitic acid, branched-chain amino acids and insulin resistance in young obese subjects. *Diabetes Res Clin Pract* 2015; 108:84–93.
46. Robinson MM, Soop M, Sohn TS, *et al.* High insulin combined with essential amino acids stimulates skeletal muscle mitochondrial protein synthesis while decreasing insulin sensitivity in healthy humans. *J Clin Endocrinol Metab* 2014; 99:E2574–E2583.
47. Everman S, Mandarino LJ, Carroll CC, Katsanos CS. Effects of acute exposure to increased plasma branched-chain amino acid concentrations on insulin-mediated plasma glucose turnover in healthy young subjects. *PLoS one* 2015; 10:e0120049. An acute and short-term increase of circulating BCAAs in healthy subjects did not decrease insulin sensitivity. Although limited to short-term exposure, this supports the suggestion that BCAAs are not harmful in healthy individuals.
48. Jewell JL, Kim YC, Russell RC, *et al.* Metabolism differential regulation of mTORC1 by leucine and glutamine. *Science* 2015; 347:194–198.
49. Neishabouri SH, Hutson SM, Davoodi J. Chronic activation of mTOR complex 1 by branched chain amino acids and organ hypertrophy. *Amino Acids* 2015; 47:1167–1182.
50. Lynch CJ, Kimball SR, Xu Y, *et al.* Global deletion of BCATm increases expression of skeletal muscle genes associated with protein turnover. *Physiol Genomics* 2015. [Epub ahead of print]
51. Glynn EL, Piner LW, Huffman KM, *et al.* Impact of combined resistance and aerobic exercise training on branched-chain amino acid turnover, glycine metabolism and insulin sensitivity in overweight humans. *Diabetologia* 2015; 58:2324–2335.
52. Amaral AU, Leipnitz G, Fernandes CG, *et al.* Alpha-ketoisocaproic acid and leucine provoke mitochondrial bioenergetic dysfunction in rat brain. *Brain Res* 2010; 1324:75–84.
53. Tomoda K, Kubo K, Hino K, *et al.* Branched-chain amino acid-rich diet improves skeletal muscle wasting caused by cigarette smoke in rats. *J Toxicol Sci* 2014; 39:331–337.
54. Kawaguchi T, Taniguchi E, Sata M. Effects of oral branched-chain amino acids on hepatic encephalopathy and outcome in patients with liver cirrhosis. *Nutr Clin Pract* 2013; 28:580–588.
55. Pedroso JA, Zampieri TT, Donato J Jr. Reviewing the effects of L-leucine supplementation in the regulation of food intake, energy balance, and glucose homeostasis. *Nutrients* 2015; 7:3914–3937.
56. Gannon MC, Nuttall FQ. Amino acid ingestion and glucose metabolism: a review. *IUBMB Life* 2010; 62:660–668.
57. Jakubowicz D, Froy O. Biochemical and metabolic mechanisms by which dietary whey protein may combat obesity and Type 2 diabetes. *J Nutr Biochem* 2013; 24:1–5.
58. Lu M, Zhang X, Zheng D, *et al.* Branched-chain amino acids supplementation protects streptozotocin-induced insulin secretion and the correlated mechanism. *Biofactors* 2015; 41:127–133. This study explored signalling factors involved in the ameliorating effects of BCAAs on the β -cell.
59. Pencharz PB, Elango R, Ball RO. Determination of the tolerable upper intake level of leucine in adult men. *J Nutr* 2012; 142:2220S–22204S.
60. Mihalik SJ, Goodpaster BH, Kelley DE, *et al.* Increased levels of plasma acylcarnitines in obesity and type 2 diabetes and identification of a marker of glucolipotoxicity. *Obesity* 2010; 18:1695–1700.
61. Giesbertz P, Ecker J, Haag A, *et al.* An LC-MS/MS method to quantify acylcarnitine species including isomeric and odd-numbered forms in plasma and tissues. *J Lipid Res* 2015. [Epub ahead of print]
62. Su X, Magkos F, Zhou D, *et al.* Adipose tissue monomethyl branched-chain fatty acids and insulin sensitivity: effects of obesity and weight loss. *Obesity* 2015; 23:329–334. An association between insulin sensitivity and adipose tissue content of monomethyl branched-chain fatty acids, which are likely derived from BCAAs, is demonstrated, providing novel potential BCAA-related biomarkers in diabetes.

1 **Signatures of acylcarnitine and acyl-CoA suggest specific regulation of**
2 **mitochondrial oxidation pathways in mouse models of obesity and diabetes**

3
4 Pieter Giesbertz¹, Katrin Müller², Dietmar Schomburg², Hannelore Daniel¹

5
6
7
8
9
10 ¹Nutritional Physiology, Technische Universität München, Gregor-Mendel-Straße 2, 85350 Freising-
11 weihenstephan, Germany

12
13 ²Institute for Biochemistry, Biotechnology and Bioinformatics, Technische Universität Braunschweig,
14 Langer Kamp 19B, 38106, Braunschweig, Germany

15
16
17
18
19
20
21
22
23
24
25
26 **Key words**

27 **Abstract**

28 Obesity, insulin resistance and diabetes are characterized by changes in plasma metabolite
29 markers of amino acid and fatty acid metabolism. We sought to determine changes in
30 individual metabolic routes of mitochondrial amino acid and fatty acid oxidation by
31 determining acylcarnitine profiles in plasma and tissues derived from mouse models
32 representing different stages of obesity and diabetes. The *ob/ob* mouse with a leptin
33 deficiency served as a model for insulin resistance with pancreas hypertrophy whereas the
34 *db/db* mouse is a model for obesity and insulin resistance with pancreatic failure and
35 consequently severe hyperglycemia. Streptozotocin-induced insulin-deficient mice served as
36 a model for type I diabetes or end-point stage type II diabetes with extreme hyperglycemia
37 and ketoacidosis. A sensitive LC-MS/MS method was used to quantify about 60 acylcarnitine
38 species including isomers derived from individual pathways of fatty acid and amino acid
39 oxidation. We furthermore determined concentrations of odd-numbered fatty acids. Since
40 acylcarnitines are derived from the conversion of acyl-CoA we additionally quantified acyl-
41 CoA species in liver and determined the correlation with the corresponding hepatic
42 acylcarnitines. Particularly strong increases in acylcarnitine species derived from branched-
43 chain amino acid metabolism in plasma and tissues of all mouse models were found and
44 were most pronounced in streptozotocin-treated animals. All models also displayed
45 increased concentrations of odd-numbered acylcarnitine species in liver while dicarboxylic
46 acylcarnitines derived from fatty acid omega-oxidation were strongly decreased in the obese
47 *ob/ob* and *db/db* mice. Correlations between acylcarnitine and acyl-CoA concentrations in
48 liver were strongest for monocarboxylic metabolites, while dicarboxylic acylcarnitines like
49 malonylcarnitine and succinylcarnitine showed no or negative correlations with their
50 respective acyl-CoA species. In summary, alterations of metabolic profiles in specific
51 pathways of fatty acid and amino acid oxidation were found in the mouse models and could
52 be associated with conditions of obesity, hyperinsulinemia, and diabetes. These changes give
53 further hints on the involvement of specific metabolic routes of mitochondrial oxidation
54 during diabetes progression.

55

56 **Introduction**

57 Metabolomics studies have identified acylcarnitines as important markers and predictors of
58 obesity-induced insulin resistance and type 2 diabetes. Increases in these conditions were
59 reported for medium-chain acylcarnitines, BCAA-derived acylcarnitines [1], and
60 succinylcarnitine [2]. Acylcarnitines are derived from the conversion of acyl-CoA species via
61 the action of carnitine acyltransferases. The origin for acylcarnitines in plasma is not known
62 but it is suggested that the conversion of acyl-CoA to acylcarnitines prevents the
63 accumulation of acyl-CoA species if mitochondrial or peroxisomal function is impaired. This
64 would allow the recovery of the inner-mitochondrial/peroxisomal free CoA pool and the
65 release of potentially toxic fatty acid intermediates to the cytosol and ultimately to the
66 plasma. It was previously shown that plasma acylcarnitine levels poorly reflect acylcarnitine
67 concentrations in tissues, possibly because plasma levels results from the contribution of
68 various tissues [3]. Furthermore, active transport processes maintain concentration
69 gradients between plasma and tissues. A dominant role of liver in the determination of
70 plasma acylcarnitine levels was recently demonstrated in a porcine model via transorgan flux
71 analysis. However, other tissues as well release acylcarnitines or take up acylcarnitines for
72 oxidation. The underlying processes causing the marked alterations in plasma acylcarnitine
73 species and levels in states of obesity, insulin resistance and diabetes are in essence
74 unknown and understanding these changes requires a global interpretation of metabolic
75 changes in tissues. In addition, it is not known to which extent acyl-CoA species are
76 converted into acylcarnitines under these conditions. Acylcarnitines can be formed from the
77 whole range of Acyl-CoA species via the concerted action of carnitine acetyl-, octanoyl- and
78 palmitoyltransferases. However, correlations between acyl-CoA and acylcarnitine levels in
79 tissue might depend on the localization of the enzymes at the cytosolic or
80 mitochondrial/peroxisomal side of membranes and on the acyl-CoA pools in individual cell
81 compartments such as cytosol, mitochondrion, or peroxisome.

82 We here employ three mouse models representing different stages of diabetes development
83 and study concentrations of acylcarnitine species in plasma and in different tissues (liver,
84 muscle, kidney, and adipose tissue). We use leptin-deficient ob/ob mice as a model of
85 obesity-induced insulin resistance at an early stage with normoglycemia, due to a pancreas
86 hypertrophy. Leptin-resistant db/db mice are used to study a more advanced stage of

87 diabetes with obesity-induced insulin resistance associated with hyperglycemia. As a model
88 for type I diabetes or end-point stage type II diabetes, a streptozotocin-treated insulin-
89 deficient mouse with severe hyperglycemia and ketoacidosis is used. For quantitation of
90 acylcarnitine concentrations a sensitive LC-MS/MS method was developed which covers
91 acylcarnitine species derived from fatty acid and amino acid breakdown pathways as well as
92 odd-numbered acylcarnitine species with chain-length between C3 and C17. Next to that, we
93 measure acyl-CoA levels in liver and determine correlations between individual
94 concentrations of acylcarnitine and acyl-CoA. With this approach we aimed to better
95 understand the origins for the changes in plasma acylcarnitine levels observed in obesity and
96 diabetes.

97

98 **Materials and Methods**

99 **Leptin-signaling deficient *ob/ob* and *db/db* mice**

100 Male *db/db* mice and C57BLKS/J wild-type littermates ($n=6-10$ per group) were purchased
101 from Charles River Laboratories (Sulzfeld, Germany) at an age of 5 weeks. Male *ob/ob* mice
102 and C57BL6/J wild-type littermates ($n=6-10$ per group), bred at the Research Center of
103 Nutrition and Food Sciences (ZIEL), were obtained at the age of 5 weeks. Mice were kept on
104 a standard-chow diet (ssniff V1534-0 R/M-H) for 3 weeks and were then placed on a
105 chemically defined control diet (CCD; ssniff E15000-04 EF R/M Kontrolle) for 12 weeks. All
106 mice had ad libitum access to food and water and were housed in the same open mouse
107 facility. Body weight was determined weekly, and blood glucose was measured shortly
108 before the end of the feeding trial. Animals were killed in a non-fasted state at an age of 20
109 weeks. Animal handling was conducted in accordance with the Principles of Laboratory Care
110 and was approved by the Veterinary Inspection Services.

111 **Streptozotocin-induced insulin-deficient diabetic mice**

112 C57BL6/N mice ($n=10$) at an age of 12 weeks were injected intraperitoneally with a single
113 high dose of streptozotocin (180 mg/kg body weight; streptozotocin was dissolved in 0.1 M
114 citric acid buffer). C57BL6/N mice ($n=10$) injected intraperitoneally with citric acid buffer
115 were used as controls. All mice were kept at a standard chow diet (ssniff V1534-0 R/M-H)

116 during the whole study and were not fasted. Mice were killed five days post-injection. Body
117 weight and blood glucose were measured daily. Blood glucose was measured using tail-vein
118 puncture. All experiments were conducted according to the German guidelines for animal
119 care and were approved by the state of Bavaria (Regierung von Oberbayern) ethics
120 committee (Reference number: 55.2.1-54-2532-22-11).

121 **Plasma and tissue collection**

122 Blood was collected into EDTA-coated tubes via cardiac puncture and centrifuged at 1200 g
123 and at 4°C to separate plasma. Plasma and tissues (liver, quadriceps muscle, and epididymal
124 adipose tissue) were collected, snap-frozen in liquid nitrogen, and stored at -80°C. Frozen
125 tissues were ground in liquid nitrogen prior to extraction of metabolites.

126 **Acylcarnitine profiling via targeted HPLC-MS/MS**

127 Acylcarnitine profiles of plasma and tissues were determined using LC-MS/MS as described
128 recently [4]. Briefly, metabolites were extracted from 10 µl of plasma or 40 mg of ground
129 tissue (wet weight). For plasma measurements, 10 µl of plasma was dissolved under ultra-
130 sonication in 100µl ice-cold methanol containing internal standard (ChromSystems,
131 München, Germany) with deuterium-labeled amino acid and acylcarnitine species. Samples
132 were then dried in a vacuum concentrator (SPD111V SpeedVac™ Thermo Savant™,
133 Germany). For tissue analysis, 40 mg of ground tissue were dissolved in 1800 µl 100% ice-
134 cold methanol and shaken for 20 min at room temperature. Samples were subsequently
135 centrifuged at 10.000 g for 10 minutes and supernatants were transferred to a new reaction
136 tube. For muscle and adipose tissue, with lower concentrations of acylcarnitines compared
137 to kidney and liver tissue, 200 µl of the extracts were mixed with 20 µl of the labeled amino
138 acid and acylcarnitine standard and vacuum-dried. For liver and kidney, 200 µl of sample
139 were mixed with 50 µl internal standard and vacuum-dried. Acylcarnitines were derivatized
140 to their butyl esters as described by Gucciardi et al. [5]. Briefly, 100 µl *n*-butanol containing
141 5% v/v acetyl choline was added to the dried samples, incubated at 60°C for 20 minutes and
142 subsequently evaporated to dryness. Samples were reconstituted in 100 µl (for plasma
143 samples) or 200 µl (for tissue samples) of acetonitrile/water and transferred to glass vials.

144 Samples were automatically injected (PAL HTC-xt, CTC analytics AG, Zwingen, Switzerland)
145 and chromatographic separation was yielded on a Zorbax Eclipse XDB-C18 column (length

146 150 mm, internal diameter 3.0 mm, particle size 3.5 μm , Agilent, USA) using the Agilent 1260
147 Infinity Quaternary LC System. The mobile phase consisted of 0.1% formic acid, 2.5 mM
148 ammonium acetic acid and 0.005% heptafluorobutyric acid in water (mobile phase A) or 0.1%
149 formic acid, 2.5 mM ammonium acetic acid and 0.005% heptafluorobutyric acid in acetonitrile
150 (mobile phase B). Mass spectrometric detection was done using the QTRAP5500 LC-MS/MS
151 system (AB SCIEX | 500 Old Connecticut Path, Framingham, MA 01701, USA) with positive
152 electron spray ionization and operating in multiple reaction monitoring (MRM). Peak
153 integration and quantification was done using Analyst 1.5[®] software (AB SCIEX | 500 Old
154 Connecticut Path, Framingham, MA 01701, USA).

155

156 **Acyl-CoA profiling using targeted HPLC-MS/MS**

157 Coenzyme A esters were extracted from frozen, ground tissue samples, which were lysed
158 using a Precellys 24 homogeniser (Peqlab, Germany) at -10 °C in 1 ml methanol containing
159 biochanin A as internal standard. The procedure included three cycles of homogenisation
160 (6800 rpm, 30 s with equivalent breaks). The lysate was transferred to 10 ml of ice cold
161 ammonium acetate (25 mM, pH 6) and centrifuged (5 min at 10,000 g, 4 °C). CoA derivatives
162 were extracted on a Strata XL-AW solid phase extraction column (Phenomenex, Germany).
163 The column was equilibrated with 1 ml methanol followed by 1 ml methanol: H₂O: formic
164 acid (50: 45: 5) and 1 ml H₂O. Cell lysate was loaded onto the column (800-900 mbar
165 vacuum, 5 min), washed with 1 ml ammonium acetate (25 mM, pH 7.2) and 1 ml methanol,
166 followed by short drying. CoA esters were eluted in 1000 μl methanol, containing 5 % (v/v)
167 ammonia. The eluate was dried in a vacuum concentrator with rotation (15 °C, overnight).

168 Buffers, eluents, column and flow rates for HPLC-MS analysis of CoA derivatives were used
169 as described by [6]. Dried extracts were resolved in 200 μl sample buffer (25 mM ammonium
170 acetate pH 3.5, 2 % methanol) and 50 μl were injected on a Dionex ultimate 3000 system
171 (Thermo Scientific Inc., Germany) coupled to a Bruker MicroTOF QII mass spectrometer
172 (Bruker Daltonik GmbH, Germany) equipped with an electrospray ionisation interface.
173 Separation of CoA-intermediates was carried out on a C₁₈ analytical column (Gemini 150 · 2.0
174 mm, particle size 3 μm ; Phenomenex, Germany) at a constant temperature of 35 °C using
175 the following gradient: 1 min 5 % B (methanol): 95 % A (50 mM formic acid: ammonia pH
176 8.1), 18 min gradient to 30 % B: 70 % A, 7 min gradient to 95 % B: 5 % A and a final step at 95

177 % B: 5 % A for 4 min. MS analysis was done using positive ESI mode with 3 Hz data
178 acquisition and automated MS² acquisition with full scan mass spectra from 90 to 1178 m/z.

179 Data export to mzXML format and internal mass calibration using sodium formiate cluster
180 was carried out with DataAnalysis software (version 4.0 SP 5 (Build 283)). Raw data were
181 processed using the XCMS package [7-9] for R (version 3.0.3). After peak detection The XCMS
182 methods 'group' and 'rector' in two iterations were used for peak alignment and retention
183 time correction and missing values were estimated using the 'fill peaks' method. Retention
184 times of available CoA standards and the accurate masses of M + 2H ions were used for peak
185 identification. If no synthetic standard was available for a certain compound, calculation of
186 molecular mass from M + 2H and M + H ions, sum formula prediction from the accurate
187 mass and isotopic pattern were combined for identification, using the DataAnalysis software.
188 Whenever possible, MS² fragmentation was used to confirm the presence of the CoA moiety.
189 Data were normalised to the median relative peak area of all metabolites detected in at least
190 36 of the 45 samples, including the internal standard biochanin A.

191 **Statistics and data integration**

192 Plasma and tissue concentrations in streptozotocin-treated mice were compared to healthy
193 control mice and significantly-changed metabolites were calculated using unpaired two-
194 sided Student's t-tests, assuming unequal variance. A significance threshold of alpha < 0.05
195 was applied. Pairwise Pearson correlations were determined for metabolite concentrations
196 within tissues and between plasma and tissues. These were visualized using correlation
197 matrices and correlation networks. The statistical software environment R was used for
198 calculations and visualizations using the packages 'corrplot', 'gplots' and 'qgraph'.

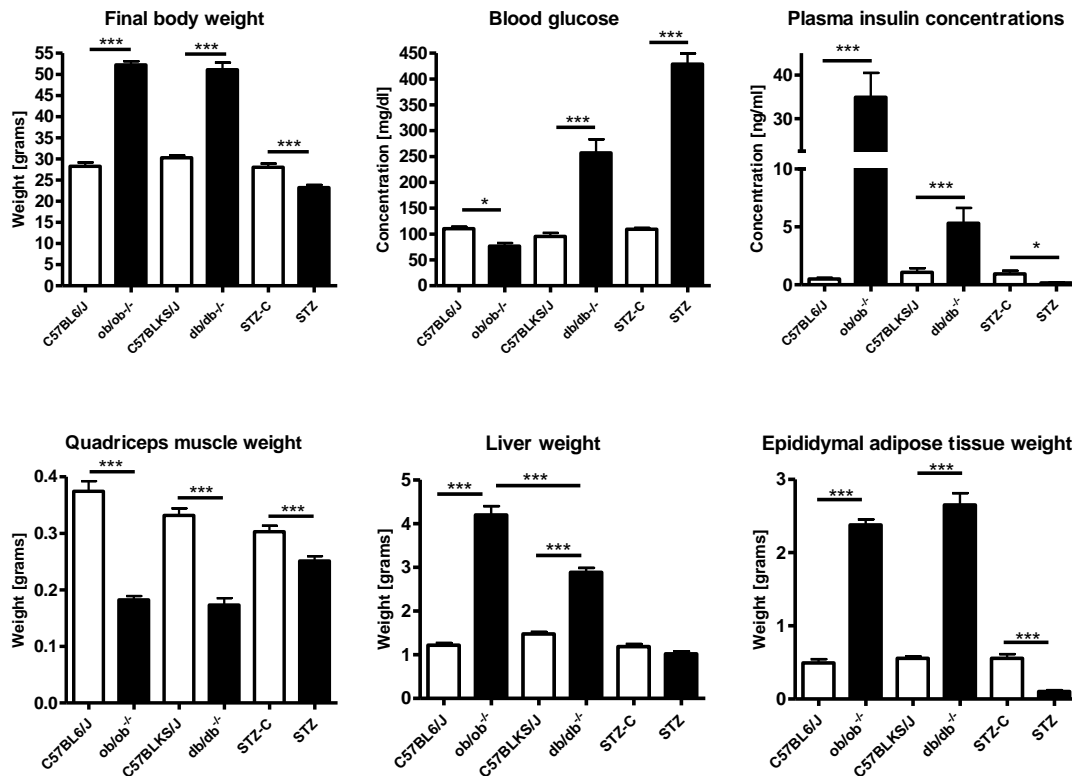
199

200

201 **Results**

202 **Body and tissue weights, blood glucose and plasma insulin levels**

203



204

205 **Figure 1. Phenotypic parameters of the different mouse models used in the study. A) Body weight. B) Blood**
 206 **glucose concentrations. C) Plasma insulin concentrations. D) Quadriceps muscle weight. E) Liver weight. F)**
 207 **Epididymal adipose tissue weight.**

208 Figure 1 shows the phenotypic parameters of the studied mice. For the ob/ob and db/db
 209 mice, animals were analyzed at an age of 20 weeks. For the streptozotocin-treated mice,
 210 measurements were obtained five days after streptozotocin injection. Leptin signaling-
 211 deficient ob/ob and db/db mice showed a dramatic increase in body weight associated with
 212 increased liver and adipose tissue weights, while their muscle mass decreased. In contrast,
 213 STZ-mice displayed a dramatic reduction in body weight of around 20% five days after
 214 injection and this was reflected by a complete depletion of white adipose tissue and a
 215 reduction in liver mass while muscle mass was only slightly reduced. Kidney weight did not
 216 change between mouse groups. While ob/ob mice displayed dramatically increased plasma
 217 insulin levels and a normoglycemia, the hyperinsulinemia in db/db mice was much less
 218 pronounced and was accompanied by increased blood glucose levels. For streptozotocin-

219 treated mice, blood glucose levels followed the well-described three-phasic response,
 220 consisting of an initial short hyperglycemic phase, followed by a rapid decrease into
 221 hypoglycemia and finally a permanent severe hyperglycemic phase. Plasma insulin in
 222 streptozotocin-diabetic mice was reduced to levels below detection.

223 **Changes in acylcarnitine profiles in plasma and tissues**

224
 225 Acylcarnitine concentrations were quantified in plasma and different tissues. The
 226 concentration ranges of individual acylcarnitine species in plasma and tissues are shown in
 227 Figure 2. Generally, liver and kidney displayed the highest concentrations of acylcarnitines,
 228 while concentrations in plasma were lowest. Short-chain saturated acylcarnitine species
 229 were at highest concentrations whereas odd-numbered species had lowest levels.
 230 Dicarboxylic acylcarnitine species were generally highest in liver and were very low in
 231 muscle.

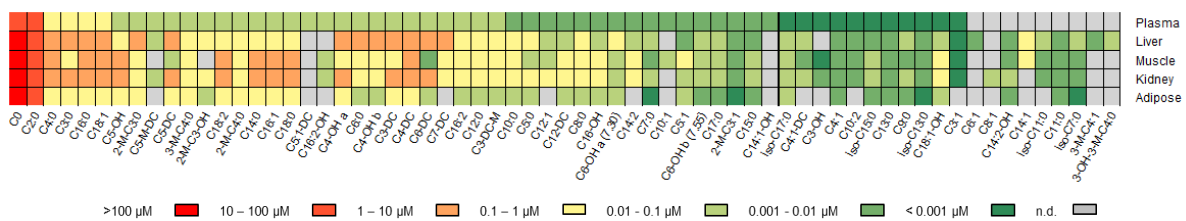


Figure 2. Level plot showing the concentration range of individual acylcarnitine species in plasma and different tissues.

236 Tables 1 to 4 display changes in acylcarnitine concentrations relative to the levels in
 237 corresponding control mice for amino acid-derived, fatty acid-derived, dicarboxylic, and odd-
 238 numbered acylcarnitines, respectively. All models displayed increases in BCAA-derived
 239 acylcarnitine species with most prominent increases for propionyl-, methylmalonyl-,
 240 succinyl-, isovaleryl-, and 2-methylbutyrylcarnitine. In ob/ob mice, these increases were
 241 found in liver and kidney, while decreased levels were found in adipose tissue. A similar
 242 trend for liver and kidney was observed in db/db mice, although less pronounced. STZ-mice
 243 additionally showed increases of BCAA-derived species in muscle. Glutarylcarnitine, an
 244 intermediate in lysine and tryptophan breakdown, showed a strong reduction in ob/ob and
 245 db/db mice in all tissues and in plasma.

Table 1. Amino acid-derived acylcarnitines in plasma and tissues
 (expressed as ratios relative to control mice)

short name	full name	Ratio OB/WT					Ratio DB/WT			Ratio STZ/CTRL			
		Plasma	Liver	Muscle	Kidney	Adipose	Plasma	Liver	Kidney	Plasma	Liver	Muscle	Kidney
C2:0	acetylcarnitine	1.36	1.28	1.07	1.16	0.51	0.72	0.99	0.96	0.64	0.96	1.14	< LOQ
C4:0	butyrylcarnitine	6.81	2.08	1.52	1.33	0.41	1.43	1.53	1.14	1.03	2.08	1.20	1.36
2-M-C4:0	2-methylbutyrylcarnitine	2.46	3.04	0.97	1.52	0.66	1.02	2.60	1.30	1.36	4.10	4.18	1.61
2-M-C4:1	tiglylcarnitine	1.35	1.43	1.05	1.90	1.23	1.46	0.62	2.41	1.89	2.42	3.98	2.46
2-M-C4-OH	2-methyl-3-hydroxybutyrylcarnitine	1.10	0.95	1.01	0.92	0.51	0.97	1.04	1.28	0.76	1.41	2.02	1.02
C3:0	propionylcarnitine	1.33	1.90	1.14	1.23	0.32	0.84	1.08	1.08	1.73	1.96	1.52	< LOQ
C4-DC	succinylcarnitine	1.70	2.05	1.07	1.63	0.48	1.13	1.37	1.56	2.07	1.53	1.48	1.22
C3-DC-M	methylmalonylcarnitine	1.55	2.50	1.06	1.56	0.29	1.46	2.41	1.53	1.39	1.88	1.35	0.65
C5-M-DC	methylglutaryl carnitine	0.89	0.52	< LOQ	1.11	< LOQ	1.06	0.85	0.73	0.44	2.14	< LOQ	0.87
3-M-C4:0	isovaleryl carnitine	2.88	1.53	1.32	1.69	0.44	1.45	1.91	1.62	2.34	4.15	6.59	3.16
3-M-C4:1	3-methylbutyrylcarnitine	< LOQ	< LOQ	< LOQ	< LOQ	< LOQ	< LOQ	< LOQ	< LOQ	< LOQ	1.82	< LOQ	< LOQ
3-OH-3-M-C4:0	3-hydroxyisovaleryl carnitine	< LOQ	< LOQ	< LOQ	< LOQ	< LOQ	< LOQ	< LOQ	< LOQ	< LOQ	1.45	< LOQ	< LOQ
C5-DC	glutaryl carnitine	0.61	0.20	0.56	0.43	0.11	0.72	0.24	0.19	1.21	1.44	1.14	0.48
C5:1-DC	glutaconyl carnitine	< LOQ	< LOQ	< LOQ	< LOQ	< LOQ	0.78	< LOQ	< LOQ	1.82	< LOQ	< LOQ	< LOQ
C4:1	crotonyl carnitine	< LOQ	1.19	2.84	1.40	0.63	0.72	2.05	1.96	< LOQ	1.21	2.16	1.31
C4-OH a	3-hydroxybutyrylcarnitine	0.65	1.32	1.71	1.22	1.45	0.48	0.83	1.23	1.42	0.96	1.31	1.47
2-M-C3:0	isobutyrylcarnitine	2.10	1.02	0.92	1.11	0.43	0.75	1.12	0.58	1.01	1.79	4.89	1.18
2-M-C3:1	methacrylylcarnitine	< LOQ	1.06	0.84	1.41	1.04	0.84	2.37	2.46	< LOQ	1.16	4.59	2.85
2-M-C3-OH	3-hydroxyisovaleryl carnitine	0.67	0.90	< LOQ	0.62	0.53	1.07	0.55	0.44	0.40	0.71	< LOQ	0.59

Increased, p < 0.01 Increased, 0.01 < p < 0.05 Decreased, 0.01 < p < 0.05 Decreased, p < 0.01

248
249

250 Table 2 displays the changes observed in fatty acid-derived acylcarnitine species. Most
251 pronounced in ob/ob mice were the elevated levels of short- and medium-chain
252 acylcarnitines, as well as of hexadecanoyl- and octadecanoylcarnitine in liver, which were
253 partially observed as well in plasma. The increase in short- and medium-chain acylcarnitines
254 was much less pronounced in livers of db/db mice and significant changes were only found
255 for octanoylcarnitine. In addition, db/db mice displayed elevated hepatic concentrations of
256 3-hydroxybutyrylcarnitine, a metabolite derived from the ketone body D-3-hydroxybutyrate.
257 Most prominent in STZ-mice were the decreases of medium- and long-chain acylcarnitine
258 species in muscle, which were partially also found in kidney.

259
260

**Table 2. Fatty acid-derived acylcarnitines in plasma and tissues
(expressed as ratios relative to control mice)**

short name	full name	Ratio OB/WT					Ratio DB/WT			Ratio STZ/CTRL			
		Plasma	Liver	Muscle	Kidney	Adipose	Plasma	Liver	Kidney	Plasma	Liver	Muscle	Kidney
C2:0	acetylcarnitine	1.36	1.28	1.07	1.16	0.51	0.72	0.99	0.96	0.64	0.96	1.14	< LOQ
C4:1	crotonyl carnitine	< LOQ	1.19	2.84	1.40	0.63	0.72	2.05	1.96	< LOQ	1.21	2.16	1.31
C4:0	butyrylcarnitine	6.81	2.08	1.52	1.33	0.41	1.43	1.53	1.14	1.03	2.08	1.20	1.36
C4-OH a	3-hydroxybutyrylcarnitine	0.65	1.32	1.71	1.22	1.45	0.48	0.83	1.23	1.42	0.96	1.31	1.47
C4-OH b	3-hydroxybutyrylcarnitine	1.23	1.67	1.43	1.12	1.30	0.55	2.18	0.77	0.83	0.94	1.39	1.78
C6:0	hexanoylcarnitine	5.66	3.29	0.92	0.87	0.71	0.57	3.13	1.07	0.48	2.22	0.61	1.12
C6-OH a	hydroxyhexanoylcarnitine	0.30	2.47	0.92	0.80	3.55	0.50	1.75	1.43	1.38	1.76	0.73	1.01
C6-OH b	hydroxyhexanoylcarnitine	0.50	1.64	0.65	0.76	1.92	0.51	1.41	1.24	0.52	1.70	0.73	0.59
C8:0	octanoylcarnitine	1.78	4.25	0.62	0.65	0.84	0.47	2.84	0.84	0.67	1.52	0.48	0.76
C10:0	decanoylcarnitine	1.22	3.51	0.58	0.69	0.73	0.53	1.40	0.82	0.53	1.01	0.34	0.58
C10:2	decadienoylcarnitine	< LOQ	1.37	< LOQ	1.76	< LOQ	0.93	1.41	2.85	< LOQ	< LOQ	0.38	1.10
C12:0	dodecanoylcarnitine	1.34	1.61	0.62	0.92	1.06	0.51	0.53	0.91	0.65	0.67	0.26	0.50
C12:1	dodecenoylcarnitine	0.84	< LOQ	0.58	< LOQ	< LOQ	< LOQ	< LOQ	< LOQ	< LOQ	0.92	0.40	0.77
C14:0	tetradecanoylcarnitine	1.05	1.38	0.60	0.97	1.10	0.54	0.56	0.96	0.73	0.52	0.23	0.55
C14:1	tetradecenoylcarnitine	< LOQ	< LOQ	< LOQ	< LOQ	< LOQ	< LOQ	< LOQ	< LOQ	< LOQ	0.63	0.37	< LOQ
C16:0	hexadecanoylcarnitine	0.85	2.44	1.01	0.99	1.49	0.58	0.75	1.04	0.83	0.86	0.32	0.67
C16:1	hexadecenoylcarnitine	2.91	2.34	1.00	1.14	1.35	0.68	1.57	1.32	0.37	0.37	0.25	0.64
C16:2	hexadecadienoylcarnitine	< LOQ	< LOQ	0.58	0.90	0.73	< LOQ	< LOQ	1.12	0.97	1.08	0.52	1.15
C16-OH	hydroxyhexadecanoylcarnitine	< LOQ	0.52	0.88	0.94	4.08	< LOQ	0.54	0.78	1.86	0.84	0.24	0.68
C18:0	octadecanoylcarnitine	0.92	3.28	0.80	0.94	0.64	0.68	1.39	1.13	1.15	1.43	0.35	0.69
C18:1	octadecenoylcarnitine	2.84	24.27	1.83	1.29	2.02	0.85	2.88	1.47	0.72	0.85	0.44	0.89
C18:2	octadecadienoylcarnitine	1.45	7.05	0.76	0.81	1.01	0.76	0.77	1.04	1.06	1.59	0.59	1.21
C18:1-OH	hydroxyoctadecanoylcarnitine	< LOQ	3.98	1.38	1.17	4.00	< LOQ	2.11	1.23	0.76	0.89	0.36	1.14

Increased, p < 0.01 Increased, 0.01 < p < 0.05 Decreased, 0.01 < p < 0.05 Decreased, p < 0.01

261
262

263 A number of dicarboxylcarnitine species were measured which originate partially from
264 amino acid degradation and from microsomal omega oxidation (Table 3). The ob/ob and
265 db/db mice display elevated hepatic and renal concentrations of amino acid-derived

266 methylmalonyl- and succinylcarnitine, while longer chain dicarboxylcarnitine species were
 267 all reduced. This is in contrast to STZ-mice which displayed the strongest elevation of
 268 methylmalonyl- and succinylcarnitine in muscle and plasma, while liver is characterized by
 269 elevations of methylglutaryl- and pimeloylcarnitine.

270 **Table 3. Dicarboxylic acylcarnitines in plasma and tissues**
 271 **(expressed as ratios relative to control mice)**
 272

short name	full name	Ratio OB/WT					Ratio DB/WT			Ratio STZ/CTRL			
		Plasma	Liver	Muscle	Kidney	Adipose	Plasma	Liver	Kidney	Plasma	Liver	Muscle	Kidney
C3-DC	malonylcarnitine	1.42	1.00	0.84	1.33	0.40	<LOQ	1.40	0.75	0.93	0.76	1.19	0.77
C4-DC	succinylcarnitine	1.70	2.05	1.07	1.63	0.48	1.13	1.37	1.56	2.07	1.53	1.48	1.22
C3-DC-M	methylmalonylcarnitine	1.55	2.50	1.06	1.56	0.29	1.46	2.41	1.53	1.39	1.88	1.35	0.65
C4:1-DC	fumarylacarnitine	<LOQ	0.01	1.00	0.30	<LOQ	1.05	0.10	0.61	0.86	1.73	<LOQ	1.34
C5-DC	glutarylacarnitine	0.61	0.20	0.56	0.43	0.11	0.72	0.24	0.19	1.21	1.44	1.14	0.48
C5:1-DC	glutaconylcarnitine	<LOQ	<LOQ	<LOQ	<LOQ	<LOQ	0.78	<LOQ	<LOQ	1.82	<LOQ	<LOQ	<LOQ
C6-DC	adipoylcarnitine	0.87	0.22	0.56	0.70	0.05	0.53	0.17	0.40	<LOQ	0.67	0.76	0.50
C7-DC	pimeloylcarnitine	0.49	0.05	0.67	0.36	<LOQ	0.66	0.09	0.29	2.36	1.97	<LOQ	1.97
C5-M-DC	methylglutarylacarnitine	0.89	0.52	<LOQ	1.11	<LOQ	1.06	0.85	0.73	0.44	2.14	<LOQ	0.87
C12-DC	dodecanoylcarnitine	0.84	133.46	0.79	0.95	0.71	0.80	1.51	1.23	0.93	1.57	0.34	0.69

273 **Increased, p < 0.01** **Increased, 0.01 < p < 0.05** **Decreased, 0.01 < p < 0.05** **Decreased, p < 0.01**

274
 275 Next to propionyl-, 2-methylbutyryl-, and isovalerylcarnitine, derived from BCAA
 276 metabolism, all models display increased hepatic concentrations of longer-chain odd-
 277 numbered acylcarnitine species of up to 13 carbons (see Table 4). Similar changes were also
 278 found in kidney, while muscle tissue of ob/ob and STZ-mice displayed decreased levels of
 279 odd-numbered acylcarnitine species of carbon chain length between C9 and C17.

280 **Table 4. Odd-numbered acylcarnitines in plasma and tissues**
 281 **(expressed as ratios relative to control mice)**

short name	full name	Ratio OB/WT					Ratio DB/WT			Ratio STZ/CTRL			
		Plasma	Liver	Muscle	Kidney	Adipose	Plasma	Liver	Kidney	Plasma	Liver	Muscle	Kidney
C3:0	propionylcarnitine	1.33	1.90	1.14	1.23	0.32	0.84	1.08	1.08	1.73	1.96	1.52	<LOQ
C5:0	valerylcarnitine	2.42	2.27	1.36	1.76	0.30	1.02	1.80	1.29	1.94	2.57	2.44	1.83
2-M-C4:0	2-methylbutyrylcarnitine	2.46	3.04	0.97	1.52	0.66	1.02	2.60	1.30	1.36	4.10	4.18	1.61
3-M-C4:0	isovalerylcarnitine	2.88	1.53	1.32	1.69	0.44	1.45	1.91	1.62	2.34	4.15	6.59	3.16
C7:0	heptanoylcarnitine	<LOQ	2.63	1.01	1.57	0.64	0.78	2.54	1.29	1.88	1.93	0.83	1.81
iso-C7:0	isoheptanoylcarnitine	<LOQ	2.48	1.07	1.20	0.70	<LOQ	3.45	0.94	<LOQ	2.83	2.26	1.37
C9:0	nonanoylcarnitine	<LOQ	3.15	1.74	1.32	0.87	0.52	2.94	1.20	<LOQ	1.54	0.48	1.17
C11:0	undecanoylcarnitine	<LOQ	2.89	0.59	1.11	0.76	<LOQ	2.28	1.06	<LOQ	1.02	0.42	0.93
iso-C11:0	isoundecanoylcarnitine	<LOQ	7.37	<LOQ	0.94	<LOQ	<LOQ	6.58	1.14	<LOQ	1.85	0.26	0.82
C13:0	tridecanoylcarnitine	<LOQ	3.55	0.53	0.97	0.83	0.78	0.84	1.11	1.21	1.03	0.40	0.91
iso-C13:0	isotridecanoylcarnitine	<LOQ	<LOQ	0.42	0.72	1.16	0.83	2.76	1.12	1.15	1.39	0.36	0.86
C15:0	pentadecanoylcarnitine	0.69	1.39	0.48	1.06	0.93	0.69	0.58	1.10	1.25	1.09	0.39	1.00
iso-C15:0	isopentadecanoylcarnitine	<LOQ	<LOQ	0.45	0.83	0.87	0.70	1.30	1.04	1.64	1.10	0.38	1.01
C17:0	heptadecanoylcarnitine	0.71	1.40	0.65	0.86	0.85	0.72	0.76	1.20	1.25	1.62	0.46	1.03
iso-C17:0	isoheptadecanoylcarnitine	<LOQ	1.72	0.51	0.76	0.75	0.74	1.40	1.20	1.42	1.48	0.47	1.07

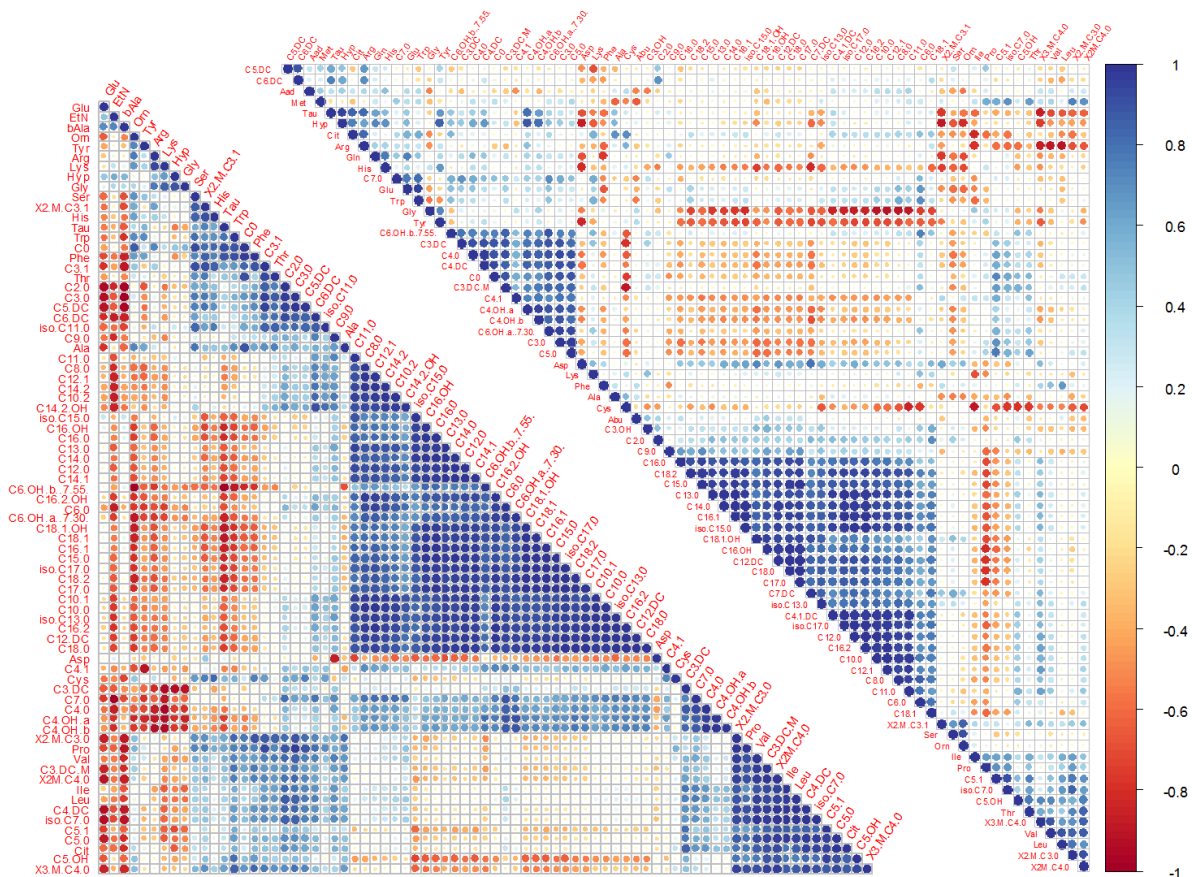
282 **Increased, p < 0.01** **Increased, 0.01 < p < 0.05** **Decreased, 0.01 < p < 0.05** **Decreased, p < 0.01**

284 **Correlations between concentrations of acylcarnitines and amino acids within tissues**

285 We previously reported changes in amino acid concentrations from the mice in this study
 286 [10, 11]. Individual concentrations of acylcarnitines and amino acids within tissues were
 287 cross-correlated. Correlation matrices for ob/ob mice for a very early stage and STZ-mice for
 288 a final stage of diabetes development are shown in Figure 3 for muscle and in Figure 4 for

289 liver. In both models BCAA concentrations and levels of BCAA-derived acylcarnitines
290 correlate in muscle, albeit much stronger in streptozotocin-treated than in ob/ob mice.
291 Medium- and long-chain acylcarnitine species correlate as well and form a large cluster in
292 both models, while amino acids other than BCAA display poor correlations amongst each
293 other and with acylcarnitines. A different clustering of butyryl- (C4) and
294 hydroxybutyrylcarnitine (C4-OH) is observed between both models. In ob/ob mice, these
295 metabolites correlate positively with other short-chain acylcarnitines and negatively with
296 medium- and long-chain acylcarnitines. In contrast, C4 and C4-OH species correlate
297 positively with longer-chain acylcarnitines in STZ-mice.

298 Compared to muscle, both models displayed less obvious correlations between BCAAs and
299 BCAA-derived acylcarnitines in liver. However, a clustering of medium- and long-chain
300 acylcarnitines is observed. Whereas in STZ-mice, odd- and even-numbered species form a
301 single large cluster, a specific clustering of odd- and even-numbered species in individual
302 clusters is seen in ob/ob mice. The cluster of odd-numbered species includes succinyl- (C4-
303 DC), propionyl- (C3), valeryl- (C5), heptanoyl- (C7), nonanoyl- (C9), and tridecanoylcarnitine
304 (C13), as well as branched odd-numbered species like a methyl-branched
305 undecanoylcarnitine (C11).



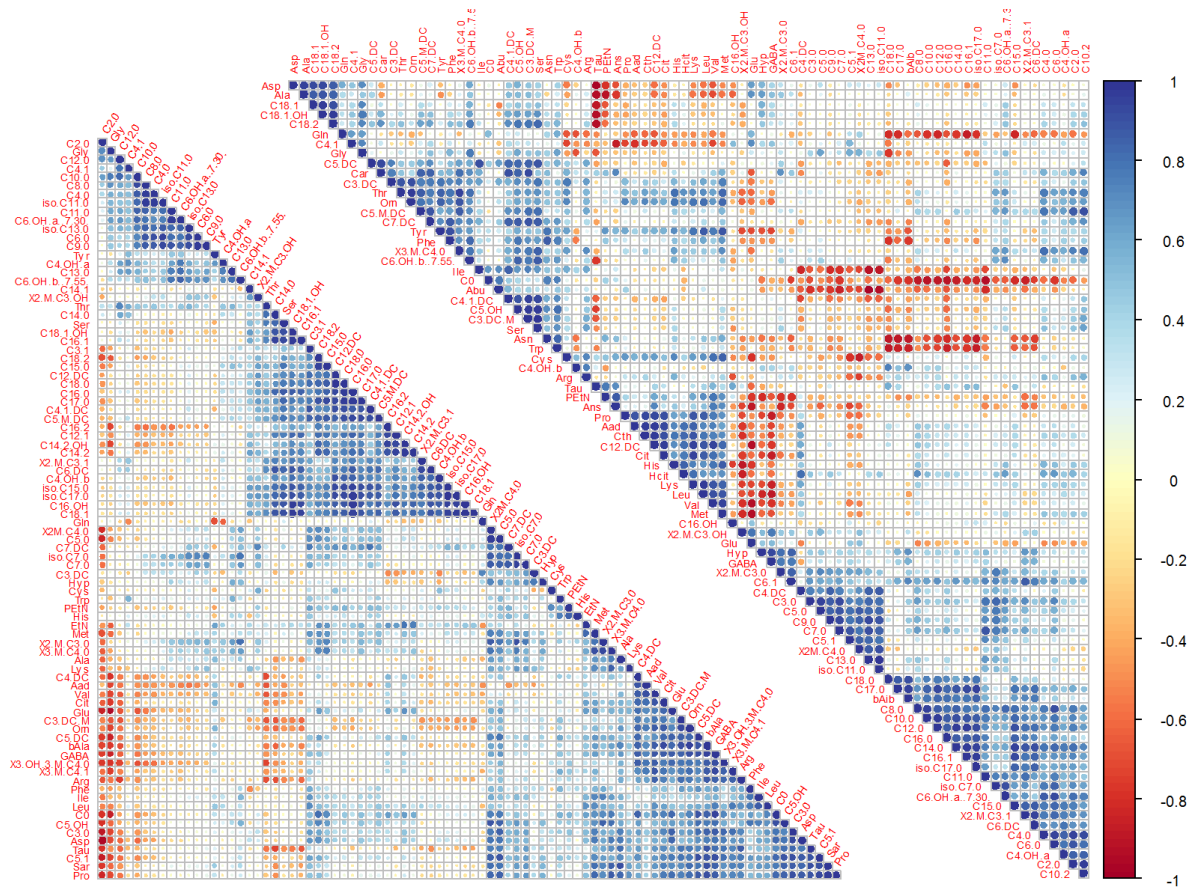
306

307

308

309

Figure 3. Correlation matrices for metabolite concentrations in muscle of STZ-mice (lower triangle) and ob/ob mice (upper triangle).



310

311

Figure 4. Correlation matrices for metabolite concentrations in liver of STZ-mice (lower triangle) and ob/ob mice (upper triangle).

312

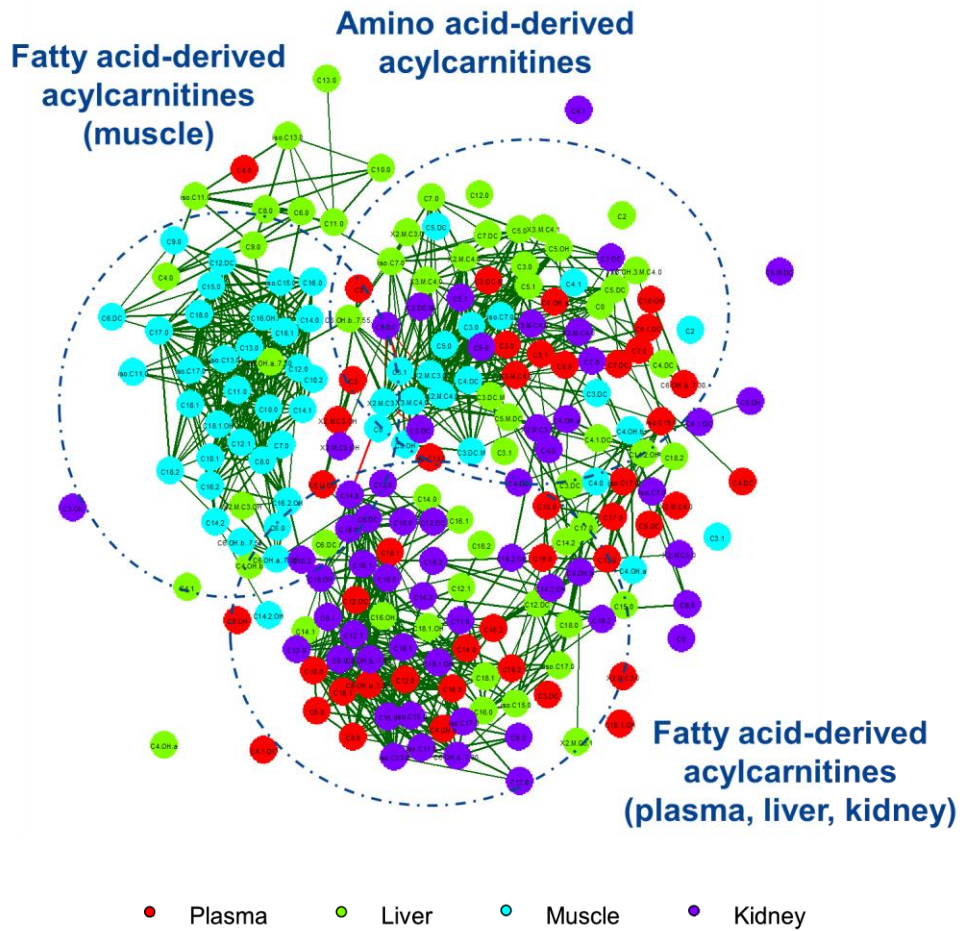
313

Correlations of acylcarnitine concentrations between plasma and tissues

314

Correlation network analysis was used to explore the correlations between plasma and tissues. Correlation networks are shown in Figure 5 for STZ-mice and in Figure 6 for ob/ob mice. In STZ animals, three main clusters were identified. Plasma levels of amino-acid derived acylcarnitines clustered with those in muscle, kidney, and liver as one group. Fatty acid-derived acylcarnitine levels correlated with those in liver and kidney, but not with those in muscle. Concentrations of fatty acid-derived acylcarnitines in muscle correlated amongst each other, forming a separate third group.

320



321

322

323

324

Figure 5. Correlation network of acylcarnitine levels in plasma and individual tissue compartments in streptozotocin-treated mice.

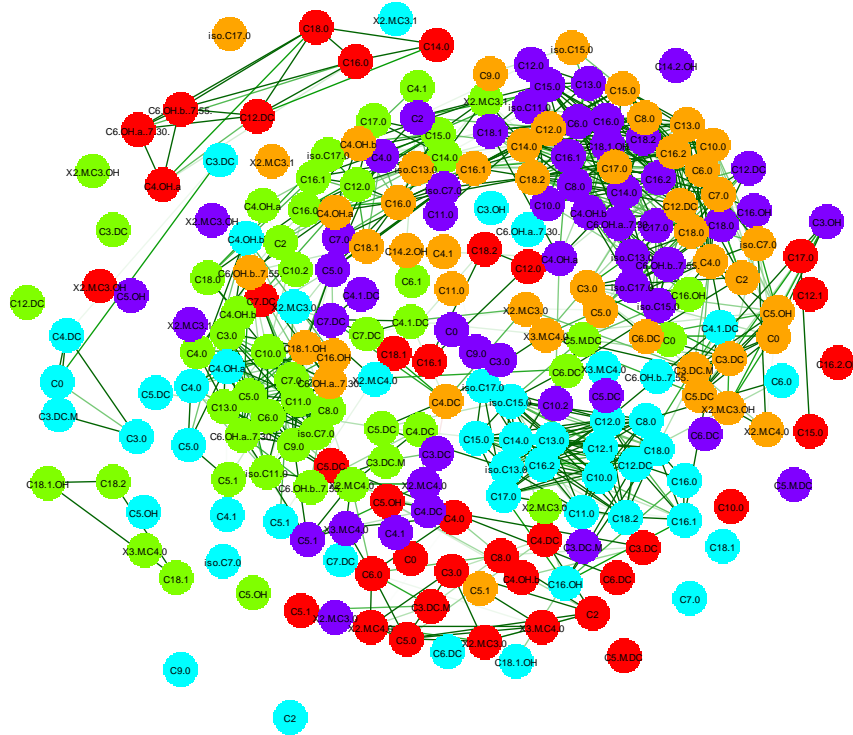
325

326

327

328

The correlation network obtained for samples of ob/ob mice showed weaker correlations between plasma and tissue compartments. Here, BCAA-derived acylcarnitines in plasma correlate with each other but not with those in tissues. Most obvious were the correlations between fatty acid-derived acylcarnitine species in kidney and adipose tissue.



329

330 ● Plasma ● Liver ● Muscle ● Kidney ● Adipose

331

332 **Figure 6. Correlation network of acylcarnitine levels in plasma and individual tissue compartments in ob/ob mice.**

333 **Hepatic concentrations of Acyl-CoA species and correlations with acylcarnitine levels**

334 For all three models in this study, hepatic concentrations of acyl-CoA species were
 335 determined from the identical samples as used for acylcarnitine profiling. Table 5 displays
 336 changes in hepatic acyl-CoA levels relative to corresponding control mice.

337 **Table 5. Ratios of hepatic acyl-CoA levels in studied diabetes models**
 338 **(expressed relative to those in control animals)**

full name	short name	OB/WT	DB/WT	STZ/CTRL
free CoA	Free CoA	1.01	1.24	1.32
acetyl-CoA	C2-CoA	0.87	0.88	0.61
propionyl-CoA	C3:0-CoA	1.26	0.83	1.37
butyryl-CoA	C4:0-CoA	1.18	1.34	0.99
isobutyryl-CoA	2-M-C3:0-CoA	0.90	1.05	1.54
2-methylbutyryl-CoA	2-M-C4:0-CoA	1.39	1.43	1.63
isovaleryl-CoA	3-M-C4:0-CoA	1.33	1.72	2.73
hydroxybutyryl-CoA	C4-OH-CoA	0.84	1.15	0.77
2-methyl-hydroxybutyryl-CoA	2-M-C4-OH-CoA	0.87	0.94	1.35
crotonyl-CoA	C4:1-CoA	1.19	1.21	1.51
3-methylcrotonyl-CoA	3-M-C4:1-CoA	1.11	0.89	2.47
succinyl-CoA	C4-DC-CoA	0.76	0.56	0.82
methylmalonyl-CoA	C3-DC-M-CoA	1.25	1.18	5.75
glutaryl-CoA	C5-DC-CoA	0.39	0.37	3.25
methylglutaconyl-CoA	C5:1-M-DC-CoA	1.06	0.39	1.53
hydroxymethylglutaryl-CoA	C5-M-DC-OH-CoA	0.93	1.21	0.87
glutaconyl-CoA	C5:1-DC-CoA	1.10	0.56	0.56
glutaconyl-CoA	C5:1-DC-CoA	1.08	0.77	0.36
methylsuccinyl-CoA	C4-DC-M-CoA	1.30	1.87	1.42
acetoacetyl-CoA	3-O-C4-CoA	0.86	1.03	0.88
hydroxypropionyl-CoA	C3-OH-CoA	0.88	1.06	0.84
pentanoyl-CoA	C5:0-CoA	1.40	1.32	1.38
hexanoyl-CoA	C6:0-CoA	1.58	2.12	1.22
heptanoyl-CoA	C7:0-CoA	1.21	2.01	1.25
octanoyl-CoA	C8:0-CoA	1.97	3.11	1.53
hydroxyhexanoyl-CoA	C6-OH-CoA	1.30	1.79	0.90
hexenoyl-CoA	C6:1-CoA	1.76	2.06	1.28
hydroxyoctanoyl-CoA	C8-OH-CoA	1.12	1.35	0.80
octenoyl-CoA	C8:1-CoA	1.27	1.17	1.23
malonyl-CoA	C3-DC-CoA	0.92	0.67	0.82
adipoyl-CoA	C6-DC-CoA	0.25	0.24	0.53
pimeloyl-CoA	C7-DC-CoA	0.34	0.09	0.71

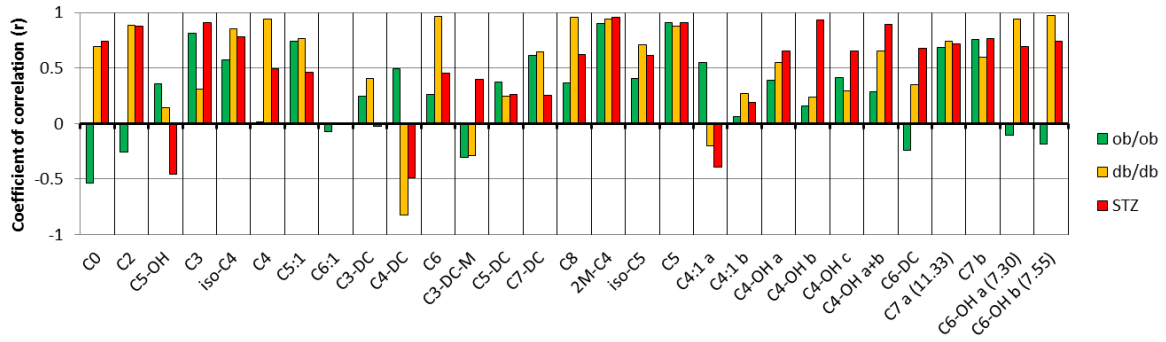
339

340

Increased, p < 0.01	Increased, 0.01 < p < 0.05	Decreased, 0.01 < p < 0.05	Decreased, p < 0.01
---------------------	----------------------------	----------------------------	---------------------

341 All models displayed increased hepatic concentrations of BCAA intermediates (propionyl-
342 CoA, isobutyryl-CoA, 2-methylbutyryl-CoA and isovaleryl-CoA). In addition, ob/ob and db/db
343 mice displayed increases in medium-chain acyl-CoA species, including pentanoyl- and
344 heptanoyl-CoA whereas reduced levels of dicarboxylic acyl-CoA species were observed in all
345 three models but most pronounced in db/db mice.

346 A total of 23 acyl chains were both quantified as acyl-CoA and acylcarnitine. Figure 7 displays
347 the correlations between hepatic acyl-CoA and corresponding acylcarnitine species.
348 Concentrations of most acyl-CoA and acylcarnitine species correlated positively. Strongest
349 correlations were found for species with saturated acyl-chains, such as 2-methylbutyryl- and
350 pentanoyl-CoA/carnitine. Differences for some metabolite pairs, including acetyl-
351 CoA/carnitine, adipoyl-CoA/carnitine, and hydroxyhexanoyl-CoA/carnitine were found
352 between the non-diabetic ob/ob mice and the diabetic models. Lowest correlations were
353 found for concentrations of dicarboxylic fatty acid species. Concentrations of succinyl-
354 CoA/carnitine even showed negative correlations in the diabetic mice. In Figure 8,
355 correlations in diabetes models are plotted against correlations in corresponding control
356 groups. It becomes clear that more acyl-CoA/carnitine show stronger correlations in
357 diabetes models as compared to control groups (metabolites located below diagonal). In
358 particular metabolites marked with the blue circle display correlations above 0.8 in diabetes
359 models, while a correlation in control lines is lacking.



360

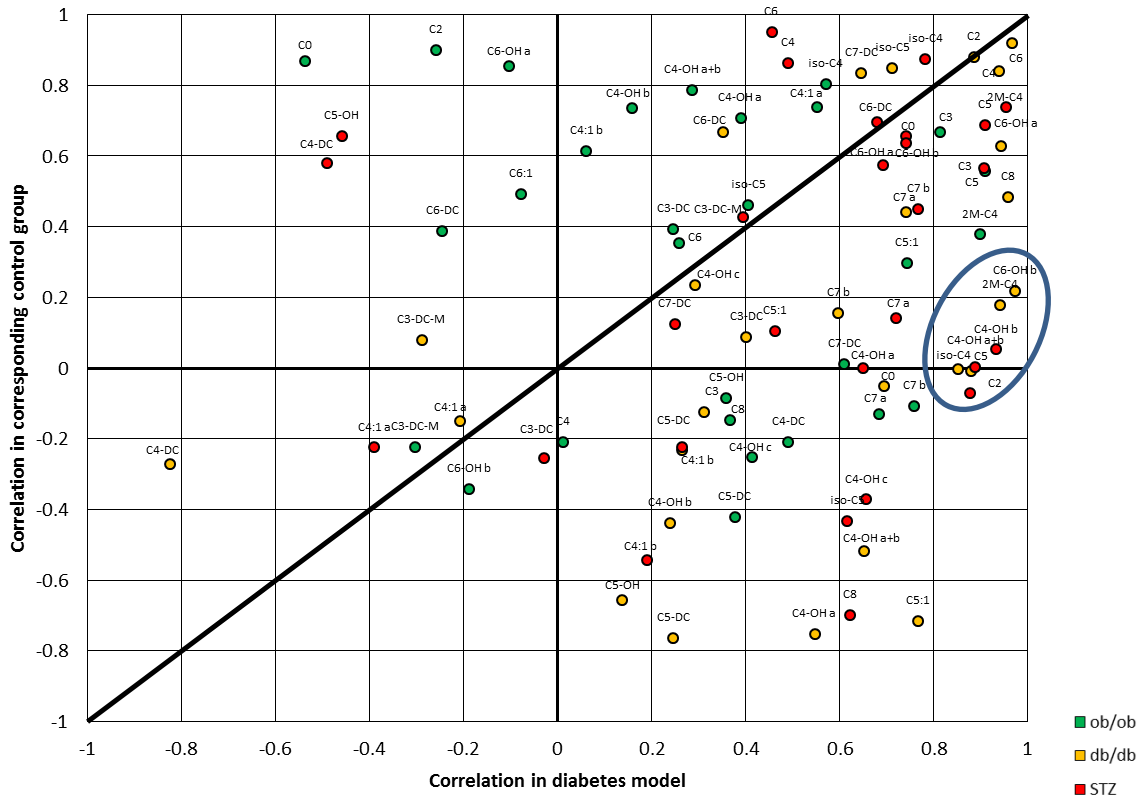
361

Figure 7. Correlations between hepatic acylcarnitine and acyl-CoA species in the three mouse models with coefficient of correlation plotted against acyl-CoA/carnitine pairs

362

363

Correlations acyl-CoA/carnitine Diabetic mice vs Controls



364

365

Figure 8. Correlations between hepatic acylcarnitine and acyl-CoA species in the diabetes models (x-values) plotted against the correlations in corresponding control groups (y-values). Every point above the diagonal indicates metabolite pairs with higher correlations in controls why every point below it represents stronger correlations in diabetes models.

366

367

368

369 Discussion

370 Elevated levels of BCAA-derived acylcarnitines are apparent in different stages of diabetes 371 development but might have different origins

372 Changes in levels of acylcarnitines derived from branched-chain amino acids have been
373 repeatedly reported as early markers of insulin resistance and diabetes with disease-
374 predictive quality [1, 2, 12]. We here describe that non-diabetic ob/ob mice already show
375 such increases in BCAA-derived acylcarnitines in plasma, liver and kidney, while such
376 changes were also observed in severely diabetic STZ-mice in plasma and all tissues analyzed
377 here. We recently speculated that the origin of these increases might differ in early and late
378 stages of diabetes development [13]. In animal models and human subjects with an early
379 state of obesity-induced insulin resistance, increases in BCAA and BCAA-derived compounds
380 are thought to originate from adipose tissue dysfunction, accompanied by a decreased
381 activity of BCKDH, the rate limiting enzyme in BCAA breakdown [14]. In support of this, we
382 previously reported decreased gene expression of BCKDH in ob/ob mice [11]. We observed
383 here that only the adipose tissue of ob/ob mice contained decreased levels of BCAA-derived
384 acylcarnitines, including isovaleryl-, propionyl-, methylmalonyl-, and succinylcarnitine. It is
385 thus very likely that a decreased BCAA breakdown in adipose tissue causes the increased
386 plasma BCAA levels observed in obesity and diabetes. In contrast to adipose tissue, the
387 increased levels of BCAA-derived acylcarnitines in liver suggest an increased breakdown of
388 BCAAs in this tissue. An increased BCKDH activity in liver to compensate for the decreased
389 activity in adipose tissue was previously discussed for obese mice fed a high fat diet [15].
390 Furthermore, elevated levels of BCAA-derived acylcarnitines in kidney could relate to an
391 increased excretion of these metabolites, which was previously described in obese Zucker
392 rats [16].

393 In contrast to the ob/ob mice, STZ-mice show a loss of adipose tissue mass which can be
394 explained by increased lipolysis [17]. As increased proteolysis was reported as well, these
395 animals will eventually lose skeletal muscle mass [18]. The elevated levels of BCAA
396 intermediates in STZ-mice could result from an increased proteolysis and increased amino
397 acid oxidation rates, as caused by the lack of insulin, which strongly inhibits proteolysis in a
398 healthy condition. The increased levels of BCAA-derived acylcarnitine in muscle and the close

399 proximity of the muscle for these metabolites in the correlation network, suggests a more
400 dominant role of muscle in determining plasma levels of BCAA-derived acylcarnitines in the
401 STZ model. A further indication of elevated amino acid breakdown in muscle tissue of STZ-
402 mice is the correlation of acylcarnitine concentrations that could be grouped according to
403 their degradation pathway and the corresponding amino acid precursor.

404 **Fatty acid-derived acylcarnitine concentrations differ between obese and non-obese mice**

405 Strongest differences in levels of fatty acid-derived acylcarnitines were found between the
406 obese mice and the non-obese STZ-mice and may relate to an effect of the hyperinsulinemia
407 observed in ob/ob and db/db mice. It is described that these mice display a partial
408 impairment of hepatic insulin signaling pathways. While insulin's inhibitory action on
409 gluconeogenesis is impaired, stimulation of de novo lipogenesis via SREBP-1c remains intact
410 and is amplified in hyperinsulinemic conditions [19]. The observed increases of hexadecenoyl
411 (C16:1)- and oleoyl (C18:1)-carnitines match with the reported increases of free C16:1 and
412 C18 fatty acids in plasma and liver and are in line with an increased activity of stearoyl-CoA
413 desaturase [11]. In accordance with this, the hypoinsulinemic STZ-mice display decreased
414 levels of C16:1 and C18-carnitines as well as most other fatty acid-derived acylcarnitine
415 species.

416 **Changes in medium-chain dicarboxylic acylcarnitine concentrations indicate differences in** 417 **hepatic omega oxidation**

418 The difference of anabolic and catabolic signaling between the obese animals and the lean
419 and diabetic STZ mice might as well be the cause of the changes observed in dicarboxylic
420 acylcarnitines. Except for methylmalonyl-, and succinylcarnitine, derived from amino acids,
421 the ob/ob and db/db mice showed dramatic decreases in hepatic concentrations of medium-
422 chain dicarboxylic acylcarnitines. Recently, these medium-chain dicarboxylic acylcarnitines
423 were described as markers of peroxisomal omega oxidation in liver [20]. A decreased omega
424 oxidation was previously proposed in ob/ob mice based on the finding of decreased urinary
425 adipic acid secretion compared to lean mice [21]. Reduced fatty acid oxidation might be
426 expected since ob/ob and db/db mice are hyperinsulinemic and lack leptin signaling, thus
427 favouring the conservation of fatty acids.

428 In contrast, STZ-mice displayed increased levels of glutaryl (C5-DC)- and pimeloyl (C7-DC)-
429 carnitine.

430 **Odd-numbered acylcarnitines as products from the elongation of BCAA-derived**
431 **intermediates**

432 Odd-numbered acylcarnitine species with more carbon units than the amino acid-derived C3
433 and C5 species were found at increased concentrations most strongly in livers of ob/ob mice
434 (up to chain length C13) but also in livers of db/db and STZ-mice (up to C7). Changes in
435 concentrations of odd-numbered fatty acids have been described in conditions of impaired
436 insulin signaling and diabetes but they might have different origins. Only very recently, the
437 synthesis of odd-numbered fatty acids from BCAAs and BCAA-derived methylmalonyl-CoA
438 shown in adipocytes [22]. This dates back to the 1960s were the synthesis of odd-numbered
439 fatty acids from propionyl-CoA was shown in mammalian adipocytes [23]. A similar
440 mechanism of fatty acid synthesis from propionyl- or methylmalonyl-CoA may be speculated
441 in liver in obese and hyperinsulinemic conditions as in ob/ob mice and may even be
442 enhanced as the precursor levels are also elevated. In support of this is the clustering of odd-
443 numbered acylcarnitine species that separate from even-numbered species in livers of ob/ob
444 animals. This is in contrast to the other tissues and animal models in which even- and odd-
445 numbered acylcarnitines form a mixed cluster with metabolites clustering according to chain
446 length (i.e. C18 correlates best with C17, etc.) Furthermore, the finding of increased levels of
447 methyl-branched longer chain acylcarnitines such as isoheptanoyl- and
448 isotridecanoylcarnitine suggests that also branched fatty acyl-CoAs such as isovaleryl-CoA or
449 isobutyryl-CoA might be used in fatty acid de novo synthesis and elongation. This is in
450 support of our previous findings showing increases of monomethyl branched fatty acids in
451 db/db mice [11]. Alternatively, it may well be that peroxisomal alpha oxidation – shown to
452 be increased in a STZ rat model [24] - causes the generation of the odd-numbered
453 acylcarnitines. Alpha oxidation, however, cannot be responsible for the increase in the levels
454 of branched acylcarnitine forms.

455 **Hepatic acyl-CoA and acylcarnitines correlate best for BCAA-derived and worst for**
456 **dicarboxylic compounds**

457 Hepatic levels of acylcarnitine and acyl-CoA correlated well for most saturated short-chain
458 species. Best correlations were observed for BCAA-derived species. This is in support of
459 previous findings comparing acylcarnitine and acyl-CoA species in mice fed a high-fat diet
460 [25]. Specifically in the STZ-mice, a strong positive correlation was observed for the ketone-
461 derived hydroxybutyryl-CoA/carnitine pair. BCAA-derived acyl chains as well as the ketone-
462 derived hydroxybutyrylcarnitine in STZ-mice are all compounds that accumulate in these
463 animals. This is in line with the concept that the formation of acylcarnitines from acyl-CoA
464 species is important in conditions of accumulating CoA species which might become toxic at
465 high levels. Since it is the spill-over that leads to an increased formation of acylcarnitines,
466 particularly accumulating species display 'sharp' correlations. The conversion of non-
467 accumulating CoA species and their carnitine conjugates are less synchronized.

468 In contrast, only weak correlations were found for several dicarboxylic acylcarnitine species.
469 Succinyl-CoA and succinylcarnitine even displayed negative correlations in the diabetic mice.
470 Whereas hepatic succinylcarnitine levels were increased in all three models, succinyl-CoA
471 levels were reduced. The reason for this poor correlation between CoA and carnitine species
472 is not known. It is intriguing that the enzyme responsible for the conversion of dicarboxylic
473 acyl-CoA to acylcarnitines has not been identified yet [26] and only a low conversion rate of
474 long-chain CoA species (C14 and C16-CoA) to carnitine species was reported in liver
475 homogenates [27]. In contrast, a microsomal dicarboxylyl-CoA synthetase was previously
476 described [28]. Nevertheless, considerable concentrations of succinylcarnitine can be found
477 in plasma and tissues. In this respect, it is important to consider the different cellular
478 compartments and locations of carnitine acyltransferases. Whereas carnitine
479 acetyltransferase and palmitoyltransferase 2 are located at the matrix side of the
480 mitochondrion, carnitine palmitoyltransferase 1 is located at the cytosolic side and carnitine
481 octanoyltransferase is located in peroxisomes. Succinyl-CoA is generated as the end-product
482 of amino acid breakdown (BCAAs, threonine and methionine) and is as well an intermediate
483 in the peroxisomal breakdown of dicarboxylic fatty acids such as suberic and sebacic acid,
484 which are generated by microsomal omega oxidation. Characterization of the different
485 cellular compartments in view of dicarboxylic acid metabolism is an interesting subject for
486 future studies to understand the lack of correlation for dicarboxylic species.

487 Taken together, we studied mouse models resembling different stages of human type 2
488 diabetes development - from obesity to insulin resistance and insulin deficiency - and
489 showed marked alterations in acylcarnitine profiles in plasma and selected organs. Overall,
490 the changes observed in plasma match with those reported from human studies along the
491 disease trajectory. We extended the set of marker compounds by using a targeted and highly
492 sensitive LC-MS/MS method. We also obtained tissue profiles of acylcarnitines and used
493 correlation network analysis to obtain indications on the origin of the plasma changes. Via
494 the parallel assessment of corresponding CoA and carnitine derivatives in liver tissue, we
495 demonstrate that the majority of acyl-CoA/acylcarnitine pairs, especially accumulating
496 species, display positive correlations, defining carnitine derivatives as good reporters of
497 changes in CoA pools. However, for dicarboxylic species, in particular succinyl-CoA/carnitine
498 even an inverse hepatic relationship was observed.

499

500 Literature

- 501 1. Newgard CB, An J, Bain JR, et al. A branched-chain amino acid-related metabolic signature
502 that differentiates obese and lean humans and contributes to insulin resistance. *Cell metabolism*.
503 2009;9(4):311-26.
- 504 2. Mihalik SJ, Goodpaster BH, Kelley DE, et al. Increased levels of plasma acylcarnitines in
505 obesity and type 2 diabetes and identification of a marker of glucolipototoxicity. *Obesity*.
506 2010;18(9):1695-700.
- 507 3. Schooneman MG, Achterkamp N, Argmann CA, et al. Plasma acylcarnitines inadequately
508 reflect tissue acylcarnitine metabolism. *Biochimica et biophysica acta*. 2014;1841(7):987-94.
- 509 4. Giesbertz P, Ecker J, Haag A, et al. An LC-MS/MS method to quantify acylcarnitine species
510 including isomeric and odd-numbered forms in plasma and tissues. *Journal of lipid research*. 2015.
- 511 5. Gucciardi A, Pirillo P, Di Gangi IM, et al. A rapid UPLC-MS/MS method for simultaneous
512 separation of 48 acylcarnitines in dried blood spots and plasma useful as a second-tier test for
513 expanded newborn screening. *Analytical and bioanalytical chemistry*. 2012;404(3):741-51.
- 514 6. Peyraud R, Kiefer P, Christen P, et al. Demonstration of the ethylmalonyl-CoA pathway by
515 using ¹³C metabolomics. *Proceedings of the National Academy of Sciences of the United States of*
516 *America*. 2009;106(12):4846-51.
- 517 7. Smith CA, Want EJ, O'Maille G, et al. XCMS: processing mass spectrometry data for
518 metabolite profiling using nonlinear peak alignment, matching, and identification. *Anal Chem*.
519 2006;78(3):779-87.
- 520 8. Tautenhahn R, Bottcher C, Neumann S. Highly sensitive feature detection for high resolution
521 LC/MS. *BMC bioinformatics*. 2008;9:504.
- 522 9. Benton HP, Want EJ, Ebbels TM. Correction of mass calibration gaps in liquid
523 chromatography-mass spectrometry metabolomics data. *Bioinformatics*. 2010;26(19):2488-9.
- 524 10. Sailer M, Dahlhoff C, Giesbertz P, et al. Increased plasma citrulline in mice marks diet-induced
525 obesity and may predict the development of the metabolic syndrome. *PloS one*. 2013;8(5):e63950.
- 526 11. Giesbertz P, Padberg I, Rein D, et al. Metabolite profiling in plasma and tissues of ob/ob and
527 db/db mice identifies novel markers of obesity and type 2 diabetes. *Diabetologia*. 2015;58(9):2133-
528 43.
- 529 12. Perng W, Gillman MW, Fleisch AF, et al. Metabolomic profiles and childhood obesity. *Obesity*.
530 2014;22(12):2570-8.
- 531 13. Giesbertz P, Daniel H. Branched-chain amino acids as biomarkers in diabetes. *Curr Opin Clin*
532 *Nutr Metab Care*. 2015.
- 533 14. She P, Van Horn C, Reid T, et al. Obesity-related elevations in plasma leucine are associated
534 with alterations in enzymes involved in branched-chain amino acid metabolism. *American journal of*
535 *physiology Endocrinology and metabolism*. 2007;293(6):E1552-63.
- 536 15. Lynch CJ, Adams SH. Branched-chain amino acids in metabolic signalling and insulin
537 resistance. *Nature reviews Endocrinology*. 2014;10(12):723-36.
- 538 16. She P, Olson KC, Kadota Y, et al. Leucine and protein metabolism in obese Zucker rats. *PloS*
539 *one*. 2013;8(3):e59443.
- 540 17. Tsujita T. Basal lipolysis in epididymal fat cells from streptozotocin-induced diabetic rats. *J*
541 *Nutr Sci Vitaminol (Tokyo)*. 2006;52(1):47-53.
- 542 18. Smith OL, Wong CY, Gelfand RA. Skeletal muscle proteolysis in rats with acute streptozocin-
543 induced diabetes. *Diabetes*. 1989;38(9):1117-22.
- 544 19. Brown MS, Goldstein JL. Selective versus total insulin resistance: a pathogenic paradox. *Cell*
545 *metabolism*. 2008;7(2):95-6.
- 546 20. Fiamoncini J, Lima TM, Hirabara SM, et al. Medium-chain dicarboxylic acylcarnitines as
547 markers of n-3 PUFA-induced peroxisomal oxidation of fatty acids. *Mol Nutr Food Res*.
548 2015;59(8):1573-83.
- 549 21. Lai RK, Goldman P. Urinary organic acid profiles in obese (ob/ob) mice: indications for the
550 impaired omega-oxidation of fatty acids. *Metabolism: clinical and experimental*. 1992;41(1):97-105.

- 551 22. Green CR, Wallace M, Divakaruni AS, et al. Branched-chain amino acid catabolism fuels
552 adipocyte differentiation and lipogenesis. *Nat Chem Biol.* 2016;12(1):15-21.
- 553 23. Horning MG, Martin DB, Karmen A, Vagelos PR. Fatty acid synthesis in adipose tissue. II.
554 Enzymatic synthesis of branched chain and odd-numbered fatty acids. *The Journal of biological*
555 *chemistry.* 1961;236:669-72.
- 556 24. Takahashi T, Takahashi H, Takeda H, Shichiri M. Alpha-oxidation of fatty acids in fasted or
557 diabetic rats. *Diabetes research and clinical practice.* 1992;16(2):103-8.
- 558 25. Liu X, Sadhukhan S, Sun S, et al. High-Resolution Metabolomics with Acyl-CoA Profiling
559 Reveals Widespread Remodeling in Response to Diet. *Mol Cell Proteomics.* 2015;14(6):1489-500.
- 560 26. Violante S, Ijlst L, Ruiten J, et al. Substrate specificity of human carnitine acetyltransferase:
561 Implications for fatty acid and branched-chain amino acid metabolism. *Biochimica et biophysica acta.*
562 2013;1832(6):773-9.
- 563 27. Vamecq J, Draye JP. Comparison between the formation and the oxidation of
564 dicarboxylcarnitine esters in rat liver and skeletal muscle: possible implications for human inborn
565 disorders of mitochondrial beta-oxidation. *Journal of inherited metabolic disease.* 1989;12(1):58-63.
- 566 28. Vamecq J, de Hoffmann E, Van Hoof F. The microsomal dicarboxyl-CoA synthetase. *The*
567 *Biochemical journal.* 1985;230(3):683-93.

568